

AN IMPROVED SERIAL SEARCH PN CODE ACQUISITION SCHEME FOR LOW SNR DS-CDMA SYSTEMS

by
Rehan Ahmad Warsi



**DEPARTMENT OF ELECTRICAL ENGINEERING
INDIAN INSTITUTE OF TECHNOLOGY KANPUR**

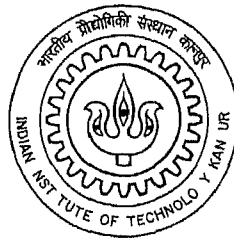
April 2000

TH
EE/2000/M
W2612

AN IMPROVED SERIAL SEARCH PN CODE ACQUISITION SCHEME FOR LOW SNR DS-SSMA SYSTEMS

*A Thesis Submitted
in Partial Fulfillment of the Requirements
for the Degree of
Master of Technology*

by
Rehan Ahmad Warsi



to the
DEPARTMENT OF ELECTRICAL ENGINEERING
INDIAN INSTITUTE OF TECHNOLOGY, KANPUR
INDIA
April 2000

23 MAY 2000 | EE
CENTRAL LIBRARY
IIT KANPUR

A 134830

11

11



A130930

20.04
2004

Certificate

It is certified that the work contained in the thesis entitled "An Improved Serial Search PN Code Acquisition Scheme For Low SNR DS-CDMA Systems" by *Rehan Ahmad Warsi* has been carried out under my supervision and this work has not been submitted elsewhere for a degree

Dated April 20th, 2000



A K Chaturvedi

Assistant Professor

Department Of Electrical Engineering

I I T Kharpur Pin 208016

Abstract

In this dissertation the problem of PN code acquisition for DS CDMA systems operating in low SNR environments has been investigated. Among the various techniques Serial search code acquisition technique has been used and improved upon. The modified strategy has been analyzed from fixed and adaptive threshold detection point of view in unfaded and faded environments characterized by Nakagami fading. Important acquisition parameters namely mean (\overline{T}_{acq}) and variance (σ_{acq}^2) of acquisition time have been derived using the signal flow graph technique. The results obtained demonstrate that for low SNR improvement of one order of magnitude is possible in the aforesaid acquisition parameters when compared with existing techniques.

Acknowledgement

I would like to record my deepest sense of gratitude and indebtedness towards *Dr A K Chaturvedi* for his erudite guidance, invaluable motivation, full encouragement and constructive criticism that has made this humble piece of work possible in its present form. He is always very patient and cooperative to me while discussing the various aspects of the work. Despite his busy schedule, he is always accessible to me.

Words are not enough to express my feelings towards my parents, brothers and sister. They have always been a constant source of inspiration for me.

I would like to express my sincere thanks to my wife and three years old son (*extremely naughty and always full of energy*) for their extended love, care and the patience during my hard days. I always found them standing by my side whenever I felt depressed and lonely.

Sincere thanks are also due to my friends and colleagues from Doordarshan especially, P. R. Sahu, Amit Sharma, Rajender Kumar and N. V. Raman for providing me a competitive environment and making my stay at I. I. T Kanpur a memorable one besides helping me directly or indirectly.

Last but not the least, I would like to thank a lot to Mr. *R. K. Gupta*, Chief engineer and Mr. *V. K. Agarwal*, Director engineering, Doordarshan Directorate, New Delhi, for providing me an opportunity to study at this esteemed Institution.

Rehan Ahmad Warsi
Assistant Director Engineering
Doordarshan Directorate
New Delhi - 110 001

***Dedicated
To
My Brother
Imran***

Contents

List of Figures	v
1 Introduction	1
1.1 Introduction	1
1.2 Synchronization in Spread Spectrum System	3
1.3 The Acquisition problem	4
1.4 Aim of thesis	5
1.5 Thesis preview	7
2 PN Code Synchronization in Direct Sequence Spread Spectrum Receivers	8
2.1 Introduction	8
2.2 Literature survey	8
2.3 Spreading codes	11
2.3.1 Maximal length (m) sequences	13
2.3.2 Rapid acquisition sequences	14
2.4 Coarse synchronization in direct sequence SS systems	16
2.4.1 Serial search fixed integration time single dwell acquisition scheme	17
2.4.2 Multiple dwell acquisition scheme	19
2.4.3 Sequential estimation method	20
2.4.4 Sequential probability ratio testing	20
2.4.5 Matched filter approach	23
2.5 Fine synchronization in direct sequence SS systems	24
2.5.1 The delay locked loop	25
2.5.2 The Tau Dither loop	26
3 The Single Dwell Serial Search PN Acquisition System in Low SNR CDMA Systems	28
3.1 Introduction	28
3.2 Recirculation principle	29

3 3	Adaptive CFAR approach	30
3 4	Adaptive CFAR vs fixed threshold approach	31
3 5	Improved Serial search hypothesis testing model for low SNR CDMA systems	32
3 5 1	Probability density function of decision variable	34
3 6	Evaluation of detection and false alarm probability in terms of PN acquisition parameters	38
3 6 1	Unfaded signal in AWGN Fixed Threshold method	39
3 6 2	Unfaded signal in AWGN Adaptive Threshold method	40
3 6 3	Nakagami m faded signal in AWGN Adaptive threshold method	41
3 7	Signal flow graph based analysis	41
3 7 1	Serial search acquisition parameters in the absence of code doppler	42
4	Results and Discussions	47
4 1	Fixed threshold detection performance	47
4 1 1	Detection performance for unfaded signal in AWGN	47
4 2	Adaptive threshold detection performance	48
4 2 1	Detection performance for unfaded signal in AWGN	49
4 2 2	Detection performance for Nakagami m faded signal in AWGN	54
4 3	Acquisition time performance Fixed threshold method	54
4 4	Acquisition time performance Adaptive threshold method	55
4 5	Acquisition time performance in Nakagami m fading environment Adaptive threshold method	56
5	Conclusions and Suggestions for Further Work	64
5 1	Scope for further work	64
	References	66
	Appendices	69
A	Derivation of Acquisition Time Parameters	70
A 1	Mean acquisition time for serial search	70
A 2	Variance of acquisition time for serial search	71
B	Probability Density Function of Decision Variable	72
B 1	Pdf of decision variable for no post detection integration case Unfaded signal in AWGN	72

B 2	Pdf of decision variable for post detection integration case	Unfaded signal in AWGN	73
B 3	Pdf of decision variable for post detection integration case	Nakagami m faded signal in AWGN	76
C	Evaluation of Detection Probabilities P_{FA} and P_D		78
C 1	Unfaded signal in AWGN	Fixed threshold case	78
C 1 1	Probability of false alarm for post detection case		78
C 1 2	Probability of false alarm for no post detection integration case		79
C 1 3	Probability of detection for post detection integration case		79
C 1 4	Probability of detection for no post detection integration		80
C 2	Unfaded signal in AWGN	Adaptive threshold case	80
C 2 1	Probability of false alarm for post detection integration case		80
C 2 2	Probability of false alarm for no post detection integration case		81
C 2 3	Probability of detection for post detection integration case		81
C 2 4	Probability of detection for no post detection integration case		82
C 3	Nakagami m faded signal in AWGN	Adaptive threshold case	82
C 4	Rayleigh faded signal in AWGN	Adaptive threshold case	84

List of Figures

1 1	(a) A simple direct sequence spread spectrum transmitter (b) Receiver [3]	2
2 1	Structure of detectors for code acquisition [20]	9
2 2	Classification of acquisition schemes [6]	12
2 3	(a) Auto correlation function of a m-sequence (b) Power spectral density of m-sequence	14
2 4	A simple direct sequence modulator	16
2 5	Single dwell serial search PN acquisition system [6]	18
2 6	Multiple (N) dwell PN acquisition system [6]	19
2 7	A rapid acquisition by sequential estimation (RASE) technique	21
2 8	Sequential probability testing block diagram	22
2 9	(a) Low pass version of matched filter acquisition (b) A digital correlator implementation of matched filter	24
2 10	(a) A non-coherent delay lock loop (DLL) (b) Error signal and auto correlations for $\Delta = T_c$	25
2 11	A Tau Dither Loop for PN code tracking	27
3 1	(a) Accumulator recirculation loop (b) correlation pulses at the output of correlator	30
3 2	Recirculation loop output with $q = 2L$, $L = 127$ and recirculation delay $T_p = 254LT$	31
3 3	A CA-CFAR based decision processor	32
3 4	Code acquisition loop employing recirculation principle and adaptive decision processor	33
3 5	Decision process signal flow graph for serial search code acquisition system of Fig 3 4	46
4 1	Probability of false alarm P_{FA} vs normalized threshold level η^*	48
4 2	Detection probability vs SNR for three retrace cycles	49

4 3	Detection probability improvement factor vs SNR for four retrace cycles	50
4 4	Detection probability improvement factor vs SNR for four retrace cycles	51
4 5	False alarm probability vs threshold coefficient for $N_B = 4$ and $N_B = 6$	51
4 6	False alarm probability vs threshold coefficient for $N_B = 8$ and $N_B = 16$	52
4 7	Detection probability vs SNR for $P_{FA} = 0.1$, $N_B = 4$ and $M = 4, 8$ Adaptive threshold method	52
4 8	Detection probability vs SNR for $P_{FA} = 0.01$, $N_B = 4$ and $M = 4, 8$ Adaptive threshold method	53
4 9	Detection probability vs SNR for $P_{FA} = 0.01$, $N_B = 6$ and $M = 6$ Adaptive threshold method	53
4 10	pdf of decision variable Z^* for Nakagami-m faded received signal	57
4 11	Detection probability vs SNR for Nakagami m faded received signal	58
4 12	Improvement in mean acquisition time Fixed threshold method	59
4 13	Improvement in variance of acquisition time Fixed threshold method	60
4 14	Improvement in mean acquisition time Adaptive threshold method	61
4 15	Improvement in variance of acquisition time Adaptive Threshold method	62
4 16	Improvement in Mean of the acquisition time Nakagami-m faded received signal using adaptive threshold method	63
4 17	Improvement in variance of the acquisition time Nakagami-m faded received signal using adaptive threshold method	63

Chapter 1

Introduction

1.1 Introduction

A Spread Spectrum (SS) system produces a signal whose energy is distributed over a bandwidth much wider than the message bandwidth. As such it is characterized by a bandwidth expansion factor N defined as the ratio of bandwidth required to transmit a SS signal (W) to the message signal bandwidth (B) i.e.

$$N \triangleq \frac{W}{B} \quad (1.1)$$

The most commonly discussed spread spectrum systems are Direct Sequence (DS) and Frequency Hopping (FH) [2, 4, 6–9]. Less commonly discussed are chip and time hopping [9]. Additionally these techniques can be combined to present a hybrid system which combines the attractive features of individual techniques. Of the number of possible techniques, we restrict our attention to Direct Sequence Spread Spectrum (DS-SS).

Figure 1.1(a) is a simplified block diagram of a DS-SS transmitter [3]. The baseband data waveform is first converted into the binary signal. The resulting *symbol* rate is denoted as $\frac{1}{T}$. The next operation is multiplication with the binary pseudorandom (PN) sequence whose *chip* rate is denoted as $\frac{1}{T_c}$. The PN code chip rate is chosen much faster than the symbol rate so that $T_s = NT_c$. As illustrated in Fig 1.1(a) the effect of this operation is to “spread” the bandwidth of the waveform by a factor N which for the same signal power causes the spectral density of waveform to be quite low and *noise* like. The signal power as indicated in Fig 1.1(b) is reduced by a factor of $\frac{1}{N}$ from its level without spreading.

At the receiver, “despreading” (multiplication by the same binary antipodal spread

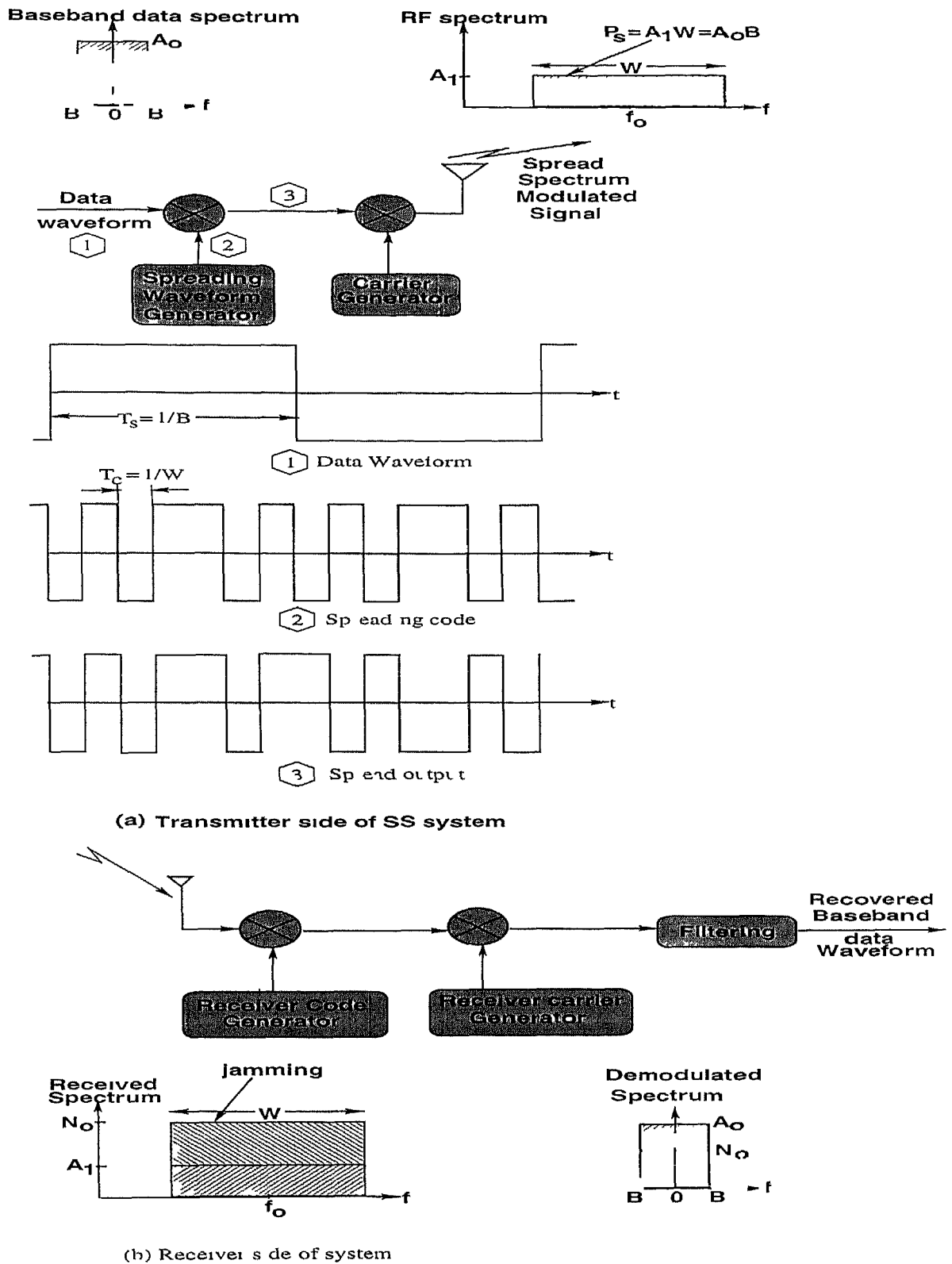


Figure 1.1 (a) A simple direct sequence spread spectrum transmitter (b) Receiver [3]

ing waveform as at the transmitter) is performed first and then removal of the carrier modulation is done to restore the original base band data waveform allowing the receiver to filter out a large part of wide band interference. Assuming as in Fig 1.1(b) the receiver front end filter admits the W hertz wide desired signal. The interference or jamming within this bandwidth (BW) will also be admitted by the receiver. However level of interference (denoted as \mathcal{N}_0 in Fig 1.1(b)) can be considerably larger than the received signal (denoted as A_1), implying an RF signal to noise ratio $(SNR)_{RF} = \frac{A_1}{\mathcal{N}_0} < 1$. But after despreading the bandwidth of desired signal is reduced to its original value B while the bandwidth of the interference remains W . Thus filtering to the signal bandwidth can be used to eliminate interference power resulting in the base band data SNR

$$(SNR)_{baseband} = \frac{A_0 B}{\mathcal{N}_0 B} = N \frac{A_1}{\mathcal{N}_0} = \frac{W}{B} (SNR)_{RF} \quad (1.2)$$

Therefore DS-SS is a method of using a periodic PN code to generate a large BW signal having considerably low power spectral density (PSD) as compared to conventional systems. Unlike most other signalling schemes or communication systems which are typically bandwidth limited, spread spectrum is converse.

Historically DS-SS has its roots in the military arena where desirable communications require Jammer resistance, Low Probability of Intercept (LPI) and Low Probability of Detection (LPD) and Low Probability of Exploitation (LPE) as discussed in [7, 8, 9]. However DS-SS has gained interest in civilian communications community as the basis of the multiple access scheme known as Code Division Multiple Access (CDMA). A well known commercial system is **IS-95** (originally designed by Qualcomm). Many chip sets are being developed in support of CDMA not only by Qualcomm but also Stanford Technologies and Loral (paramox) [35].

1.2 Synchronization in Spread Spectrum System

In a typical spread spectrum system, any meaningful transmitted information can be extracted from the received signal if

- Code at the receiver is accurately aligned with the spreading code contained in the received signal i.e., the two codes must have identical chips and their edges (timing) must precisely coincide
- The transmitted and receiver carrier are accurately aligned

If the two codes are out of alignment by as little as one chip, insufficient signal energy will reach the receiver data demodulator for reliable data recovery. The process of precisely aligning the two codes is termed as *Code Synchronization* [1, 2]. It plays a cardinal role in the proper functioning of any spread spectrum system. The process of code synchronization is performed in two steps, namely **code acquisition** and **code tracking**. *Code acquisition* is a process of successive decisions wherein the ultimate goal is to bring the two codes into coarse time alignment within one code chip interval. After this condition is detected and verified, the tracking system is activated. *Tracking*, also called **fine synchronization**, is the operation by which synchronization errors are further reduced or at least maintained within certain bounds [9, 20]. Coupled with the code synchronization issue is the synchronization of transmitted carrier with that of receiver carrier. The code and carrier synchronization are inter linked and one can not be achieved without the help of other. Therefore, following steps are involved for achieving the two synchronizations.

- 1 Coarse carrier frequency estimation to get an idea of nominal carrier frequency in use
- 2 PN code acquisition
- 3 PN code tracking
- 4 Coarse carrier phase estimation
- 5 Fine alignment of carrier frequency and phase

Thus, PN sequence timing can be acquired and tracked accurately and hence spreading can be removed without the knowledge of carrier phase and with only rough estimate of carrier frequency. Once code timings has been acquired, carrier phase and frequency can be accurately estimated using the conventional phase locked loop techniques in the same way as for any digital communication system [1].

This thesis deals with the first part of code synchronization namely ‘*Code Acquisition*’

1.3 The Acquisition problem

In a DS-SS systems, the complexity and random nature of initial code acquisition process is due to a number of factors such as 1) initial uncertainty about code phase offset

- 2) channel distortion (e.g. fading channels) and additive interference (intentional or unintentional)
- 3) unknown carrier phase and possibly carrier frequency offset (Doppler)
- 4) front end receiver additive white Gaussian noise (AWGN)

The set of design parameters for the acquisition procedure include threshold settings, correlation time i.e. number of test per code chip and system complexity as manifested by the choice of search strategy, verification logic etc. Also implicit is the knowledge of important parameters such as design SNR, code rate, code length, code uncertainty region etc. As a result of the above factors, *the time to acquire the code* also called **acquisition time** (T_{acq}) is a random variable and its complete statistical description requires probability distribution function. Although the problem of determining the distribution function of acquisition time can be solved in principle, it is very difficult to obtain in practice, at least in closed form. However, as pointed out in [2, 6, 20], the first two moments, namely **mean acquisition time** \bar{T}_{acq} and **variance** of acquisition time σ_{acq}^2 provide sufficiently accurate statistical description for most practical purposes.

1.4 Aim of thesis

The code acquisition problem in spread spectrum systems has attracted considerable research in recent past [15, 16, 17, 18, 20]. As shown in fig. 2.2, a number of viable search strategies are possible for code acquisition. Prominent among those are *maximum likelihood* (ML) approach, whose parallel implementation complexity is prohibitive. However, a less complex serial version for ML approach is possible, in which a decision can be made only after examining the outcome of each code phase. On the other hand, low SNR environments are characterized by strong interfering signals, deep noise, Doppler effect and rapid fading etc. therefore, multiple examination of each code phase in serial version of ML approach can not be ruled out [20]. Sequential approaches are coherent in nature and have lower implementation complexity than ML method. Their merits strongly depends on the accuracy of the initial estimates of code phase, which reduces quite rapidly with decreasing SNR and therefore, not well suited in typical low SNR environments [6]. The serial search approach, on the other hand, is characterized by its simplicity, reliability, strong interference rejection capability in hostile environment, ability to accommodate long PN sequences and low hardware requirements. Because of its attractive features, the majority of research work on PN code acquisition revolves around the serial search strategy.

Recently [15] has proposed a very attractive serial search strategy for low SNR

CDMA systems based on the recirculation loop principle in which the main reason for low SNR was cited as considerable code Doppler and received signal was assumed to be unfaded. The analytical frame work of [15] was pure probabilistic which except for the cases can not be generalized. The dynamic SNR range considered there was not sufficiently wide from spread spectrum point of view and in that range another method namely sequential estimation has better performance in terms of code acquisition parameters. Moreover to improve the detection of correct code phase the constant false alarm probability approach was utilized using a complex Adaptive Decision Threshold Level Control (ADTLC) [17]. As such the work of [15] has left many open issues which require careful addressing. Some of these issues forms the basis of work embodied in this thesis with the aim to modify the scheme of [15] on two fronts

1. The addition of post detection integration feature to widen the dynamic SNR range so that relatively simple hardware could be used for code acquisition
2. Modification in decision circuitry to achieve the constant false alarm probability by introducing Cell Averaging Constant False Alarm Rate (CA-CFAR) approach which requires relatively low hardware as compared to ADTLC method

These modification will introduce several new issues and some of them will be analyzed in this work. In particular, our attention will be on

- To provide an analytical frame work for unfaded received signal for the modified serial search strategy from detection point of view
- To perform the analysis of modified serial search strategy for low SNR operation. Here the case of low SNR due to rapid fading is chosen. For analytical frame work the Nakagami m fading model is used which is better suited for modeling of urban multi path radio channels [32]
- Use of more powerful and versatile signal flow graph based approach will be made to derive the general form of various acquisition parameters
- Finally, the issue of how much improvement the modified scheme can provide over the known serial search scheme including the one presented in [15], for important acquisition parameters in faded and unfaded environment will be considered

To summarize, *the main motivation for this work is to find new serial search algorithms suitable for all digital receiver implementation and operation at low signal to noise ratios*

1.5 Thesis preview

In chapter 2 a review of code alignment methods is presented. In chapter 3 the modifications to serial search scheme is carried out and analyzed from detection and code acquisition point of view. The unfaded and Nakagami m faded signal case is considered separately. The detection and false alarm probability expressions for the two cases have been derived. Finally using the signal flow graph approach the important acquisition parameters are derived. The detailed derivation involved in each of the above case is not included in the main body of chapter 3 rather they are provided in the appendices. In chapter 4 some of the numerical results are presented and discussed. Finally in chapter 5 scope for further investigations alongwith concluding remarks are presented.

Chapter 2

PN Code Synchronization in Direct Sequence Spread Spectrum Receivers

2.1 Introduction

This chapter examines the following areas which influence synchronization of DS-SS systems: spreading codes, coarse synchronization and fine synchronization. Spreading codes are the higher rate binary sequence of symbols which are used to spread the data sequence. Coarse synchronization or '*Acquisition*' and fine synchronization or '*Tracking*' together complete the synchronization process of received and locally generated PN code. During coarse synchronization the most important issue is usually the minimization of acquisition time, while SNR maximization and hence minimization of bit error (BER) is the issue of concern during the fine synchronization.

2.2 Literature survey

If one searches through the available PN code acquisition literature, the common denominator found among almost all the methods is that received and local PN signals are first multiplied to produce a measure of correlation between the two. This correlation measure is then processed by a suitable detector/decision rule and search strategy to decide whether the two codes are in synchronism and what to do if they are not. The difference between the various schemes depends on

- Type of detector and decision strategy used
- The nature of search algorithm which acts on the detector output to reach on the final decision of code phase acquired or not

All known detector for PN acquisition systems fall into two basic categories namely *coherent* and *non coherent*. By far the most common found in acquisition systems for DS-SS receivers is the non coherent detector which for example might be comprised of a band pass filter centered at the frequency of received carrier upon which the PN signal is directly modulated followed by a square law envelope detector, an integrate and dump circuit and a simple threshold device [34].

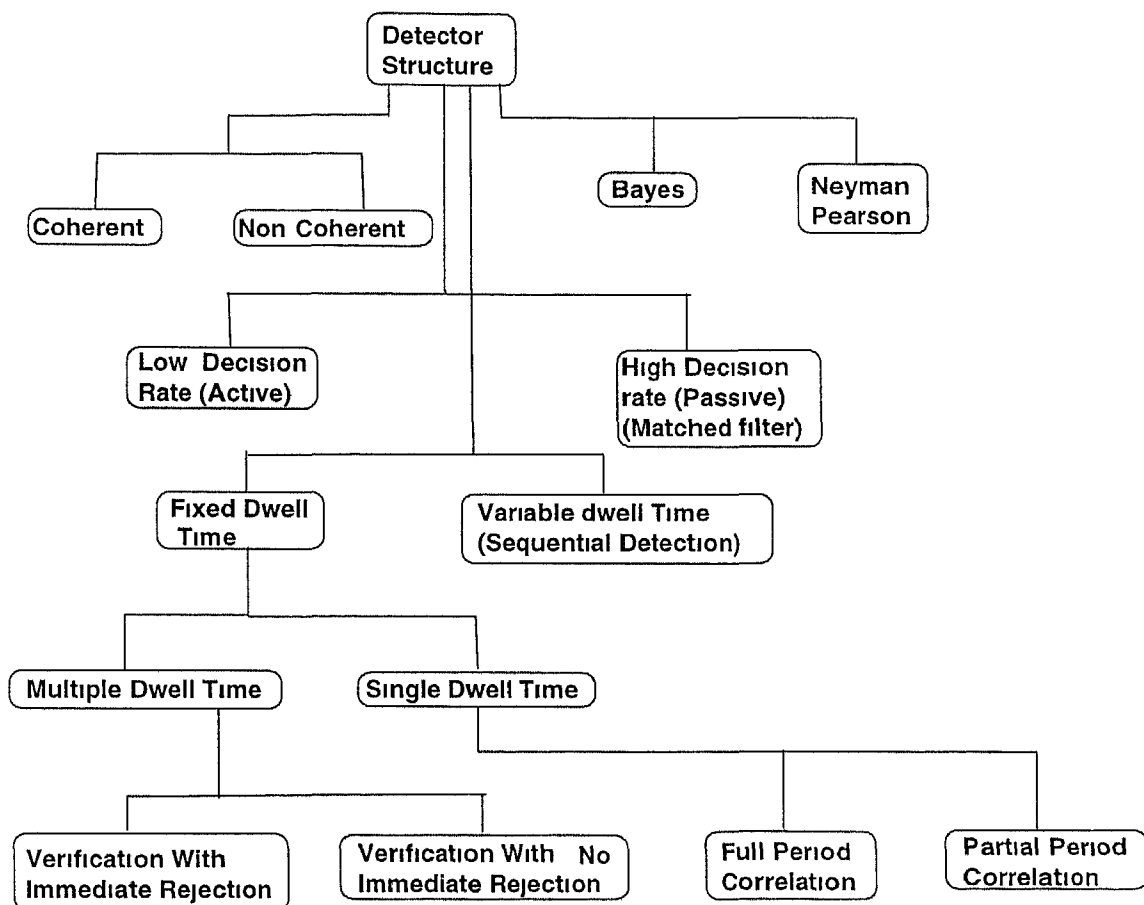


Figure 2.1 Structure of detectors for code acquisition [20]

Consideration has also been given in the literature to PN acquisition systems which employs a coherent detector, typically implemented as an integrate and-dump circuit followed by an optimum *Bayes* detector [6] or instead just a simple threshold device [25]. The inherent assumption here is that receiver is capable of determining good estimates of carrier phase and frequency offsets.

Further classification of detector is based on the type of integration time. It may be *fixed* or *variable*. Under the category of fixed integration time another subdivision is possible namely *single dwell time* [23–34] and *multiple dwell time* detector [22]. The operation of former is based on single fixed time observation of received signal plus noise while latter considers multiple such observations. Depending upon the duration of observation or equivalently the time allotted to make a decision relative to the PN code period, single dwell time detectors can be further differentiated according to whether they utilize the full period or partial period code correlation. The multiple dwell detectors differ from one another in the way in which the additional observations are used to *verify* the temporary decision made based on the first observation alone.

Finally the categories of variable integration time is reserved for those cases where the dwell time (*time for continuously integrated stochastic process to exceed a threshold*) is a random variable. Typically they employ the classical method of *sequential detection* [2–4].

The next classification of detector structure is in accordance with the rate at which the decisions are made on each code phase position under test. High decision rate detectors, such as used in *matched filter* (passive correlation) PN acquisition systems [6, 21], refer to those structures that make their decisions at a PN code chip rate or integer multiple of it. Low decision rate detectors which employ active correlation make decisions at a rate significantly slower than code chip rate.

To complete the detector classification further categorization is based upon the criterion used for deciding between in sync or out of sync hypotheses e.g. *Bayes*, *Neyman Pearson* and *Minimax* criterion.

A summary of above classification of detector structures used for PN code acquisition is illustrated in Fig 2.1.

The remaining aspect of the acquisition process is the search strategy by which one denotes the particular procedure adopted by the receiver in its search through the uncertainty region. Not unlike the classification of detector types the classification of acquisition scheme according to search strategy follows a tree structure [20] as shown in Fig 2.2. Conceptually the simplest of search techniques on the first level of the hierarchy is the *maximum likelihood* algorithm. It requires that received PN signal is correlated with all possible code positions of local PN code replica. The correct PN alignment is chosen as that local code phase position which produces the maximum detector output.

Another scheme is based on a sequential estimation of the shift register states of PN generator typical example is RASE (Rapid Acquisition by Sequential Estimation) technique first introduced by Ward [25]. In this technique the best estimate of first n chips of received PN code is loaded in the n stage local PN code generator thus defining a particular initial condition from which the generator begins its operation. The success of this scheme depends on the accuracy of initial estimate.

The serial synchronization of PN sequence was first introduced by Sage [24]. In its original version a serial search was performed by *linearly* varying the time difference between the PN modulation on the incoming carrier and the PN waveform generated at the receiver with a continuous decision process determining when synchronization is achieved. Such a system is also called *sliding correlator* [4]. Sweeping through the time uncertainty region can also be done in discrete steps where the time uncertainty region has been *quantized* into a finite number of elements called *cells* through which the receiver is stepped. Which particular search strategy is selected by the receiver is dependent on the nature of uncertainty region, available prior information, statistical quality of the tests performed, availability of stepping and rewinding mechanisms. A multitude of such search algorithm is shown in Fig 2.2. If the uncertainty region covers the whole code period a straight line search would be appropriate [19–24]. On the other hand prior information is sometimes available which suggests the use of more sophisticated strategies (*Z search* or *Expanding window search*) for better results [19]. Finally it may be noted all the above serial search techniques base their decisions on the likelihood ratios and thus, are fundamentally different from sequential estimation techniques [25, 26] whose merits decreases with the decreasing SNR.

2.3 Spreading codes

Direct Sequence (DS) systems require a pseudo random noise (sequence) generator at transmitter and receiver. The desirable properties for the spreading codes of a single transmitter and receiver pair are

- An impulse like auto correlation function (or equivalently a flat power spectral density) so that when spreading and despreading codes are not aligned a non zero correlation result which has numerous implications
 1. The larger the ratio of peak to side lobe of auto correlation function, the easier it is to determine the correct spreading code phase position and hence synchronize the despreading sequence with the received signal.

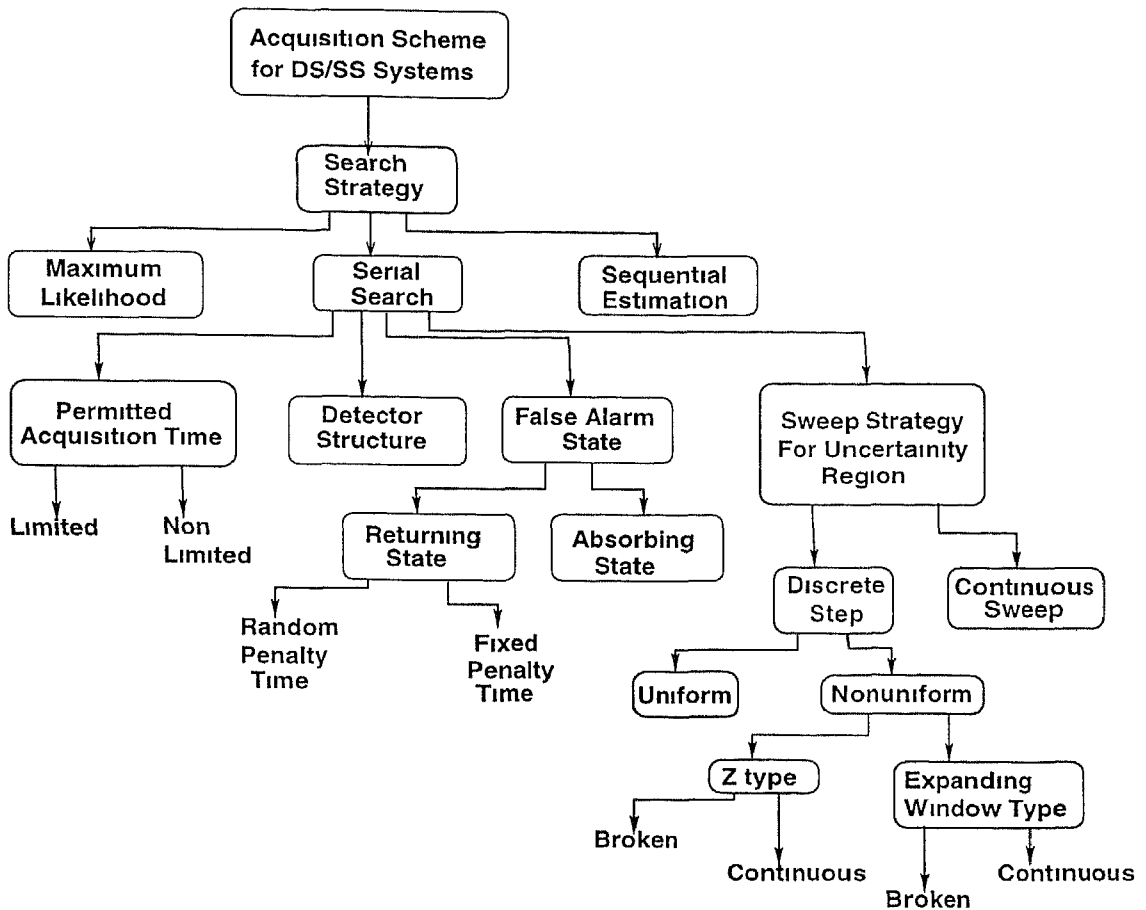


Figure 2 2 Classification of acquisition schemes [6]

- 2 Provides larger processing gain and hence better utilization of allocated spectrum leading to increased capacity
- 3 can be generated in synchronism at transmitter and receiver

The preceding properties are also desirable for multi user communications such as CDMA additional desirable properties include

- One spreading code per CDMA user i.e. sufficient number of spreading code for all users
- Orthogonality between spreading codes of different users so that the extraction of desired user's signal could be accomplished from multiple access interference (MAI)

Some of the spreading codes are Maximal Length (m) Sequences, Gold codes [29] Rapid Acquisition codes [5-28]

2.3.1 Maximal length (m) sequences

Traditionally the maximal length (m) sequences are attractive because they can be generated via a Linear Feedback Shift Register (LFSR). The length and hence also repetition period of an m sequence constructed from an n stage shift register is

$$L = 2^n - 1 \quad (2.1)$$

Maximal length sequences have a good balance of 1's and 0's and when mapped to an antipodal signalling scheme have a two valued normalized periodic auto correlation function $\theta_p(k)$ given by

$$\theta_p(k) = \begin{cases} 1 & k = lL \\ -\frac{1}{L} & k \neq lL \end{cases} \quad (2.2)$$

where l is any integer and L is the sequence period. Therefore over the interval $|\tau| \leq \frac{LT}{2}$ the auto correlation of maximal length sequence is given as

$$R_p(\tau) = \begin{cases} 1 - \left(\frac{L+1}{L} \frac{|\tau|}{T} \right) & |\tau| \leq T_c \\ -\frac{1}{L} & |\tau| > T_c \end{cases} \quad (2.3)$$

and the power spectral density (PSD) is given as [9]

$$S_p(f) = \frac{L+1}{L^2} \sum_{\substack{i = -\infty \\ i \neq 0}}^{\infty} \text{sinc}^2\left(\frac{1}{L}\right) \delta\left(f - \frac{i}{LT}\right) + \frac{1}{L^2} \delta(f) \quad (2.4)$$

The two functions are plotted in Fig 2.3(a) and (b). The PSD function consists of delta functions separated by $\frac{1}{LT}$.

As pointed out earlier the more impulse like the auto correlation function of a sequence the more preferable it is. However, the undesirable property of m sequence for DS-SS application is *cross correlation between the m sequences can be high* affecting multiuser separation and code synchronization. Another undesirable property of m sequence is that they are inherently susceptible to mathematical cryptanalysis. Thus if message security is desired when m sequence is used for spreading, the data symbols must be enciphered before they are combined with pseudo noise (PN)¹ sequence [9].

The poor cross correlation deficiency of m sequence is removed in another family of codes called **Gold codes**. A Gold code is constructed by the modulo 2 addition of specific cyclic permutations of a preferred pair of m sequences. The period of any code in the set of gold codes is L , where L is given by (2.1). The improvement in

¹In literature the term m sequence and PN sequence are used interchangeably

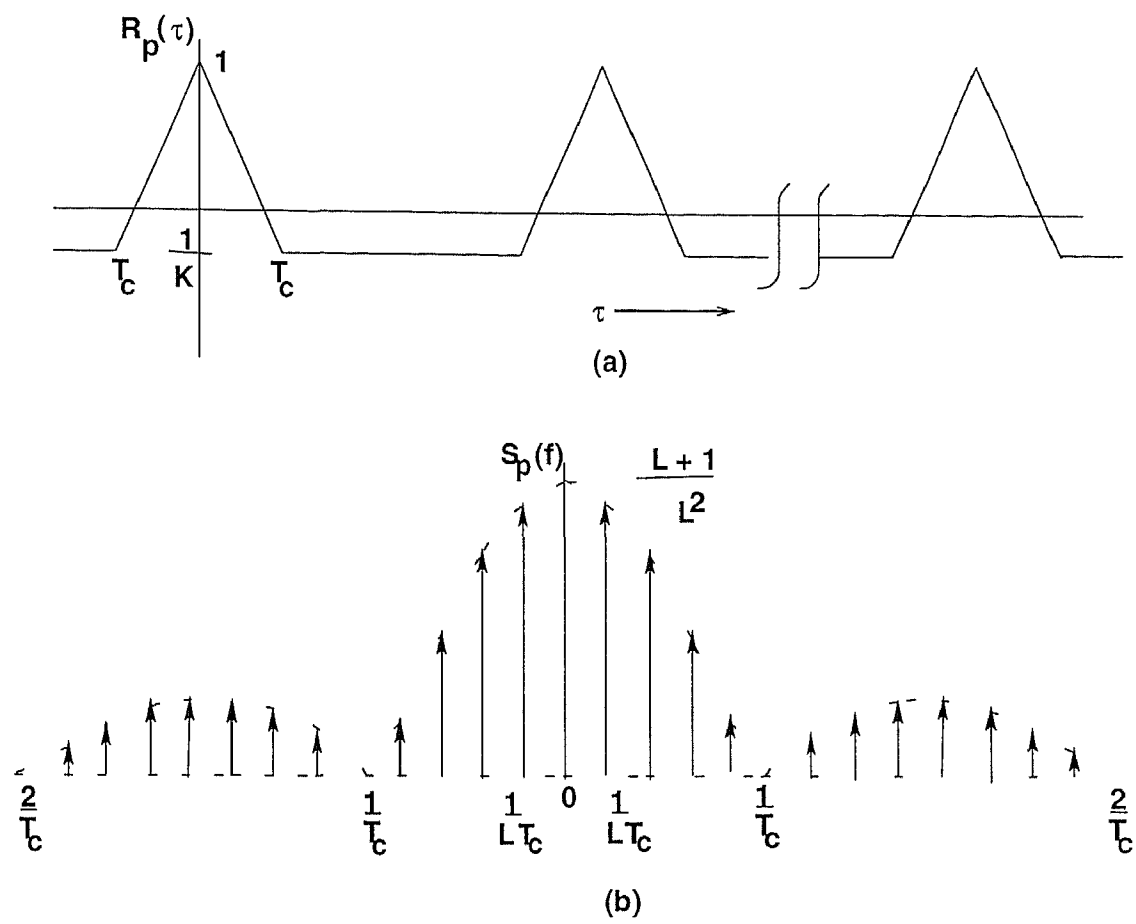


Figure 2.3 (a) Auto correlation function of a m sequence (b) Power spectral density of m sequence

cross correlation between the gold codes in a set, simple construct on of the generators and abundance makes gold codes attractive for multiuser communications. The auto correlation however is no longer as attractive as that of m sequences and consequently the acquisition process can suffer. Gold codes and their properties are considered in more detail in [29].

2.3.2 Rapid acquisition sequences

The problem of rapid code acquisition has received considerable attention. Stiffler [28] investigated the possibility of designing codes which have rapid acquisition properties. The principle of operation was that a correlation is performed and depending upon the correlation value, if another correlation is required the uncertainty region of the code is halved. Thus the average number of correlation to achieve the acquisition is reduced to $\log_2 L$ from $\frac{L}{2}$, although the correlation time for each step of acquisition process is longer than that required in a conventional system.

Suppose that the received spreading code phase uncertainty is equivalent to no longer than L chips i.e. time uncertainty region between received and local code is $\left[-\frac{LT_c}{2}, +\frac{LT_c}{2}\right]$ where T_c is code chip interval. Thus to avoid any ambiguity an acquisition code which is minimum of L chips long is required. If L is not a power of 2 choose a code length which is smallest power of 2 greater than L . Let $n = \log_2 L$ and construct a binary n -tuples

$$b_j = (\sigma_j^1, \sigma_j^2, \sigma_j^3, \dots, \sigma_j^n) \quad j = 1, 2, 3, \dots, I \quad (2.5)$$

where $\sigma_j^k = \pm 1$ such that

$$\sum_{i=1}^n \left(\frac{1 - \sigma_j^i}{2} \right) 2^{j-1} = j - 1 \quad (2.6)$$

These n -tuples are binary representations of number 0 through $L-1$ with MSB placed on the right. Given these vectors the *rapid acquisition sequence* is

$$\chi = (\xi_1, \xi_2, \xi_3, \dots, \xi_L) \quad (2.7)$$

where

$$\xi_j = \begin{cases} 1 & \text{if } \sum_{i=1}^n \sigma_j^i \geq 0 \\ -1 & \text{if } \sum_{i=1}^n \sigma_j^i < 0 \end{cases} \quad (2.8)$$

The sequence χ is transmitted periodically and the sequences which the receiver correlates with the received sequence are

$$s_i = (\sigma^1, \sigma^2, \sigma^3, \dots, \sigma^L) \quad i = 1, 2, 3, \dots, n \quad (2.9)$$

These sequences are simply the transpose of columns of a $(L \times n)$ matrix whose rows are b_j . In addition to high cross correlation between χ and s_i , the cross correlation for all s_i , $i = 1, 2, 3, \dots, n$ are equal and is given as

$$\rho = \begin{cases} \frac{1}{2^{n-1}} \binom{n-1}{\frac{n-1}{2}} & \text{for } n \text{ odd} \\ \frac{1}{2} \binom{n}{\frac{n}{2}} & \text{for } n \text{ even} \end{cases} \quad (2.10)$$

In spite of longer integration time for each binary decision, significant acquisition time improvement can be achieved with these codes. The price paid is *reduced jamming resistance* and *increased detectability* for the spread spectrum system. Both of these factors are the result of additional structure (i.e., decreased randomness) of the code.

2.4 Coarse synchronization in direct sequence SS systems

A spread spectrum receiver must generate a pseudo noise sequence that is synchronized with the received sequence—that is, the corresponding chips must precisely coincide. As shown in Fig. 2.3(a) the auto correlation function (ACF) of a PN sequence is a narrow triangular pulse of width two chips. Any misalignment causes the signal amplitude at demodulator output to fall in accordance with the auto correlation function. As such, the accurate synchronization is one of the most important functional requirement for any spread spectrum system. In an hostile environment, an acquisition system with the following feature is desired [9]

- Because successful jamming during acquisition completely disables a communication system, the acquisition system must have a strong interference rejection capability.
- The PN sequence used for acquisition system must be programmable and sufficiently long for security.
- The acquisition should be rapid so that a jammer must operate continuously during acquisition. Continuous operation reduces the amount of jamming power that can be produced.

Refer to Fig. 2.4 for a better understanding of coarse acquisition process in DS-SS system. If the PN sequence of receiver is synchronized with that in transmitted signal

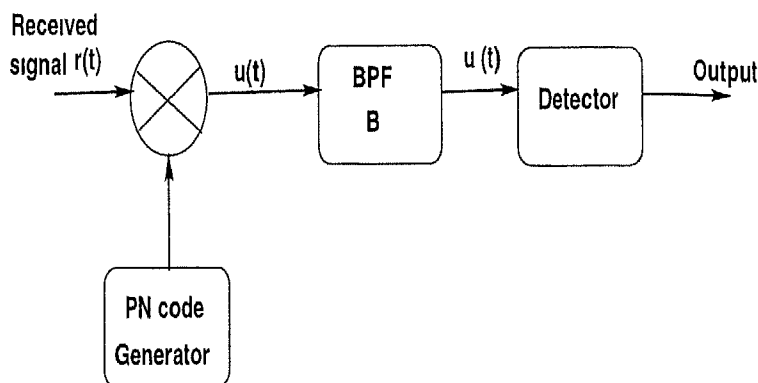


Figure 2.4 A simple direct sequence acquisition block diagram

then the received signal $r(t)$, collapses back to narrow band transmitted data stream $u(t)$. Filtering removes any remaining high frequency terms. Once the signal is

despread and passed through the filter $u(t)$ is analyzed by some detection method. However, if the received signal and locally generated PN sequence are not of the same phase, the resultant output from multiplier and then filter appears as band limited Gaussian noise. Thus, to extract any intelligible data from a spread spectrum user, the transmitter and receiver must have aligned PN codes. All methods of performing coarse synchronization involve evaluating the correlation at various delay values. Matched filter methods slide the signal past the PN code to produce the correlation $R(\tau)$ for all delays τ and wait for a peak to indicate the correct code phase. Other methods start with a guess τ_0 as to the correct delay, evaluate $R(\tau_0)$ for a possible windowed version of the code, see if it exceeds the threshold(s), and upon failure guess another delay estimate τ_0 accordingly.

For coarse acquisition of a length L periodically repeating spreading code to a resolution of $1/q^{th}$ of a chip, there are qL possible offsets between the transmit and receive spreading codes. The goal of any coarse acquisition procedure is to reduce the uncertainty regarding the actual offset value as quickly as possible subject to the constraints on the available processing power. An important research area within coarse acquisition is to determine the search strategies for searching the remaining uncertainty region [20]. That is, when a SS signal is received there is an associated uncertainty (or uncertainty region) for the locally generated PN code. A trial code phase is tested and if it is accepted code tracking (fine PN code synchronization) is invoked. If the code phase under test fails, another phase is tested. *Search strategies* are the process by which subsequent code phases are selected upon failure of the preceding code phase. A number of search strategies are possible depending upon the amount of available *a priori* knowledge of received code phase.

2.4.1 Serial search fixed integration time single dwell acquisition scheme

Serial search acquisition consists of a search, usually in discrete steps, of the possible time alignments of a receiver generated PN sequence relative to a received PN sequence [2–20]. The time uncertainty region is usually quantized into a finite number of search positions called *cells*. If the search *step size* is denoted by s and number of code chips in uncertainty region by N_u , then maximum number of cells q to be searched is given by $q = N_u/s$. Typically s is chosen to be $\frac{1}{2}$ so that $q = 2N$. The cells are serially tested until it is determined that a particular cell corresponds to the alignment of the two sequences to within a fraction of a chip i.e., only one out of these q cells

represents the correct code phase for acquisition. The simple model of a single dwell serial PN acquisition system is illustrated in Fig 2.5 which employs non coherent type (square law) detector. The fixed integration time detector is so named because the

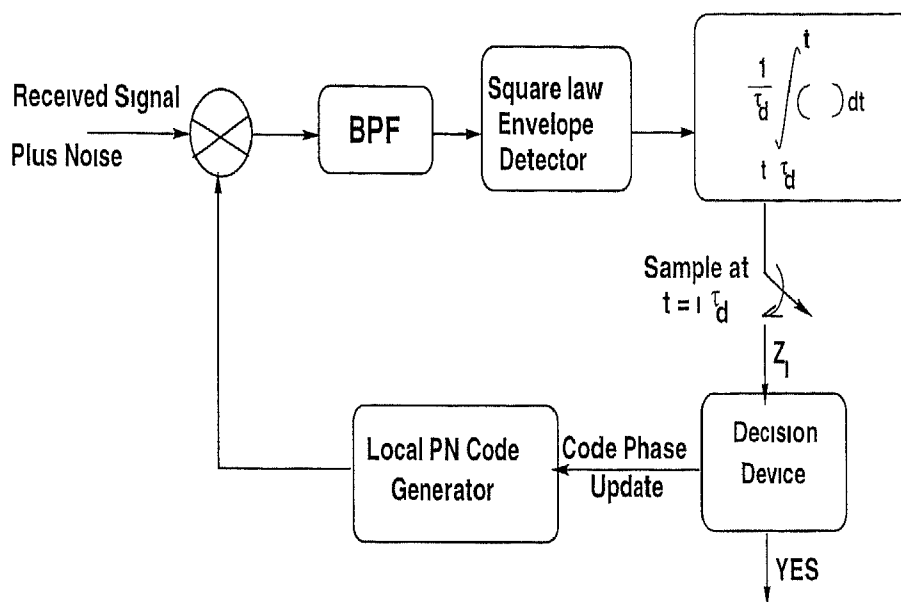


Figure 2.5 Single dwell serial search PN acquisition system [6]

integration period (correlation period) of incorrect and correct cells for this detector remains constant. The received signal plus noise is correlated with a local replica of the PN code and then passed through a band pass (pre detection) filter. The filter output is then square law envelope detected with the detector output integrated for fixed time duration τ_d (the dwell time) in an integrate and dump circuit (post detection integration) and then compared with a threshold. If the threshold is not exceeded the cell under test is rejected and phase of local sequence is advanced or retarded to test a new cell. When the threshold is exceeded search is stopped and verification is done. Once the particular cell passes the verification test control is handed over to tracking circuitry for finer alignment of the two codes [6-9]. One of the obvious disadvantages of this coarse acquisition technique is that when large uncertainty regions are involved a lot of time may be spent unnecessarily integrating the incorrect code phase cells. However it is most secure acquisition technique in hostile environment due to its extremely strong interference rejection capability [9-20]. Moreover it is best suited for low SNR spread spectrum systems when compared with other acquisition techniques [15].

2.4.2 Multiple dwell acquisition scheme

The multiple dwell detection scheme was designed to reduce the time spent in integrating the incorrect code phase cells [22]. A diagram of multiple dwell detector is shown in Fig 2.6 as taken from [6].

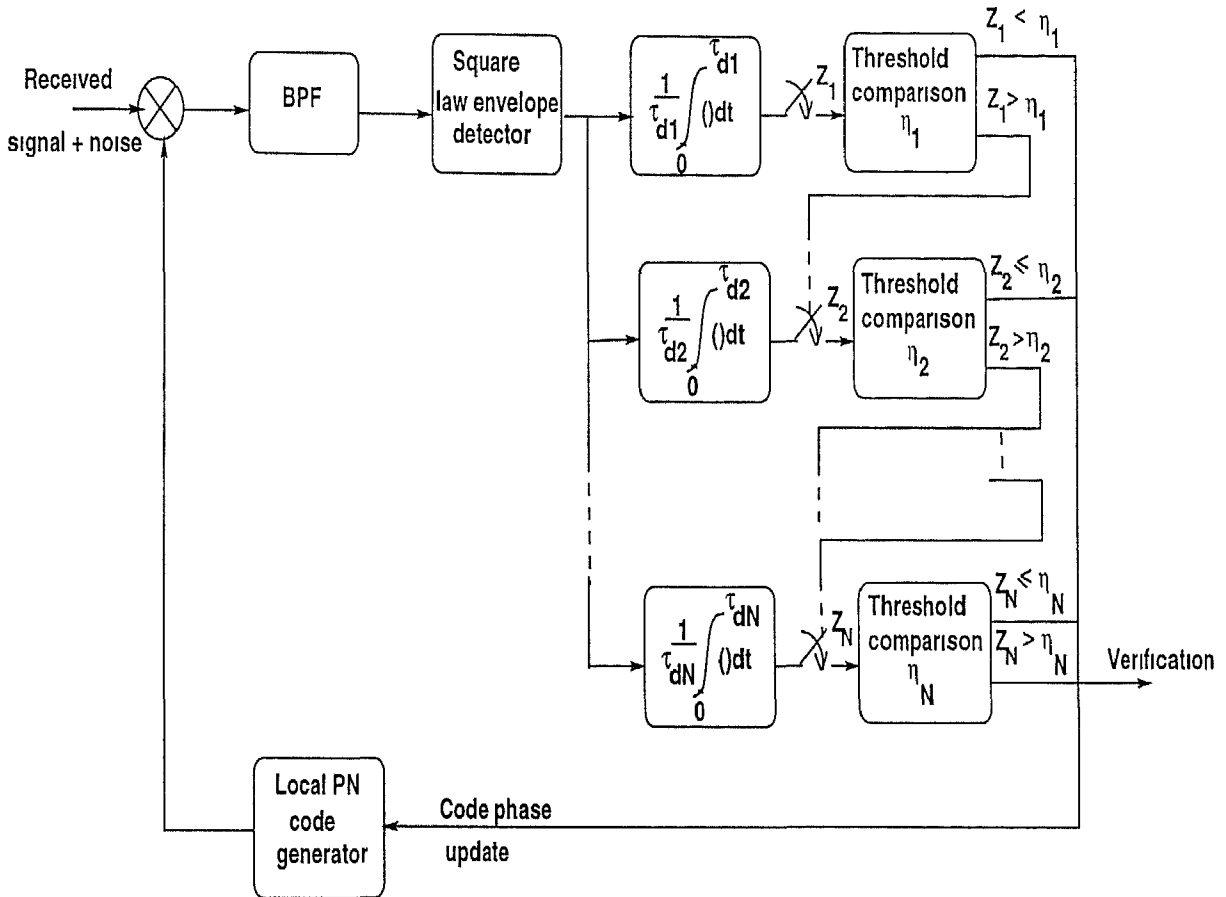


Figure 2.6 Multiple (N) dwell PN acquisition system [6]

The system begins by selecting a local code phase for evaluation multiply it with received signal plus noise. The envelope of resultant product signal is formed in a square law envelope detector. The envelope is then applied to each of the N integrators simultaneously. The integration (“dwell”) time of detectors are ordered such that

$$\tau_{d1} \leq \tau_{d2} \leq \tau_{d3} \leq \dots \leq \tau_{dN} \quad (2.11)$$

Thus all of the N integrate and dump circuits starts integration at the same time, each one dumping, however at a later time instant in view of (2.11). The search update algorithm works as follows.

The output of i^{th} integrate and dump is sampled and compared to a threshold only if all of the previous $i - 1$ integrate and dump outputs have previously exceeded their

respective thresholds. Otherwise, the first integrate and dump output to fall below its threshold causes the local code phase update and search the next cell thereby resetting all of the integrate and dump circuits. The maximum time to search a given cell is τ_{dN} while minimum time is τ_{d1} . Thus most of the cells can be dismissed after a dwell time τ_{dk} , $k \ll N$ which implies significant savings in the acquisition time as opposed to simple single dwell serial search algorithm where each cell is examined for a time equivalent to τ_{dN} .

2.4.3 Sequential estimation method

This scheme was first introduced by Ward [25, 26] and is based on a *sequential estimation* of shift register states of PN generator. In particular the RASE (Rapid Acquisition by Sequential Estimation) of Fig 2.7 makes its best estimate of first n received PN code chips (n is the number of shift register stages in the local code generator) and loads the receiver sequence generator with that estimate thus defining a particular initial condition (starting state) from which the generator begins its operation. Since a PN sequence has the property that next combination of register states depends only on the present combination of states. If all n input chips are estimated with sufficient accuracy, all the following states can be predicted based on the knowledge of only this initial condition. For this the local PN code generator is periodically loaded with new estimated n chips at a rate determined by examination period generator. When to stop the loading is determined by a threshold crossing of an in lock detector. The test statistics of the in lock detector is the cross correlation of input code with that produced by local PN generator whose shift register contents correspond to the present estimate of the input state. Once it is determined that the n detected chips provide the correct starting positions, lock detector threshold crossing inhibits further loading of PN code generator. This register is then closed within the PN tracking loop which is responsible for maintaining code phase from that time onwards. This scheme outperforms the single dwell serial search method for moderate (-10 dB) to high ($+10$ dB) input SNR [26]. However, its performance is inferior to serial search at very low SNR (i.e. below -10 dB) [6]. Despite its Rapid acquisition capability, this scheme is highly vulnerable to noise and interfering signals [30].

2.4.4 Sequential probability ratio testing

Sequential Probability Ratio Testing (SPRT) is a direct sequence acquisition method which is in some ways quite similar to the multiple dwell detector. Initially investigated

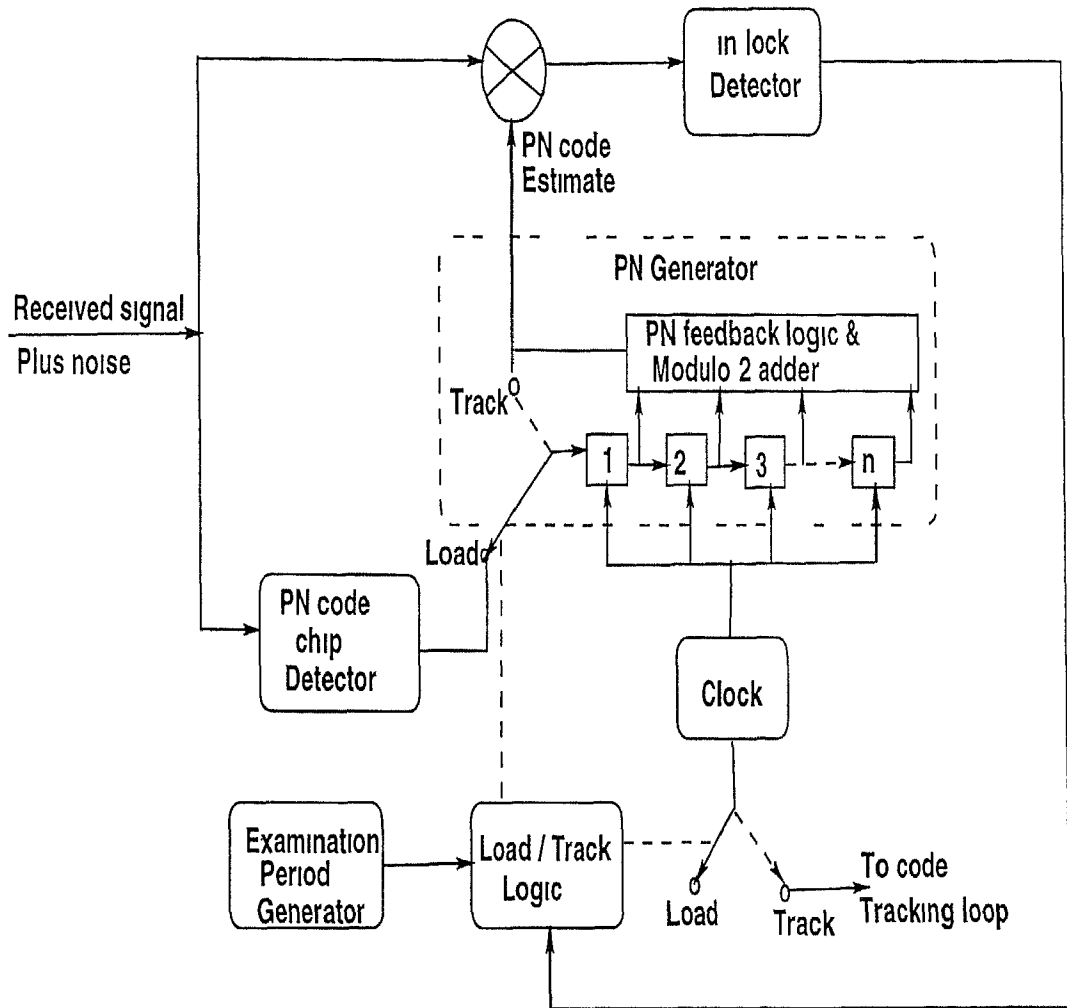


Figure 2 7 A rapid acquisition by sequential estimation (RASE) technique

by Wald [2 6] it has received considerable attention in recent years [27] Fig 2 8 depicts a block diagram of an SPRT acquisition system The difference between SPRT and other acquisition scheme lies in the decision circuitry SPRT uses a two level (A and B) threshold device whereby three possible events occur These being

- If the partial correlation is less than threshold A, declare code phase as incorrect and try a new phase and reset the integrator
- If the partial correlation is greater than Threshold $B(> A)$ then declare correct code present
- If the partial correlation falls between Threshold A and B then retain the correct code phase and integrate a little longer

The dual threshold system implements a screening test Test results which clearly show success or failure of acquisition allow a quick decision Those which are inconclusive

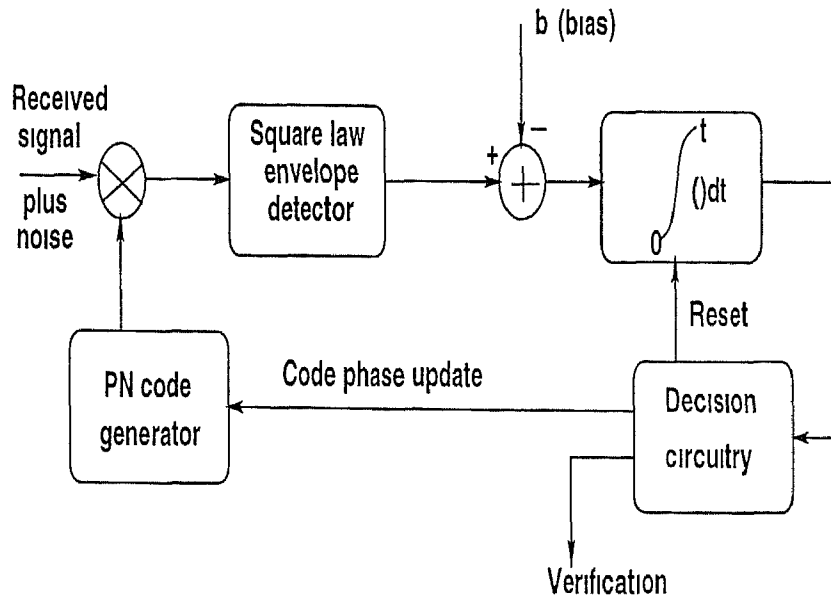


Figure 2.8 Sequential probability testing block diagram

are used to initiate further investigation in this case longer integration

As can be seen from Fig 2.8 the received sequence is correlated with the locally generated version of the PN code, product signal is square law envelope detected and a bias level is subtracted to remove any biasing effects from the squaring of noise. The residual signal is then integrated and sampled at intervals (or multiples) of chip period T_c . The sampled signal is then tested against aforementioned thresholds and appropriate decision is subsequently made. SPRT operates on the principal design philosophy of discarding false synchronization propositions quickly and accepting true ones quickly.

The system described above has many negative aspects. Firstly there are more than one threshold and a bias level from optimization point of view [6]. Secondly the typical SPRT system may suffer from the significant problem of signal remaining between threshold A and B indefinitely. The Truncated Sequential Probability Ratio Testing (TSPRT) was introduced by [27] to address this shortcoming. TSPRT essentially sets a limit on the longest correlation period and if this limit is reached a hard decision is made whether the correct code phase is acquired or not. A significant drawback of (T)SPRT is that it is difficult to analyze due to evaluation of partial correlations and the variations in integration period. Consequently mean and variance of acquisition time is best obtained via simulation [6].

2.4.5 Matched filter approach

All of the previous discussions of DS acquisition techniques incorporate a measure of correlation which was produced by an active correlation of the received signal with a locally generated PN reference code. The term active correlation is used with *multiply and integrate* type of correlation/detector structure where received signal is multiplied with the local PN code, energy detected, tested against a threshold(s) and declared as a correct or incorrect code phase. Moreover, the local PN generator is continuously running; therefore, for each successive threshold test, a completely new set of $M = \frac{T_d}{T}$ chips of received signal is used for each successive threshold test. On the other hand, matched filter based acquisition system operates on the principle of passive correlation where the input (received signal) continuously slides past a stationary replica of PN sequence. When there is a match (i.e. the two are in near synchronism), the threshold is exceeded, local PN generator is enabled and despreading can commence. If the codes do not match, the threshold is not exceeded and PN generation is not started. The main advantage of matched filter approach over the previous methods is summarized in [4-6].

The reduced synchronization time is explained by noting that the MF continuously correlates over a time interval. That is, the MF merely waits for the preselected waveform to be received.

The base band matched filter acquisition system is shown in Fig. 2.9(a). A transversal matched filter performs many more possible code phase correlations in an interval than any of the preceding methods due to its inherent parallel structure which does not require a new observation interval of received signal for each integration period. As a result, the search rate of matched filter acquisition method is considerably higher than preceding methods [1-6, 21]. The matched filters are fabricated in the following forms:

- Charge Couple Device (CCD)
- Surface Acoustic Wave (SAW) Convolvers
- Discrete Time Correlators

The last is becoming increasingly popular due to the availability of high speed Digital Signal Processors (DSPs) and flexible Field Programmable Gate Arrays (FPGAs). A digital correlator implementation of matched filter is shown in Fig. 2.9(b). Using this

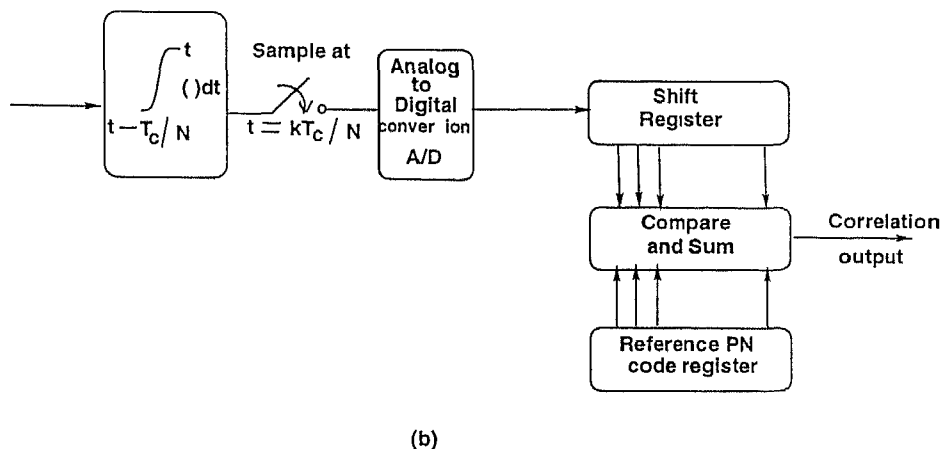
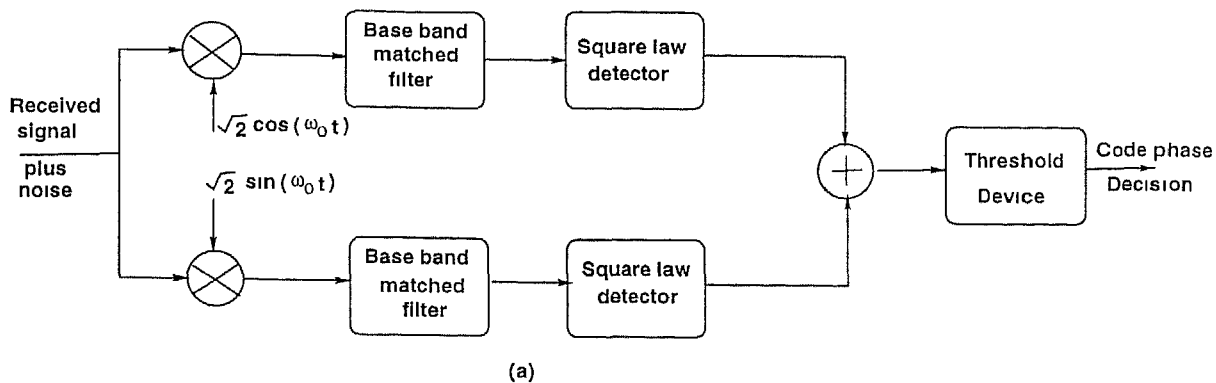


Figure 2.9 (a) Low pass version of matched filter acquisition (b) A digital correlator implementation of matched filter

implementation of matched filter in Fig 2.9(a) results in the discrete time version of the matched filter acquisition system. The correlation output is then squared, summed up and finally threshold tested to decide whether the code is acquired or not. Matched filter technique is preferred when short PN codes are used.

2.5 Fine synchronization in direct sequence SS systems

Once the coarse synchronization of PN codes is achieved, code tracking is activated. The purpose of code tracking (fine PN code alignment) is to maximize the alignment of locally generated PN code to that of received incoming PN code and in doing so to maximize the post despreading SNR. In general, code tracking loops maintain synchronization of receiver's replica of the spreading code by using the two correlators called an *early correlator* and a *late correlator*. An early correlator uses a code reference

waveform that in time by some fraction of a chip with respect to acquired PN code. A late correlator uses a code reference waveform that is delayed by some fraction of a chip. The difference between the two correlations is then used to form error signal proportional to the code misalignment and uses this error signal to shift the two codes into closer proximity. There are two basic architectures which implement the required fine closed loop functions [1, 4, 6, 30] the Delay Lock Loop (DLL) and the Tau Dither Loop (TDL).

2.5.1 The delay locked loop

A delay lock loop corrects any timing offset of the local code generator by feeding back error voltages to the local code generator. Consider the simplified block diagram

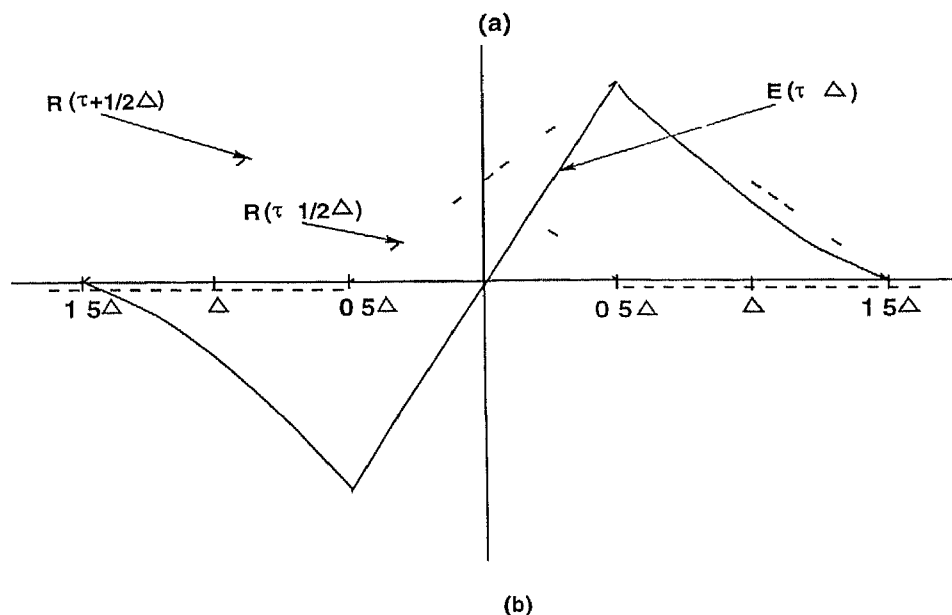
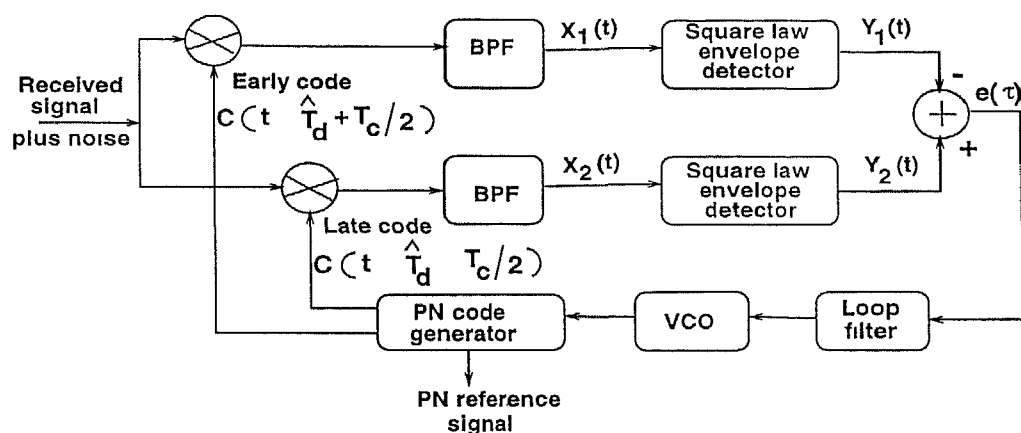


Figure 2.10 (a) A non coherent delay lock loop (DLL) (b) Error signal and auto correlations for $\Delta = T_c$

[3] as shown in Fig 2.10(a). Timing error voltages are obtained by using the local code to generate two offset sequences (advanced and delayed). These offset codes are separately multiplied with the input in the two channels of delay locked loop. The multiplied outputs are then band pass filtered and envelope detected and non coherently combined to produce a difference signal $e(\tau)$ where $e(\tau) = Y_2(t) - Y_1(t)$. This difference (or correction) signal is filtered (dampened) in the loop filter and is used to derive a voltage controlled oscillator (VCO). The VCO is a clock which drives the local PN generator faster when its clock is lagging in phase in comparison with the incoming sequence and vice versa. The rigorous treatment of DLL is given in [1-4] and a simplified version in [3]. The *normalized error* signal as obtained in [3] is given by

$$E(\tau, \Delta) \triangleq R_2^2 \left(\tau - \frac{\Delta}{2} \right) - R_1^2 \left(\tau - \frac{\Delta}{2} \right) \quad (2.12)$$

Where R_1 and R_2 are the auto correlation functions in the early and late branch of DLL. Parameter τ is delay estimator error, defined as $\tau \triangleq T_l - \hat{T}_d$. \hat{T}_d is the delay estimate and Δ = separation between early and late codes. Under the assumption of identical branches $R_1 = R_2 = R$

$$E(\tau, \Delta) \triangleq R^2 \left(\tau - \frac{\Delta}{2} \right) - R^2 \left(\tau - \frac{\Delta}{2} \right) \quad (2.13)$$

The auto correlation function as given by (2.12) and (2.13) depends on the basic chip waveform $\phi_c(t)$. For a rectangular waveform of unity amplitude in the interval $[0, T_c]$ the error signal is shown in Fig 2.10(b). By observation to the Fig 2.10(b) it can be concluded that regardless of whether Δ is positive or negative a compensating error voltage is generated which will correct the chip timing difference. However, it should also be noted that DLL is difficult to construct since the advance and delay arm of structure must be perfectly balanced requiring identical mixers, bandpass filters and envelope detectors.

2.5.2 The Tau-Dither loop

To overcome the balancing problem of delay locked loop the Tau Dither Loop (TDL) is suggested. TDL operates on the principle of time sharing a single correlator by early and late codes i.e. the incoming signal is correlated *alternately* with the early and late codes [3, 2, 30]. The Tau Dither Loop is shown Fig 2.11 [3]. This arrangement generates the same code offsets as did the previous delay locked loop, however only one multiplication branch is used at a time periodically alternating between advanced and delayed version of the code every T_p seconds where T_p is a fraction of a chip

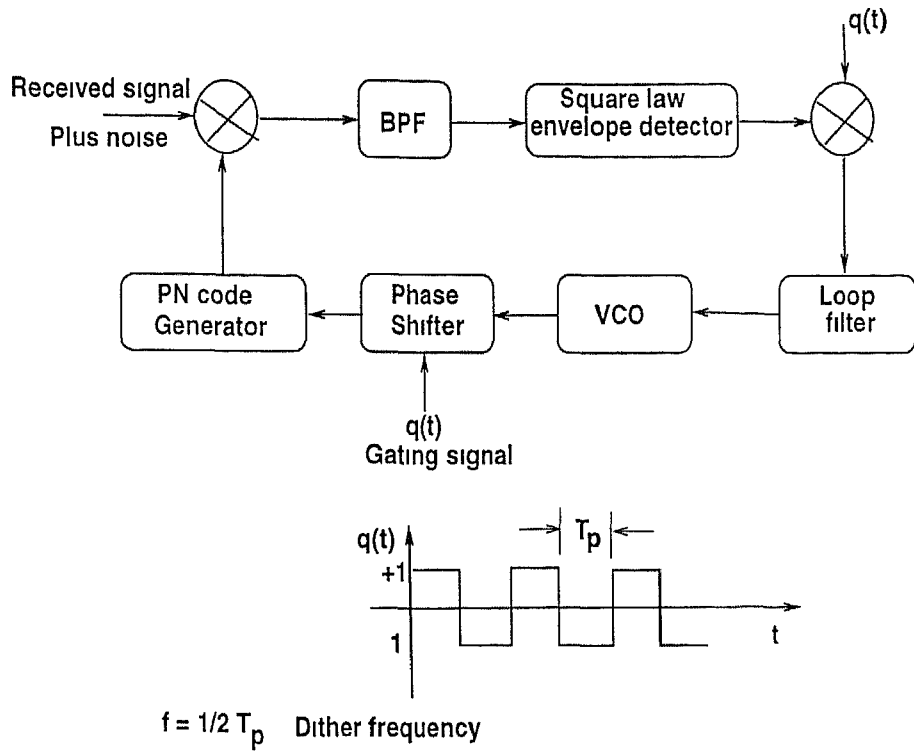


Figure 2 11 A Tau Dither Loop for PN code tracking

period (usually taken as $\frac{1}{2}$) The alternation is achieved by means of a gating signal $q(t)$ The gating signal also used to provide the resultant error signal before smoothing (averaging) in the loop filter

The normalized error function error function as given by [3] is

$$E(t, \tau, \Delta) = R^2 \left(\tau - \frac{\delta}{2} \right) - R^2 \left(\tau + \frac{\Delta}{2} \right) - q(t) \left[R^2 \left(\tau - \frac{\Delta}{2} \right) + R^2 \left(\tau + \frac{\Delta}{2} \right) \right] \quad (2.14)$$

This error function consist of two parts the first part is familiar error function of DLL as plotted in Fig 2 10(b) and the second part is sum of the squares of the early and late auto correlation functions multiplied by the dither switching function $q(t)$ which causes a net reduction in the error correction voltage

Chapter 3

The Single Dwell Serial Search PN Acquisition System in Low SNR CDMA Systems

3.1 Introduction

In a typical spread spectrum system the requirement of large processing gain is accomplished by using high chip rate PN codes. Coupled with this is the requirement of a high detector input bandwidth which in turn results in low input SNR. Channel distortions such as multi path fading causes the received signal to be random. The multiple access application of spread spectrum system such as land based mobile CDMA network (e.g. IS 95) or Low Earth Orbit (LEO) satellite systems (e.g. Globestar etc.) suffer from another phenomenon called Doppler effect which is due to relative motion between transmitter and/or receivers. It has been shown in [1, 15] that SNR at the correlator output will be drastically low if there is considerable Doppler. Low link power budget is another reason for the received SNR to be low. In general, in any CDMA network the excessive number of users approaching the system capacity limit causes the received signal to be characterized by low SNR. Since this SNR also happens to be a key parameter influencing the decisions regarding the synchronization therefore code acquisition process will also suffer heavily. The typical operational scenario in terms of input SNR at receiver is well below $-10dB$ [6] however, above factors further reduces it considerably causing severe degradation in system performance.

In this chapter the serial search code acquisition scheme of [15] has been modified for extending the low SNR operation range.

The code acquisition scheme of [15] consists of a multiplier band pass filter recirculation loop accumulator a decision circuitry acquisition and tracking control circuitry and a local PN code generator. The scheme has shown good results in the SNR range $-10dB$ to $+10dB$ from acquisition parameters point of view i.e. an improvement of 3 times in mean acquisition times and 5 times in the variance of acquisition time has been obtained compared to standard serial search approach of Fig 2.5. Comparable performance improvement is also obtainable by sequential estimation methods such as RASE [25].

However below $-10dB$ SNR the system performance needs to be re investigated since improvement is nominal (1.5 times) and for this purpose two major modifications in the scheme of [15] have been introduced with due consideration to hardware overhead. The first one being the addition of *post detection integration* (PDI) block¹ and the second one being adaptive threshold operation for achieving the constant false alarm probability using *cell averaging constant false alarm rate* (CA CFAR) approach² in contrast to the ADTLC algorithm [17] used for the same purpose in [15].

The attractive feature of the scheme presented in [15] namely the recirculation loop is retained in this work and after the above said modifications the modified serial search code acquisition scheme is presented in section 3.5. The analysis of modified scheme is then carried out in subsequent sections from detection and acquisition point of view.

3.2 Recirculation principle

The recirculation loop operates on the principle of delayed addition similar to that of a First In First Out (FIFO) accumulator queue. The samples of decision variable are fed to decision processor and the accumulator simultaneously. The delay provided by the accumulator can be chosen according to the desired application. As shown in the Fig 3.1(a) the delay in accumulator is kept $T_p \triangleq q\tau_d$ where T_p is the period of the correlation pulses at the output of sliding correlator as shown in Fig 3.1(b). q is the number of cells in the uncertainty region of code phase. τ_d is the integration (dwell) time. Therefore, recirculation loop accumulates the signal samples in each cell obtained during every new retrace of code delay uncertainty region. The addition of recirculation loop in standard single dwell serial search approach of Fig 2.5 will improve the SNR

¹The necessity of PDI is discussed in section 3.5

²CA CFAR method is discussed in section 3.3 and 3.4

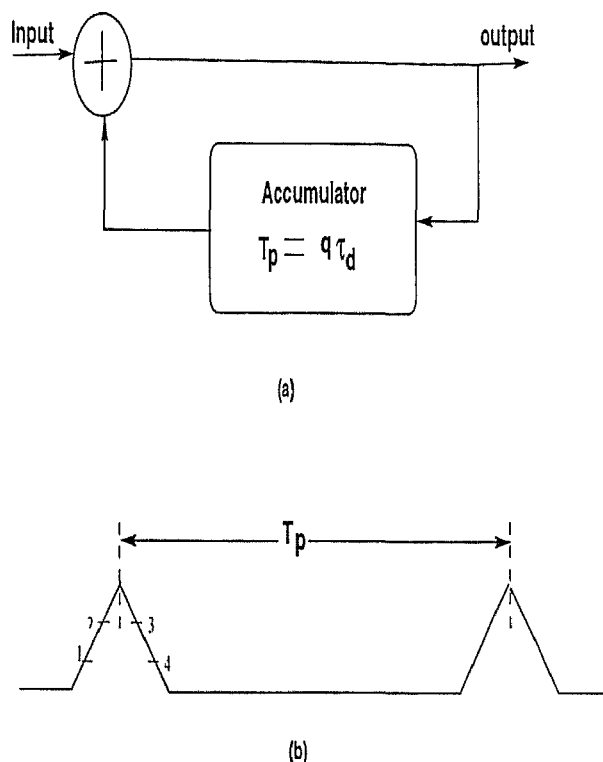


Figure 3.1 (a) Accumulator recirculation loop (b) correlation pulses at the output of correlator

of decision variable which will lead to better probability of synchronous cell detection and improved acquisition time performance. Simulation of recirculation in base band for $L = 127$, $q = 2L$ is shown in Fig 3.2

3.3 Adaptive CFAR approach

The basic cell averaging constant false alarm rate (CA CFAR) processor is illustrated in Fig 3.3. The essence of CFAR is to compare the decision statistics with an adaptive threshold, obtained from the estimate of noise or interference power after observing fixed number of noise or interference samples. This estimate may be obtained by accumulating the noise or interfering signals and adjusting the threshold in accordance with the measured noise or interfering signal so as to provide constant false alarm probability. As shown in Fig 3.3 the samples of decision variables are fed to a shift register and it is assumed that only one memory element of shift register contains signal plus noise sample while remaining elements contain only noise samples. An estimate (X) from these noise samples is then formed and multiplied by a threshold coefficient (T). T keeps on changing according to estimated noise (X) so as to form a threshold level

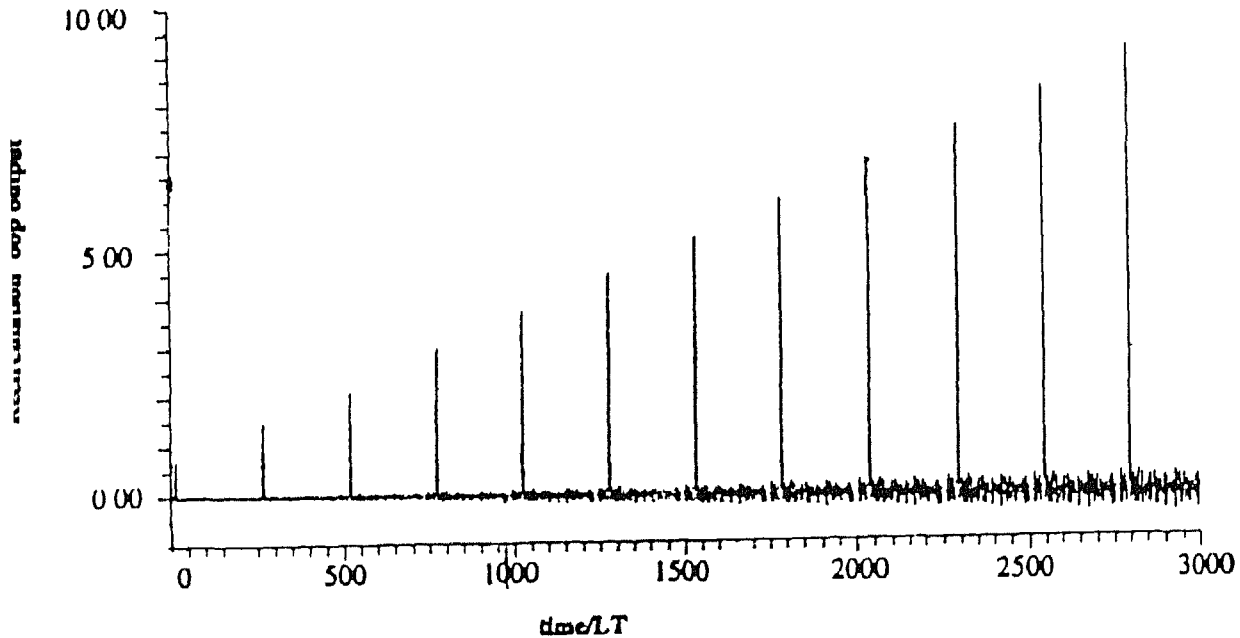


Figure 3.2 Recirculation loop output with $q = 2L$, $L = 127$ and recirculation delay $T_p = 254LT$

$\eta = T \backslash$ against which the samples of decision variable are compared and a decision is made whether signal is present or not. More details about CFAR approach are given in section 3.6.2.

3.4 Adaptive CFAR vs fixed threshold approach

The threshold level in the decision device of any communication receiver is chosen so as to achieve a desired false alarm probability. The false alarm rate is quite sensitive to the threshold level and minor variations such as changes in the noise at the input of receiver, multiple access interference, shadowing and fading in the received signal may affect the receiver's detection performance drastically. The typical mobile environment is further characterized by the relative motion between the transmitter and/or receiver which adds a new dimension to already complex code acquisition process. In the fixed threshold detection methods, the threshold level is fixed for a given false alarm probability, no matter how the associated environment of received signal is varying, and is changed only when a new value of false alarm probability is desired. It will quite often lead to too many false alarms which will reflect in an increased acquisition time, resulting in poor acquisition time performance [17–18]. On the other hand

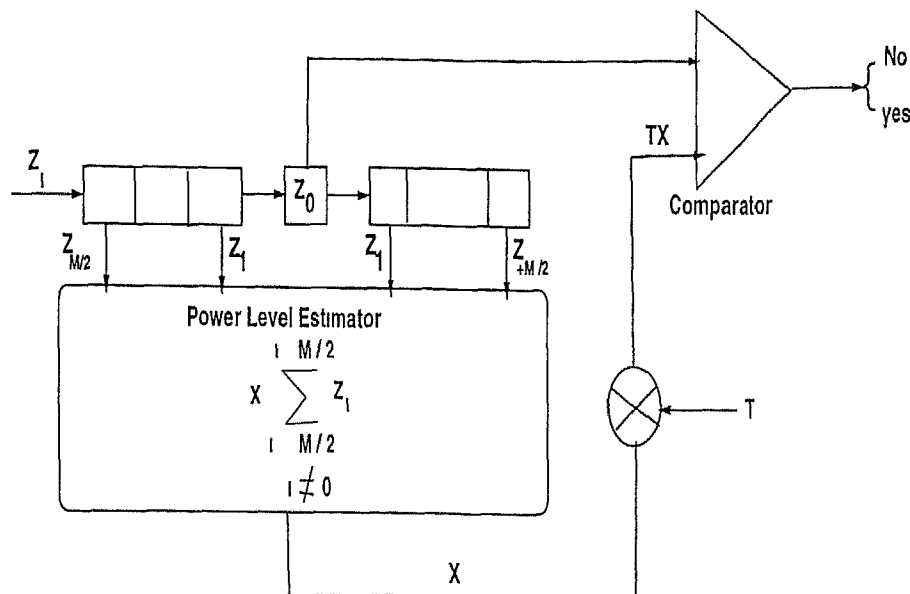


Figure 3.3 A CA CFAR based decision processor

in adaptive threshold detection methods the threshold level is continuously updated such that it provides desired false alarm probability by forming an estimate of the noise or interference in the received signal [18]. Therefore the problem of automatic threshold level control is fundamental for efficient operation of a DS-SS system and forms a key issue in decision making about the correct code phase (acquisition). One such approach for adapting the threshold level is Automatic decision threshold level control (ADTLC) [17] which comes at the cost of fairly increased hardware complexity coupled with the fact that it is SNR dependent and therefore not well suited for low SNR environment. Less demanding hardware is needed in the cell average constant false alarm rate (CA-CFAR) methods [18–31] and they are also independent of received signal's SNR.

3.5 Improved Serial search hypothesis testing model for low SNR CDMA systems

The recirculation loop of Fig. 3.1, a post-detection integration block and the adaptive decision processor of Fig. 3.3 has been added in the standard serial search approach of Fig. 2.5.

The resulting modified serial search code acquisition system is shown in Fig. 3.4 and is expected to have better performance in terms of detection probabilities and code acquisition parameters as compared to the standard serial search approach and the one

presented in [15] due to the following reasons

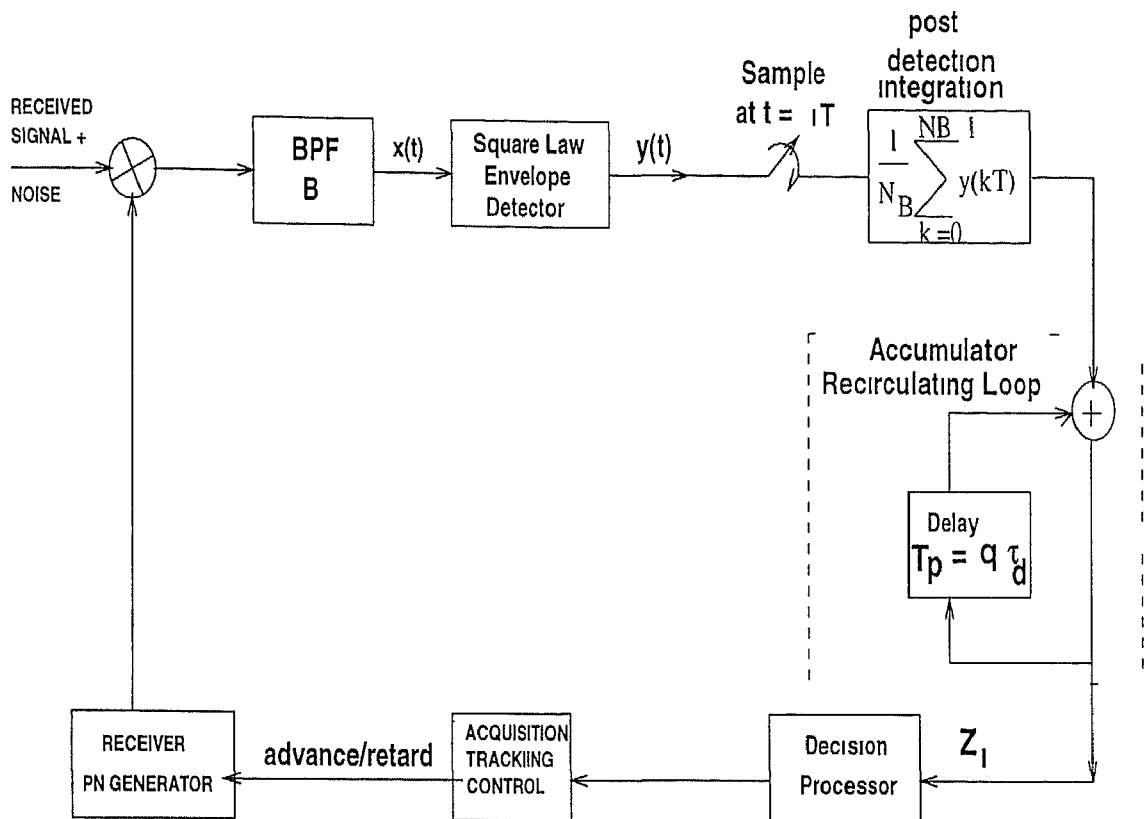


Figure 3.4 Code acquisition loop employing recirculation principle and adaptive decision processor

- Post detection integration (PDI) block is thought to be necessary for low SNR operations because the key parameter influencing the correct decision is the SNR at the multiplier output. It has been shown to be proportional to square of code correlation function multiplied by a factor of $\left[\frac{\sin(\omega_d \tau_d)}{\omega_d \tau_d}\right]^2$ due to carrier Doppler where ω_d is carrier frequency shift in radian due to Doppler effect and τ_d is integration or dwell time [1-15]. The SNR at multiplier output will be drastically low if there is considerable Doppler. Even under the assumption of no Doppler, testing the PN sequences with half chip timing error would cause square of code correlation function to be quite low and will result in several dB loss in the performance of acquisition scheme, a hardly affordable factor in low SNR environments. PDI forms unbiased estimate over the multiple samples of same hypothesis which in turn improves the SNR of decision variable thereby justifying the necessity of post detection integration.
- The adaptive CFAR decision processor being independent of SNR, has been used

to provide a constant false alarm probability (P_{FA}) during each retrace cycle of search procedure.

The improvement in SNR due to recirculation loop and post detection integration along with constant false alarm probability will increase the overall detection probability in each of the uncertainty region *cell* during every retrace cycle.

The serial search process for code acquisition comprises of multiplication of received direct sequence signal with the local PN code sequence, measurement of energy in the product signal and then comparison with a threshold in the decision processor. The samples of decision variable Z_i are also fed to the accumulator/recirculation loop. If the two sequences are not aligned, band pass filter blocks most of the power in product signal and threshold is not exceeded which results in the rejection of code under test. The phase of local sequences is then retarded or advanced for testing a new code phase. Thus each code phase corresponds to the two hypotheses when the two sequences are newly aligned, the product becomes a narrow band signal that passes through the filter with little loss of power and threshold is exceeded indicating that code has been acquired and search is stopped. Correct code verification is done and the tracking system is activated. This procedure is repeated for every code phase (*cell*) in the uncertainty region. If during the first pass the threshold is not exceeded then during the next retrace cycle of uncertainty region samples of decision variable are added to the corresponding samples of previous search cycle thereby improving the SNR of decision variable which will in principle improve the acquisition time performance.

3.5.1 Probability density function of decision variable

The complete statistical description of decision variable Z of Fig 3.4 is given by its probability density function. First the simplest case is considered in which no post detection integration is employed. Next post detection integration case is employed. In both the above cases the received signal is assumed to be unfaded. Finally the behaviour of decision variable under Nakagami m faded received signal is considered.

3.5.1.1 Unfaded signal in AWGN: No post detection integration case

Let the input data waveform be denoted by $d(t)$. The transmitted signal after spreading by PN code waveform $c(t)$ can be expressed as

$$s(t) = c(t)d(t)\sqrt{2P}\cos(\omega_0 t + \psi) \quad (3.1)$$

Where ω_0 is carrier frequency in radians and P is the power in transmitted carrier signal. The received signal in Fig 3.4 is $r(t) = s(t) + n(t)$ where $n(t)$ is assumed to be additive white gaussian noise. The local PN code generator of Fig 3.1 is assumed to be at an offset of $\pm\tau$ from the received code so that local PN code is represented as $c(t \pm \tau)$. In the worst case scenario τ may be as large as the period of PN code. The received signal after correlation and band pass filtering can be expressed as

$$r(t) = [r(t)c(t \pm \tau)]_{BPF} \quad (3.2)$$

where $[]_{BPF}$ represents band pass filtering operation. The input to square law detector then can be expressed as

$$r(t) = \sqrt{2P} \rho(t)d(t)\cos(\omega_0 t + \psi) + \sqrt{2}n_c(t)\cos(\omega_0 t + \psi) - \sqrt{2}n_s(t)\sin(\omega_0 t + \psi) \quad (3.3)$$

where $\rho(t)$ is correlation function of PN sequence and is defined as [17]

$$\rho(t) = \begin{cases} 1 & \text{if the two PN codes are synchronized i.e. signal lies on the correlation curve} \\ 0 & \text{otherwise} \end{cases} \quad (3.4)$$

Letting $1 \triangleq \rho(t)d(t)\sqrt{P}$ and recognizing A as rms signal amplitude after correlation and filtering is performed. P is the power in the received signal after correlation and band pass filtering.

Now defining the hypothesis H_1 as the case of signal present i.e. (the cell being searched corresponds to a sample value on PN correlation curve of Fig 3.1(b) and $\rho(t) = 1$) and hypothesis H_0 as the case of signal absent i.e. (the cell being searched does not correspond to a sample value on PN correlation curve of Fig 3.1(b) and $\rho(t) = 0$).

The input to square law envelope detector of serial search hypothesis device of Fig 3.4 can be expressed in the form

$$r(t) = \sqrt{2}A\cos(\omega_0 t + \psi) + \sqrt{2}n_c(t)\cos(\omega_0 t + \psi) - \sqrt{2}n_s(t)\sin(\omega_0 t + \psi) \quad (3.5)$$

$$= \sqrt{2}R(t)\cos(\omega_0 t + \psi + \theta(t)) \quad (3.6)$$

Where

$$R(t) = \sqrt{(A + n_c(t))^2 + n_s^2(t)} \quad \theta(t) = \tan^{-1} \frac{n_s(t)}{A + n_c(t)} \quad (3.7)$$

$n_c(t)$ and $n_s(t)$ are band limited independent low-pass zero mean Gaussian noise processes with variance $\sigma^2 = \frac{N_o B}{2}$. N_o is single sided noise spectral density and B is the noise bandwidth of predetection band pass filter.

The output of square law envelope detector in Fig 3.4 in response to the input $v(t)$ of (3.6) is (ignoring the second harmonics of carrier)

$$y(t) \triangleq v^2(t) = R^2(t) = (A + n_c(t))^2 + n_s(t) \quad (3.8)$$

Letting

$$\begin{aligned} A + n_c(t) &= w(t) \sim \mathcal{N}(A, \sigma^2) \\ n_s(t) &= v(t) \sim \mathcal{N}(0, \sigma^2) \end{aligned} \quad (3.9)$$

the distribution of $y(t)$ under *hypothesis* H_1 is found out in appendix B.1.1.e

$$p_1(y) = \begin{cases} \frac{1}{2\sigma} \exp\left(-\frac{y}{2\sigma} + \gamma_i\right) I_0\left(\sqrt{\frac{2y}{\sigma}}\gamma\right) & \text{for } y \geq 0 \\ 0 & \text{otherwise} \end{cases} \quad (3.10)$$

Which is *non central chi squared pdf* characterizing the square law output in all search cells that contain the signal to be acquired embedded in AWGN. γ_i is signal to noise ratio in the i^{th} retrace cycle of recirculation loop defined as $\gamma \triangleq \gamma_0$. γ_0 is predetection signal to noise ratio given by

$$\gamma_0 \triangleq \frac{A^2}{BN_o} = \frac{A^2}{2\sigma^2} \quad (3.11)$$

$I_0(\cdot)$ is modified Bessel function of first kind and zeroth order

The pdf of $v(t)$ under *hypothesis* H_0 can be obtained by substituting $A = 0$ in (3.10) and recognizing the fact that $I_0(0) = 1$

$$p_0(y) = \begin{cases} \frac{1}{2\sigma} \exp\left(-\frac{y}{2\sigma}\right) & \text{for } y \geq 0 \\ 0 & \text{otherwise} \end{cases} \quad (3.12)$$

This is *central chi squared pdf* characterizing the square law output in all search cells that contain Gaussian noise only. Equation (3.10) and (3.12) are same as those given in [6] except the fact that definition of γ is different here to account for the recirculation loop.

3.5.1.2 Unfaded signal in AWGN Post detection integration case

If band pass filter of Fig 3.4 has sharp cutoff skirts and $v(t)$ is sampled at intervals $T = \frac{1}{B}$ then the samples $(y_1, y_2, \dots, y_{N_B})$ will be approximately independent [1-6]. Therefore integrate and dump (post detection integration) output can be approximated by a summation over these sampled values, namely

$$Z \triangleq \frac{1}{\tau_d} \int_0^{\tau_d} y(t) dt \approx \frac{1}{N_B} \sum_{k=0}^{N_B-1} y_k \quad (3.13)$$

$$N_B \triangleq \frac{\tau_d}{T} = B\tau_d \quad (3.14)$$

where τ_d is dwell time. The pdf of normalized decision variable $Z \triangleq \frac{Z_{AB}}{\gamma_\sigma}$ (derived in appendix B.2) under the two hypotheses H_0 and H_1 respectively can be expressed as

$$p(Z) = \begin{cases} \frac{(Z)^{N_B-1}}{(N_B-1)!} \exp(-Z) & \text{for } Z \geq 0 \\ 0 & \text{otherwise} \end{cases} \quad (3.15)$$

and

$$p_1(Z) = \begin{cases} \left(\frac{Z}{N_B\gamma}\right)^{\left(\frac{N_B-1}{2}\right)} \exp(-Z - N_B\gamma) I_{N_B-1}(2\sqrt{N_B\gamma}Z) & \text{for } Z \geq 0 \\ 0 & \text{otherwise} \end{cases} \quad (3.16)$$

3.5.1.3 Nakagami m faded signal in AWGN

Often in the terrestrial propagation signal arrives at the receiver through different paths with relative delays and random phases. Statistically the resultant signal amplitude is modeled by the Rayleigh or Rician distribution while phase is assumed to be uniformly distributed in the interval $[0, 2\pi]$. However, as pointed out in [32] more complete and accurate statistical description of urban radio multipath fading channels is provided by Nakagami m distribution as compared to Rayleigh or Rician distribution. Also the Nakagami m is a two parameter distribution that provides more flexibility and accuracy in matching the observed signal statistics as compared to the other two distribution. For fading parameter $m < 1$ the Nakagami m distribution is used to model fading channel conditions that are more severe than the Rayleigh distribution ($m = 1$) and for $m > 1$ it is used to model the fading channel conditions less severe than Rayleigh distribution. It has been assumed in the following discussion that Nakagami m fading is slow enough that amplitude as well as phase remain constant over the one integration (dwell) time (τ_d) but fast enough that successive integration duration are essentially independent. The Nakagami m fading distribution is given by [33]

$$p(x) = \frac{2}{\Gamma(m)} \left(\frac{m}{\Omega}\right)^m x^{2m-1} \exp\left(-\frac{mx^2}{\Omega}\right) \quad (3.17)$$

where m is fading parameter and is defined as

$$m = \frac{\Omega^2}{E[x^2 - \Omega]^2} \quad (3.18)$$

and $\Omega = E(x^2)$ and $\Gamma(m)$ is gamma function. In Nakagami m fading environment the received SNR will be a random variable with distribution obtained by a change of variable in (3.17) as

$$p(\gamma_i) = \frac{\gamma_i^{m-1}}{\Gamma(m)} \left(\frac{m}{\Omega}\right)^m \exp\left(-\frac{m\gamma_i}{\Omega}\right) \quad (3.19)$$

Even in severe fading environments $p_0(Z^*)$ as given by (3.15) will remain unchanged as it does not depend upon the fading signal power. However $p_1(Z)$ as given by (3.16) will now become conditional pdf i.e. $P_1(Z/\gamma)$. Therefore pdf of decision variable Z under Nakagami m fading will then be obtained by averaging the pdf (3.16) over (3.19) i.e.

$$p_1(Z) = \int_0^\infty p_1(Z/\gamma_i) p(\gamma_i) d\gamma_i \quad (3.20)$$

This integration has been carried out in the appendix B.3 and the final result can be expressed as

$$p_1(Z) = \frac{(Z)^{N_B-1} \exp(-Z^*)}{\Gamma(m)(1+u)^m (N_B-1)!} {}_1F_1\left(m, N_B, \frac{uZ}{1+u}\right) \quad \text{hypothesis } H_1 \quad (3.21)$$

where ${}_1F_1(a, b, x)$ is the confluent hypergeometric function given as ${}_1F_1(a, b, x) = \sum_{r=0}^\infty \frac{\Gamma(b)\Gamma(r+1)x^r}{\Gamma(r+1)\Gamma(b+r+1)r!}$ and $b \neq 0, -1, -2, \dots$ [14]. u is defined as $u \triangleq \frac{\Omega N_B}{n}$ and $\Omega \triangleq E(\gamma)$. Since u is a function of average SNR in the i^{th} retrace cycle so is the $p_1(Z)$.

3.5.1.4 Rayleigh faded signal in AWGN

The Rayleigh fading distribution is a special case of Nakagami m distribution [33] it can be obtained by putting $m = 1$ in the latter distribution. Therefore for pdf of normalized decision variable Z^* under Rayleigh fading is given by

$$p_1(Z) = \frac{(Z^*)^{N_B-1} \exp(-Z^*)}{1+u} {}_1F_1\left(1, N_B, \frac{uZ^*}{1+u}\right) \quad \text{hypothesis } H_1 \quad (3.22)$$

or alternatively by

$$p_1(Z) = \frac{(Z^*)^{N_B-1} \exp(-Z^*)}{1+u} \sum_{r=0}^\infty \frac{\left(\frac{uZ^*}{1+u}\right)^r}{(N_B+r-1)!} \quad (3.23)$$

The important case of no post detection integration case under hypothesis H_1 can be obtained by putting $N_B = 1$ in (3.23). The final pdf is given as

$$p_1(Z^*) = \frac{1}{1+\Omega} \exp\left[-\frac{Z^*}{1+\Omega}\right] \quad (3.24)$$

With Z^* now given as $Z^* = \frac{Z}{2\sigma^2}$. This result is similar to one obtained in [1] except the change of notation.

3.6 Evaluation of detection and false alarm probability in terms of PN acquisition parameters

The detection probability, P_D is a salient factor in acquisition time and is defined as *probability that the code alignment is declared when the code is aligned*. If P_D is

low it is possible that multiple sweeps of all possible code phases may be necessary before acquisition occurs. Probability of false alarm P_{FA} is the probability that the correlation product of the received and reference code is sufficient to declare acquisition when in fact the correct code phase has not been acquired. The event of false alarm results in futile attempt to despread over another integration period. Both probability of false alarm and detection are parameters of code acquisition and acquisition time T_{acq} . The P_D and P_{I-1} are also functions of the integration period (dwell time), SNR and threshold voltage. The ideal scenario is to have high P_D and low P_{I-1} which is not always achievable. The variables which affect the process of determining these probabilities are inter related so that a simple change in the integration time or threshold voltage affects both of these probabilities. A high P_D and low P_{FA} imply a long integration period and consequently long acquisition time.

3.6.1 Unfaded signal in AWGN Fixed Threshold method

The probability of false alarm P_{FA} for unfaded signal in AWGN and post detection case can be obtained by integrating the likelihood pdf $P_0(Z)$ as given by (3.15)

$$P_{FA} = \int_{\eta}^{\infty} p_0(Z) dZ^* \quad (3.25)$$

The integration (3.25) is carried out in the appendix C.1 and result can be expressed as

$$P_{FA} = \exp(-\eta^*) \sum_{p=0}^{N_B-1} \frac{\eta^p}{p!} \quad (3.26)$$

where η^* is normalized threshold and is defined as $\eta^* \triangleq \frac{\eta N_B}{2\sigma}$

The probability of false alarm under no post detection integration case can be obtained by substituting $N_B = 1$ in equation (3.26) i.e.

$$P_{FA} = \exp(-\eta^*) \quad (3.27)$$

The probability of detection in the i^{th} retrace cycle of accumulation loop P_{Di} can be obtained by

$$P_{Di} = \int_{\eta}^{\infty} p_i(Z) dZ \quad (3.28)$$

The complete derivation is carried out in appendix C.1 and the final expression for detection probability is given as

$$P_{Di} = \exp(-\gamma_i N_B - \eta) \sum_{r=0}^{\infty} \frac{(N_B \gamma_i)^r}{r!} \sum_{p=0}^{N_B+r-1} \frac{(\eta)^p}{p!} \quad (3.29)$$

The detection probability for no post detection integration case may be obtained by putting $N_B = 1$ in equation (3.29) i.e

$$P_D = \exp(-\gamma_i - \eta) \sum_{r=0}^{\infty} \frac{\gamma}{r!} \sum_{p=0}^r \frac{(\eta)^p}{p!} \quad (3.30)$$

which if desired can be expressed in **Marcum Q function** form. The result will then be same as the one used in [15]

3.6.2 Unfaded signal in AWGN Adaptive Threshold method

In the CA CFAR approach (Fig 3.3) for adaptive threshold setting the samples of Z are serially sent into a shift register of length $M+1$ [31]. Each of the M reference cells is assumed to contain Gaussian noise while only one cell corresponding to Z_0 is assumed to contain the signal plus noise. Non coherent integration of N_B pulses follow the square law envelope detection for comparison with the adaptive threshold. Integrated noise power estimate from $L = MN_B$ samples is then obtained by $\lambda = \sum_{i=-M}^{+M} Z$. The threshold TX varies according to variations in the noise and the threshold coefficient T is used as a scale factor to achieve the desired false alarm probability for a given shift register of window size M . Under the assumption that surrounding M cells contains independent Gaussian noise with the same variance, the pdf of λ is obtained from (3.15) as

$$p(\lambda) = \frac{\lambda^{L-1}}{(L-1)!} \exp(-\lambda) \quad (3.31)$$

The detection probability for a given value of T is obtained by integrating the detection probability conditioned on a threshold $\eta^* = TX$ over $p(\lambda)$ [31] as

$$P_{Di} = \int_0^{\infty} p(X) \int_{TX}^{\infty} p_1(Z^*) dZ^* d\lambda \quad (3.32)$$

while threshold coefficient T is determined from a designated false alarm probability given as

$$P_{FA} = \int_0^{\infty} p(\lambda) \int_{TX}^{\infty} p_0(Z) dZ^* d\lambda \quad (3.33)$$

Substituting the (3.31) (3.15) in (3.33) (3.31) (3.16) in (3.32) and carrying out the required integrations (see appendix C.2) the final expressions are

$$P_{FA} = \frac{1}{(1+T)^{MN_B}} \sum_{p=0}^{N_B-1} \binom{MN_B + p - 1}{p} \frac{T^p}{(1+T)^p} \quad (3.34)$$

$$P_{Di} = \frac{\exp(-\gamma_i N_B)}{(1+T)^{MN_B}} \sum_{r=0}^{\infty} \frac{(N_B \gamma_i)^r}{r!} \sum_{p=0}^{N_B+r-1} \binom{MN_B + p - 1}{p} \left(\frac{T}{1+T} \right)^p \quad (3.35)$$

where notation $\binom{a}{b}$ is used to denote $\frac{a!}{b!(a-b)!}$ when a and b are positive integer and also for representing $\frac{\Gamma(a+1)}{\Gamma(l+1)\Gamma(a-b+1)}$ when a and b are positive non integer

The probability of false alarm for *no post detection integration case* may be obtained by substituting $N_B = 1$ in (3.34) i.e

$$P_{FA} = \frac{1}{(1+T)^M} \quad (3.36)$$

The detection probability for *no post detection integration case* may be obtained by simply putting $N_B = 1$ in equation (3.35) i.e

$$P_D = \frac{\exp(-\gamma_i)}{(1+T)^M} \sum_{r=0}^{\infty} \frac{\gamma_i^r}{r!} \sum_{p=0}^r \binom{M+p-1}{p} \left(\frac{T}{1+T}\right)^p \quad (3.37)$$

3.6.3 Nakagami-m faded signal in AWGN Adaptive threshold method

Substituting (3.21) and (3.31) in (3.32) and carrying out the required integration (see appendix C.3) the expression for detection probability in the i^{th} retrace of such procedure is found out to be

$$P_{Di} = \frac{1}{(1+u)^m(1+T)^L} \sum_{r=0}^{\infty} \binom{m+r-1}{r} \left(\frac{u}{1+u}\right)^r \sum_{p=0}^{N_B+r-1} \binom{L+p-1}{p} \left(\frac{T}{1+T}\right)^p \quad (3.38)$$

The detection probability in (3.38) is a function of received SNR in the i^{th} retrace cycle of serial search procedure (through parameter u) fading parameter m number of post detection integration N_B and the number of reference cells M used in the adaptive CFAR thresholding method

3.7 Signal flow graph based analysis

As pointed out earlier, the time to acquire the code (*acquisition time* T_{acq}) of an acquisition process is characterized by first two moments of acquisition time i.e mean (\bar{T}_{acq}) and variance (σ_{acq}^2). The two parameters are function of P_{FA} and P_{Di} which are already derived in previous sections. As a next step we will now determine these two moments. In the literature, there exist three approaches to analyze a code search process from acquisition time point of view

- Signal flow graph based approach [2 6 16]
- Circular state diagram approach [19 20]
- Pure probabilistic approach [4 10]

Former two approaches are z transform based and rely on search process description by a suitable flow graph or circular state diagram. Next transfer function of graph (or state diagram) is determined. Finally this transfer function is used to determine the moments of acquisition time. These approaches are quite versatile, elegant and simple to use as opposed to pure probabilistic approach which is time domain based, heuristic in nature and lacks mathematical elegance. The generalization of former two approaches to an arbitrary search process is straightforward as they completely describe the anatomy of search procedure while latter does not provide much insight into actual search process and its generalization to an arbitrary search strategy is an involved task.

In this work modified serial search system as shown in Fig 3.4 will be analyzed using the *signal flow graph* based approach. The analysis procedure and subsequent expressions obtained are general enough in the sense that they apply equally to coherent type as well as non coherent type of search strategy. The only difference between the two cases being the inter relation of parameters τ_d , P_{F1} and P_D for the type of detector used. This inter relationship is essential for computing the acquisition time performance and should be determined at the first instance.

3.7.1 Serial search acquisition parameters in the absence of code doppler

In the modeling of serial search code acquisition process by signal flow graph method the *cells* in code uncertainty region are represented as nodes and branches between the nodes as transitions from one cell to another. In such a flow graph it is customary [2 6, 16] to label each branch with the product of the transition probability associated with going from the node at the originating end of branch to the node at its terminating end, and an integer (including zero) power of a parameter denoted as z . The parameter z is used to mark the time as one proceeds through the graph and its power represents the number of time units (dwell times) spent in traversing that branch. Furthermore, sum of the branch probability (letting $z = 1$) emanating from each node equals unity. The cells³ are serially tested until it is determined that a particular cell corresponds to

³The term nodes and cells will be used interchangeably here

the alignment of two PN codes within a fraction of a chip. If the number of code chips to be searched are N_u and search proceeds in half chip increment then the number cells in the code uncertainty region are $q = 2N_u$. Only one out of these q cells represents synchronization i.e. it is assumed that correct phase lies in any one of q cells and search can begin anywhere [2-16]. The successive decision process is presented by a signal flow graph in Fig 3.5. A priori probability of achieving coarse synchronization in the i^{th} cell provided it is not present in first $(i-1)$ nodes is given as

$$P_i = \frac{1}{(q-i+1)} \quad (3.39)$$

where $q-i+1$ is the number of remaining cells to be searched (each possessing an equal probability of achieving synchronization). Starting at cell 1 (Fig. 3.5) if the synchronous state is detected the process will be completed in one dwell time (τ_d) as shown by state Γ . In z transform domain it is represented by $P_{D1}z$ weight of corresponding branch in Fig 3.5. If the synchronization has not been achieved the process will move to cell 2 and the corresponding branch weight will be $(1 - P_{D1})z$. Here it encounters either a false alarm represented by αz^{K+1} (α is false alarm probability and K is design parameter to extend the integration time τ_d for verification of false alarm $K < q$) or no false alarm represented by $(1 - \alpha)z$. At cell 2 the process will be repeated and search will proceed to check further cells until the synchronization is achieved. In case synchronization is not obtained the search process will start all over again at starting position i.e. cell 1. However now the overall probability of detection is increased in all the q cells to $P_{D1} + P_{D2}(1 - P_{D1})$ and the whole search procedure will be repeated. Since the SNR of synchronous state will be increased in each new retrace cycle after some passes synchronous state will be detected and search process will stop.

Using the standard flow graph reduction technique [16] the transfer function of overall graph $U(z)$ is determined. This function is further used in the derivation of a closed form analytical expression for mean acquisition time \bar{T}_{acq} and variance of acquisition time σ_{acq}^2 . The mean acquisition time is defined by [1-2, 6-16]

$$\bar{T}_{acq} \triangleq \tau_d \left[\frac{d \ln U(z)}{dz} \right]_{z=1} \quad (3.40)$$

While the variance of acquisition time is defined as

$$\sigma_{acq}^2 \triangleq \left[\frac{d^2 \ln U(z)}{dz^2} + \frac{d \ln U(z)}{dz} \right]_{z=1} \quad (3.41)$$

Introducing the notation $H(z) = (1 - \alpha)z + \alpha z^{K+1}$ for gain in advancing the search process from i^{th} cell to $(i+1)^{th}$ cell and β_j as overall detection probability in j^{th}

retrace cycle given as

$$\beta_j = \sum_{n=1}^j P_{Dn} \prod_{m=1}^{n-1} (1 - P_{Dm}) \quad (3.42)$$

From signal flow graph of Fig 3.5 loop gain of i^{th} loop in j^{th} retrace cycle is given as

$$L_{ji} = (1 - \beta_j) z H^{q-1}(z) \quad (3.43)$$

Forward path gain of i^{th} cell in j^{th} retrace cycle is given by

$$G_{ji} = p_i \beta_j z \quad (3.44)$$

The transfer function of i^{th} cell in j^{th} pass is given as

$$T_{ji} = \frac{P_i \beta_j z}{1 - (1 - \beta_j) z H^{q-1}(z)} \quad (3.45)$$

Now from Fig 3.5 the overall transfer function for j^{th} pass can be written as

$$\begin{aligned} U_j(z) = & T_{j1} + (1 - P_1) T_{j2} H(z) + (1 - P_1)(1 - P_2) T_{j3} H^2(z) \\ & + (1 - P_1)(1 - P_2)(1 - P_3) \dots (1 - P_{q-1}) T_{j,q} H^{q-1}(z) \end{aligned} \quad (3.46)$$

substituting $T_{j1}, T_{j2}, T_{j3}, \dots, T_{jq}$ from (3.45) and P_1, P_2, \dots, P_q from (3.39) into (3.46) and after some routine algebra the result can be expressed as

$$= \frac{\beta_j z}{1 - (1 - \beta_j) z H^{q-1}(z)} \left[\frac{1}{q} + \frac{1}{q} H(z) + \frac{1}{q} H^2(z) + \dots + \frac{1}{q} H^{q-1}(z) \right] \quad (3.47)$$

which can be further simplified i.e.,

$$U_j(z) = \frac{\beta_j z}{1 - (1 - \beta_j) z H^{q-1}(z)} \left[\frac{1}{q} \sum_{l=0}^{q-1} H^l(z) \right] \quad (3.48)$$

For N retrace cycles the overall transfer function of decision making flow graph is given as

$$U(z) = \sum_{j=1}^N \frac{\beta_j z}{1 - (1 - \beta_j) z H^{q-1}(z)} \left[\frac{1}{q} \sum_{l=0}^{q-1} H^l(z) \right] \quad (3.49)$$

Now using the definition of mean acquisition time from (3.40) and variance of acquisition time from (3.41), the two parameters are found out in the appendices A.1 and A.2 respectively. The final expression for mean acquisition time is

$$\frac{\bar{T}_{acq}}{\tau_d} = (q-1)(1 + K\alpha) \left[\left(\frac{1}{N} \sum_{j=1}^N \frac{1}{\beta_j} \right) - 0.5 \right] + 1 \quad (3.50)$$

While for variance of acquisition time is

$$\begin{aligned} \frac{\sigma_{acq}^2}{\tau_d^2} = & \left[\frac{(q-1)(1+K\alpha)}{N} \sum_{j=1}^N \frac{1-\beta_j}{\beta_j} \right] \left[3 + (q-2)(1+K\alpha) + \frac{K\alpha(K+1)}{(q-1)(1+K\alpha)} \right] \\ & + \left[\frac{2\{(q-1)(1+K\alpha)\}^2}{N} \sum_{j=1}^N \left(\frac{1-\beta_j}{\beta_j} \right)^2 - \left(\frac{(q-1)(1+K\alpha)}{N} \sum_{j=1}^N \frac{1-\beta_j}{\beta_j} \right)^2 \right] \\ & + \frac{(q-1)}{2} \left[(1+K\alpha) + (1+K\alpha)^2 \left(\frac{q-1}{6} \right) + \frac{K\alpha(K+1)}{2} \right] \quad (3.51) \end{aligned}$$

From (3.50) it is clear that mean acquisition time is a function of P_{FA} (denoted as α in the above equations), overall detection probability β_j , number of cells in the code uncertainty region q , integration time τ_d , number of retrace cycles N and false alarm penalty K . If β_j is not too low, only a few passes are required to achieve synchronization. The same can be said for the variance of acquisition time. However, given the nature and complexity of (3.51), it is difficult to draw meaningful conclusions regarding the interplay of various variables.

The mean and variance of the acquisition time for standard serial search approach of Fig. 2.5 are given as [2, 6]

$$\frac{\bar{T}_{acq}}{\tau_d} = \frac{(2 - P_D)(1 + K\alpha)(q - 1)}{2P_D} \quad (3.52)$$

and

$$\frac{\sigma_{acq}^2}{\tau_d^2} = \left\{ (1 + K\alpha)^2 q^2 \left(\frac{1}{12} - \frac{1}{P_D} + \frac{1}{P_D^2} \right) + 6q [K(K+1)\alpha(2P_D - P_D^2)(1 + K\alpha)(4 - 2P_D - P_D^2)] + \frac{1 - P_D}{P_D^2} \right\} \quad (3.53)$$

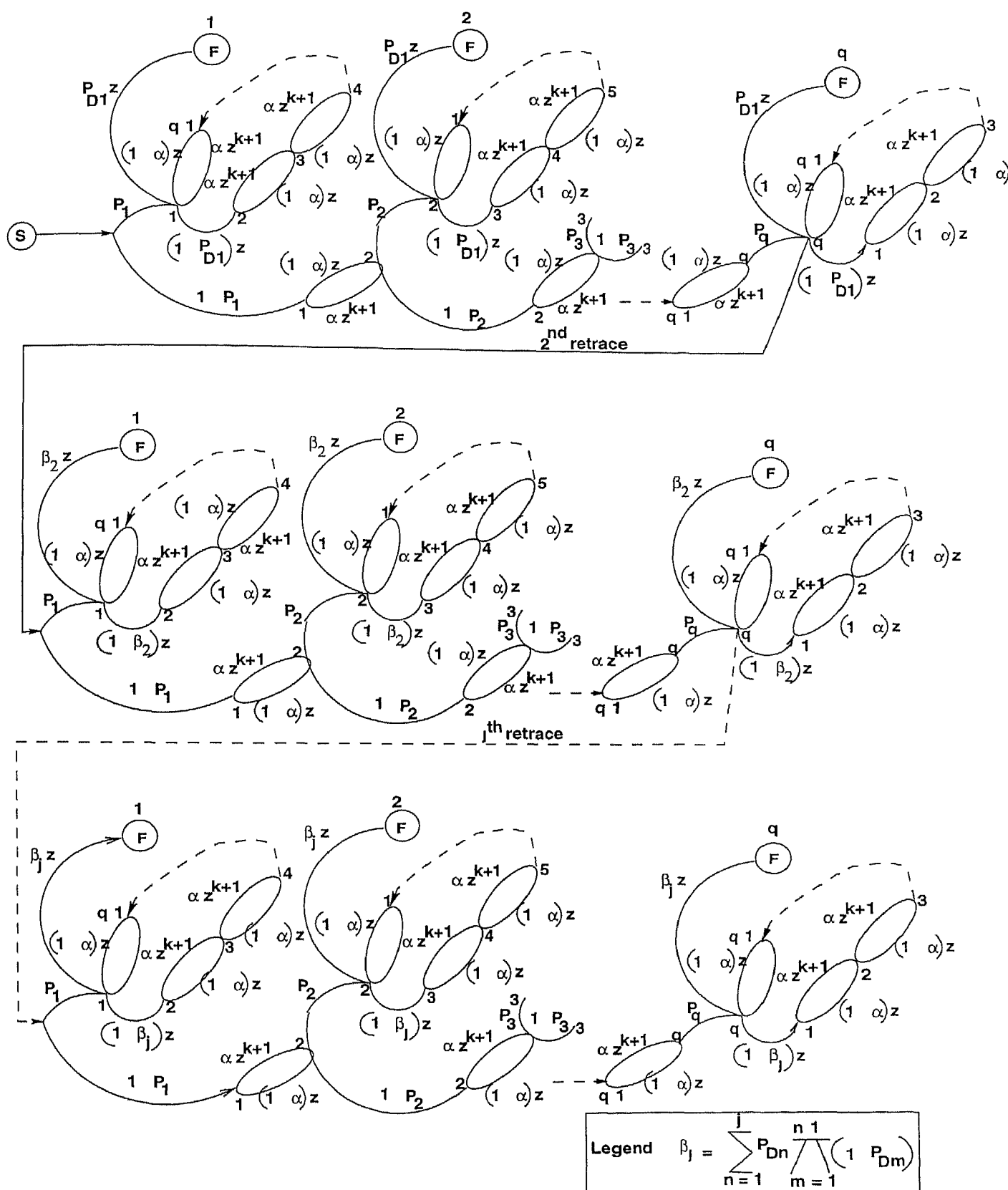


Figure 3.5 Decision process signal flow graph for serial search code acquisition system of Fig. 3.4

Chapter 4

Results and Discussions

In this chapter we present the numerical results of the analysis carried out in the chapter 3. Firstly the results for code phase detection performance of fixed threshold method is presented and discussed. Secondly the case of adaptive threshold is considered and its results are presented. The Nakagami m faded signal case is considered next and its detection performance is presented. Finally, the corresponding results from the code acquisition point of view is presented and discussed in the above order. The manner in which these results are presented is suitable for making a comparative analysis with the existing known similar techniques and to clearly demarcate the resulting improvements and/or degradations.

4.1 Fixed threshold detection performance

For a given P_{FA} and N_B the normalized threshold level η can be obtained by numerical evaluation of (3.26). Upon substitution, this η^* in (3.29) yields the P_D for that particular P_{FA} provided the other parameters are suitably chosen. The (P_{FA}) and (P_{Di}) are further used to compute the mean and variance of acquisition time in (3.50) and (3.51) respectively.

4.1.1 Detection performance for unfaded signal in AWGN

Fig 4.1 Using (3.26) P_{FA} against the threshold level (η^*) as a function of N_B is plotted in Fig 4.1. With increasing N_B larger threshold level η^* is needed for a given value of P_{FA} . For a given N_B the η^* increases with decreasing P_{FA} .

Fig 4.2 The P_{Di} as computed from (3.29) vs SNR for $P_{FA} = 0.1$, $N_B = 4$ and

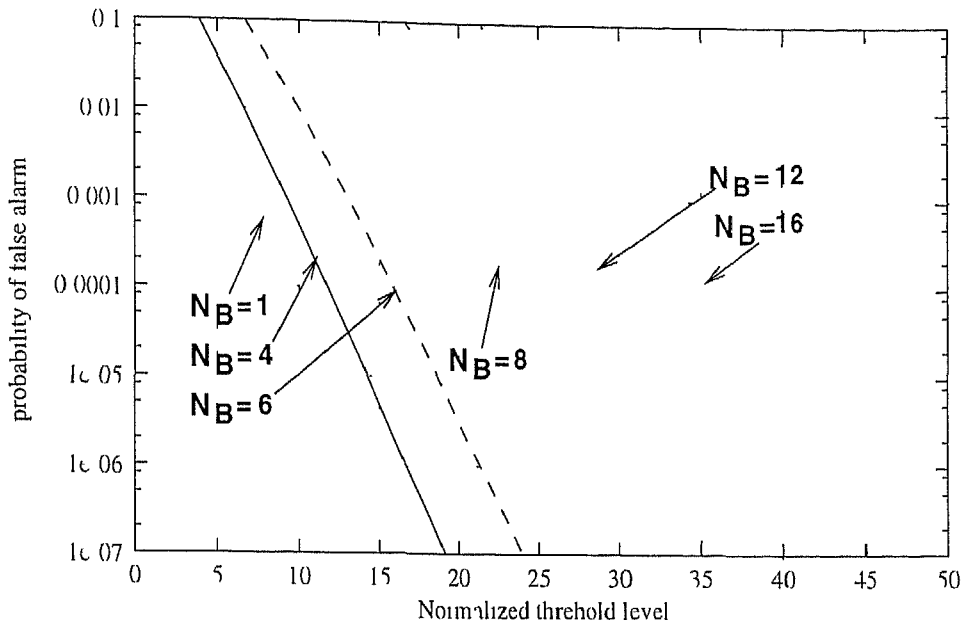


FIGURE 4.1 Probability of false alarm P_{FA} vs normalized threshold level η

as a function of number of retrace cycle of recirculation loop is plotted in Fig 4.2. In general, with increasing retrace cycles the curves shift towards the left and increase in detection probability is obtained. However, in low SNR region ($< 0dB$) sufficient number of retrace cycles are needed to achieve fairly high detection probability.

Fig 4.3 and Fig 4.4 The *improvement factor* in detection probability can also be obtained by increasing N_B , which is defined as *ratio of detection probability for a given number of post detection integration N_B to the case when no post detection integration $N_B = 1$ is employed*. The improvement factor vs SNR as a function of number of retrace cycles for $P_{FA} = 0.1$, $N_B = 4, 16$ is plotted in Fig 4.3. A peak improvement factor of 1.6 to 1.8 is obtained for $N_B = 4$ and 2.5 to 3.1 is obtained for $N_B = 16$. Similar curves for $P_{FA} = 0.01$ are shown in Fig 4.4 in which a peak improvement of 2.9 to 3.2 times for $N_B = 4$ and 8.5 to 9.2 times for $N_B = 16$ is obtained. As shown in Fig 4.3 and Fig 4.4 with decreasing false alarm probability higher improvement in detection probability is possible with increasing N_B . Moreover, the peak of the curves shift towards the left i.e. towards the low SNR region with increasing N_B .

4.2 Adaptive threshold detection performance

The threshold coefficient T for designated P_{FA} for given shift register size $M+1$ and N_B can be obtained from numerical evaluation of (3.34). Upon substitution of T along with other parameters in (3.35), one can obtain the detection probability in

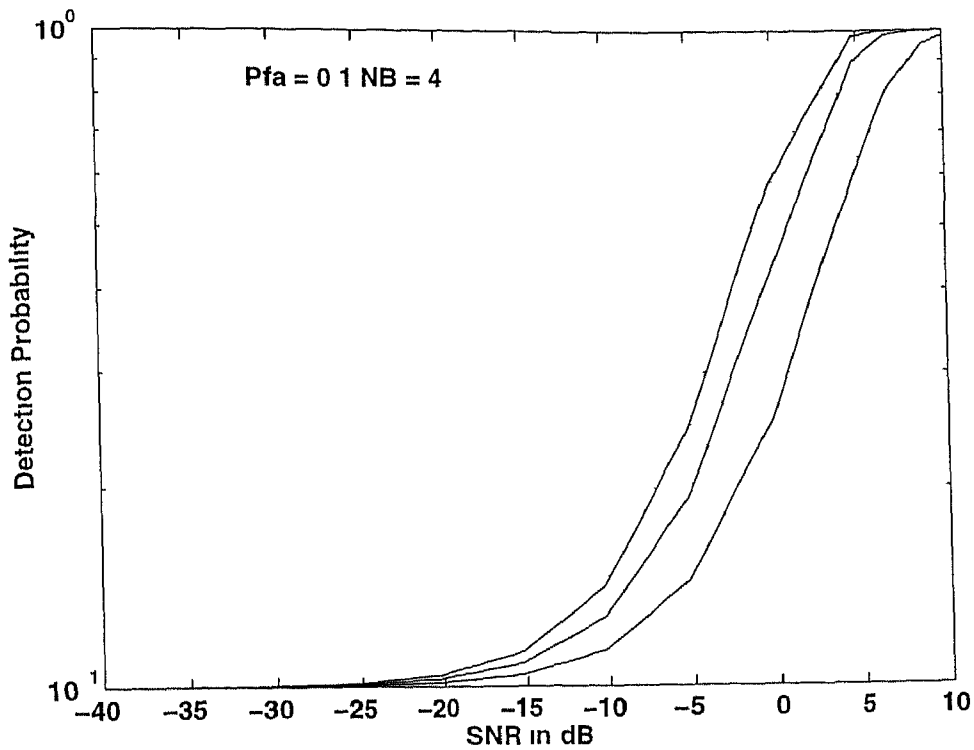


Figure 4.2 Detection probability vs SNR for three retrace cycles

every retrace cycle of recirculation loop. The mean acquisition time and variance of acquisition time then can be obtained by utilizing this P_{FA} and P_D along with other parameters in (3.50) and (3.51) respectively.

4.2.1 Detection performance for unfaded signal in AWGN

Fig 4.5 and Fig 4.6 The probability of false alarm P_{FA} against threshold coefficient T is plotted in Fig 4.5 and Fig 4.6. For specific N_B and P_{FA} , the threshold coefficient T decreases with increasing M . Moreover, for wide range of P_{FA} from 10^{-6} to 10^{-1} , the variations in the threshold coefficient decreases with increasing M . This is due to the fact that as more and more noise samples are included in the adaptive CFAR decision processor of Fig 3.3, the better will be the noise estimate and hence more accurate will be the threshold coefficient, which in turn will result in accurate threshold setting to achieve the desired false alarm probability.

Increasing the N_B , i.e., better estimation of decision variable Z_i of Fig 3.4, the whole family of curves shift towards left as shown in Fig 4.5 and Fig 4.6, indicating again a reduction in T . Moreover, for specific N_B and T , a reduction in P_{FA} is obtained with increasing M .

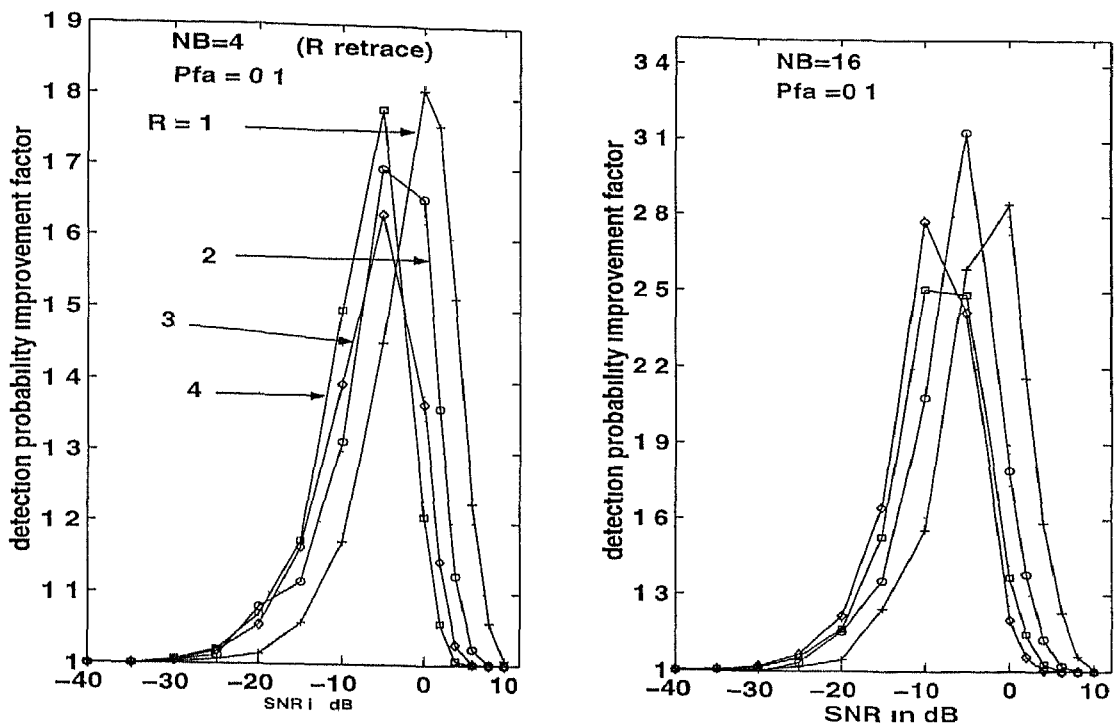


Figure 4.3 Detection probability improvement factor vs SNR for four retrace cycles

Fig 4.7, Fig 4.8 and Fig 4.9 The detection probability as obtained from the (3.35) for various SNR is shown in Fig 4.7 for designated $P_{FA} = 0.1$, $N_B = 4$ and two different M i.e., $M = 4$ and $M = 8$. The similar curves were obtained for $P_{FA} = 0.01$ and are shown in Fig 4.8. Finally Fig 4.9 shows similar curves for $P_{FA} = 0.01$, $N_B = 6$ and $M = 6$.

The important observations are as follows

- Due to recirculation loop, the detection probability curves shift towards left i.e., an improvement in detection probability is obtained in each retrace cycle. The effect of recirculation loop is most visible in SNR range -30dB to $+5\text{dB}$. Beyond 5dB all curves start saturating i.e., detection probability approaches to unity and below -30dB another few retrace cycles are needed to obtain the fairly high detection probability.
- As shown in Fig 4.7, for given P_{FA} and N_B further improvement is possible with increasing value of M in each retrace cycle of recirculation loop. The same observation is also visible in Fig 4.8.
- As shown in Fig 4.9 increasing N_B further improves the detection probability.

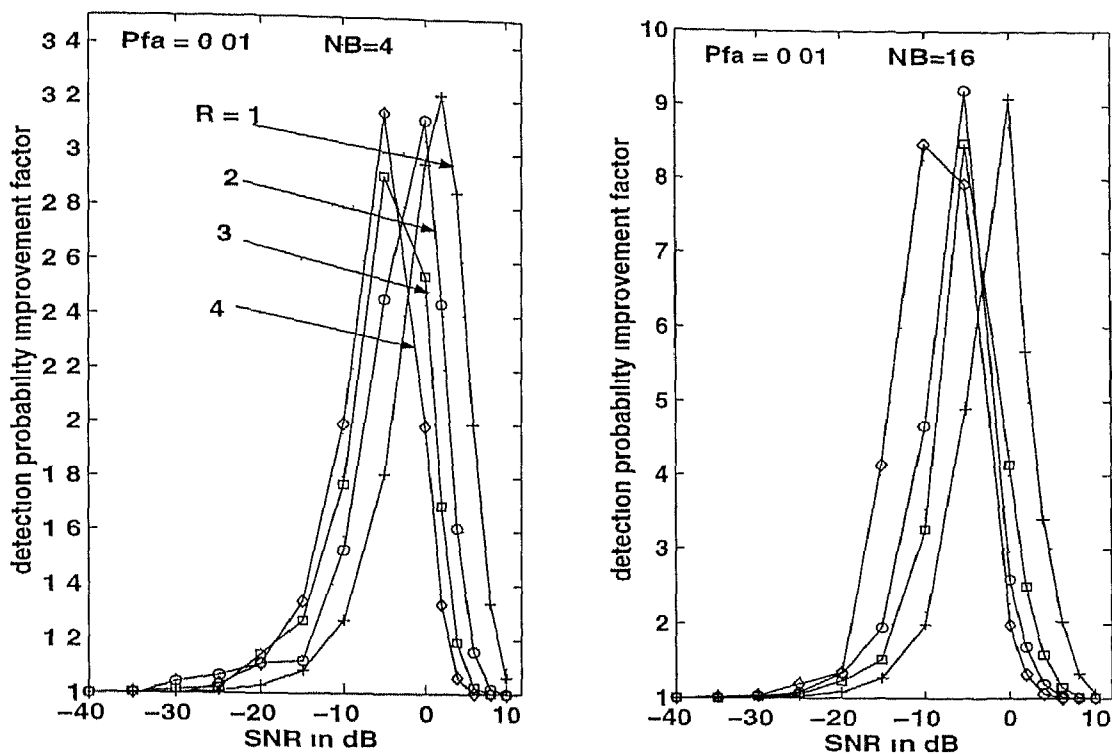


Figure 4.4 Detection probability improvement factor vs SNR for four retrace cycles

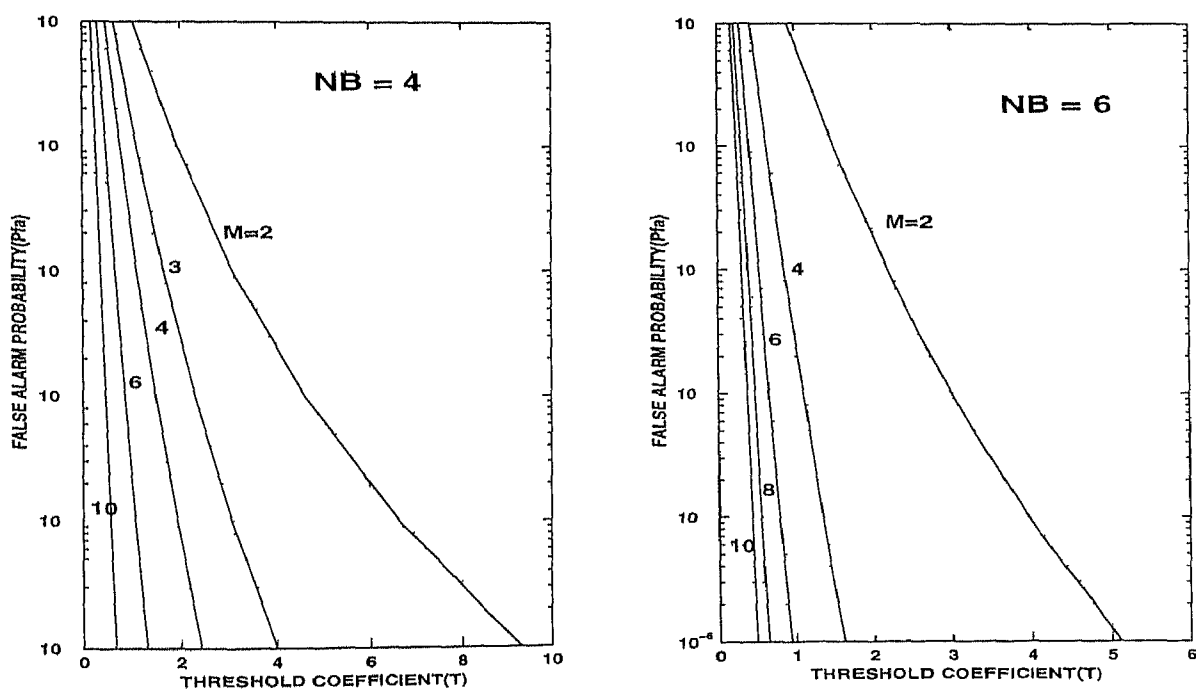


Figure 4.5 False alarm probability vs threshold coefficient for $N_B = 4$ and $N_B = 6$

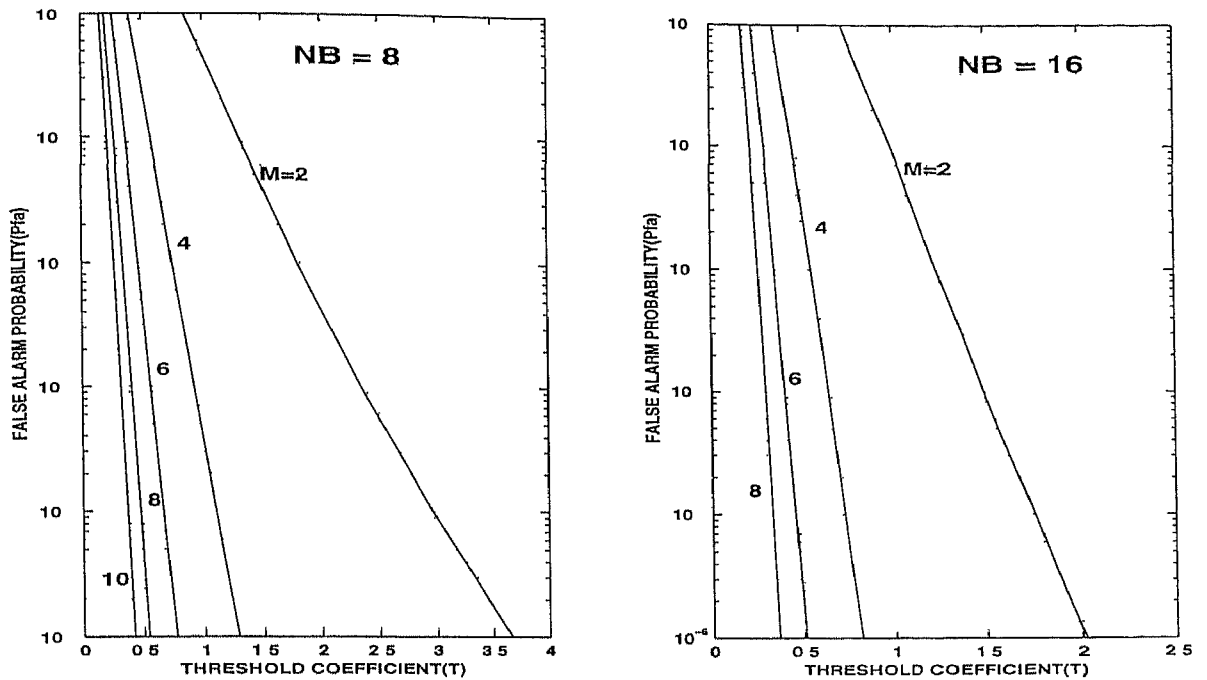


Figure 4.6 False alarm probability vs threshold coefficient for $N_B = 8$ and $N_B = 16$

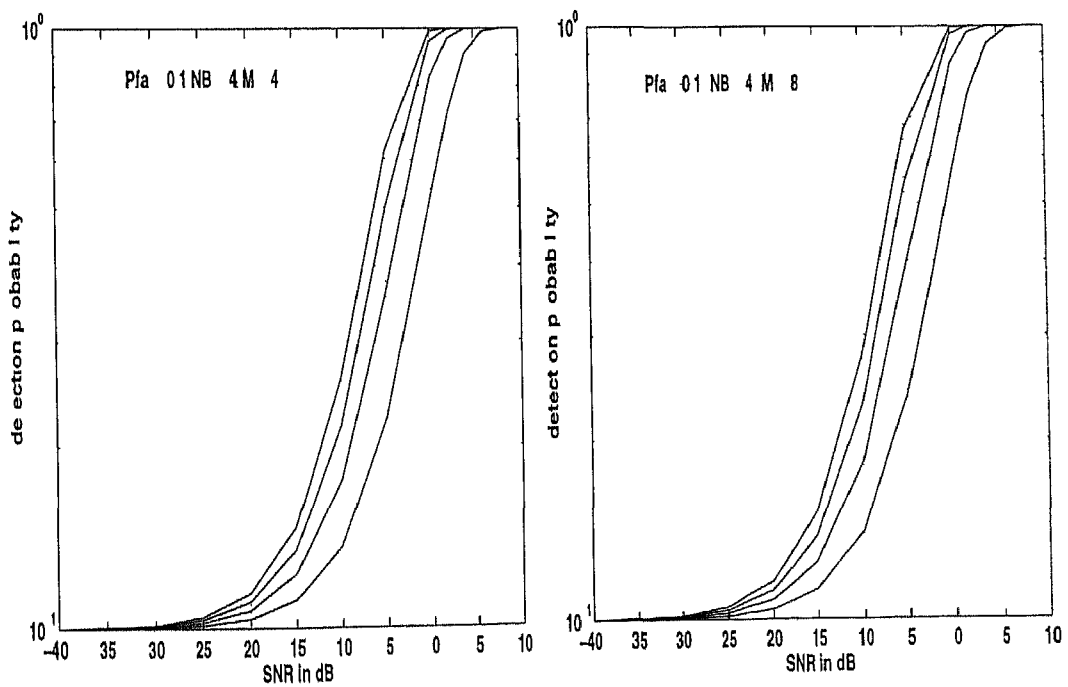


Figure 4.7 Detection probability vs SNR for $P_{FA} = 0.1$, $N_B = 4$ and $M = 4$,
8 Adaptive threshold method

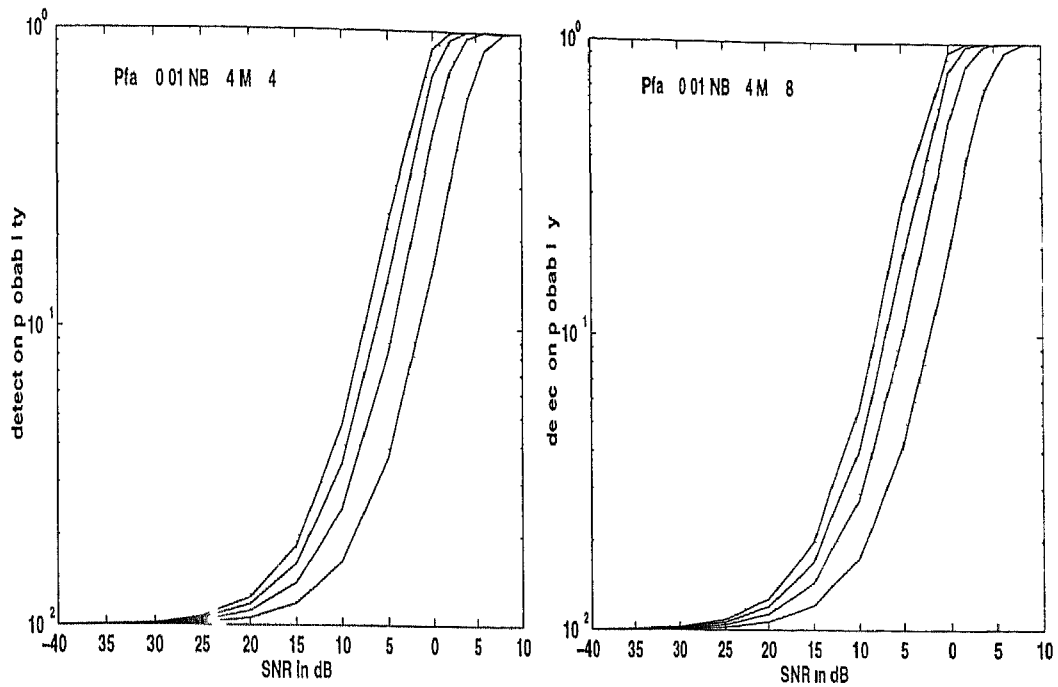


Figure 4.8 Detection probability vs SNR for $P_{FA} = 0.01$, $N_B = 4$ and $M = 4, 8$ Adaptive threshold method

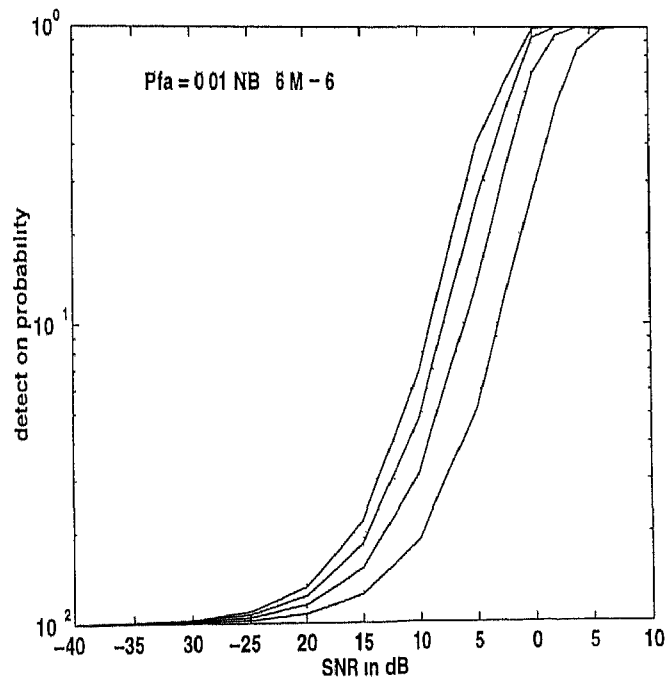


Figure 4.9 Detection probability vs SNR for $P_{FA} = 0.01$, $N_B = 6$ and $M = 6$ Adaptive threshold method

- A comparison with Fig 4.2 and Fig 4.7 shows a vast improvement in detection probability is obtained by adaptive thresholding technique of Fig 3.3

4.2.2 Detection performance for Nakagami-m faded signal in AWGN

Fig 4.10 The pdf of decision variable when the received signal is severely faded according to Nakagami-m distribution can be obtained by (3.21) as shown in Fig 4.10 and Fig 4.11 for various fading parameter m . The parameter $m < 1$ indicates that received signal is more severely faded than Rayleigh fading ($m = 1$) and $m > 1$ correspond to the cases of less severe fading than Rayleigh.

It can be observed that as m is increased the symmetry of curves increases and they become more and more peaked. For low SNR ($-10dB$) peaking occurs at larger value of m while for moderately high SNR ($0dB$) the peaking occurs at comparatively lower value of m .

Fig 4.11 The detection probability as obtained from (3.38) is shown in Fig 4.11 for the parameters $N_B = 1$, $M = 4$, $P_{FA} = 0.001$ and increasing values of fading parameter m . As can be observed in Fig 4.11 when the detection probability is in the range of 0.2 to 0.3, better detection performance is possible with the reducing fading severity (increasing m). However, below this range of detection probability better detection performance with increasing fading severity (reducing m). The phenomenon is not unusual and has been observed by many authors [13–31]. The reason behind this phenomenon is that there exist an optimum N_B for the faded received signal below and above which the performance degrades with increasing m .

4.3 Acquisition time performance: Fixed threshold method

Fig 4.12 and Fig 4.13 The mean and variance of acquisition time for modified serial search strategy of Fig 3.4 is computed from (3.50). Similarly the same parameters for standard serial search scheme of Fig 2.5 is obtained from (3.52) and (3.53) respectively. The improvement factor for mean acquisition time is defined as *ratio of mean acquisition time when no recirculation loop is present to the case when single recirculation loop is present*. A similar definition also applies to the improvement factor for variance of acquisition time.

The mean acquisition time improvement factor for the case $N_B = 1, 4, 16$ number of cells in code uncertainty region $q = 128$, false alarm overhead $K = 64$ false alarm probability $P_{FA} = 0.1$ and 0.01 is plotted in Fig 4.12 and Fig 4.13 respectively.

An improvement of 3 to 9 times is possible for mean acquisition time in the SNR range of $-40dB$ to $+10dB$. Improvement factor for the variance is shown in Fig 4.13 and 4 to 11 times improvement is obtained. With $N_B = 1$ the peak of all the curves lies in the SNR region extending from $-5dB$ to $+10dB$ while peak of the curves shift towards left with increasing N_B indicating that due to post detection integration maximum improvement is possible in extremely low SNR region. However, rapid decrease in the improvement factor for mean acquisition time can be observed beyond $-5dB$ with increasing N_B . This rapid fall is due to the fact that with increasing N_B recirculation loop increases the SNR quite rapidly while the detection probability asymptotically increases towards the unity and improvement, finally settles down to a moderate value in between 4 and 5. The same is true for variance improvement factor beyond $0dB$.

4.4 Acquisition time performance Adaptive threshold method

Fig 4.14 The improvement factor for the mean acquisition time is plotted in Fig 4.14 for the case $N_B = 1, 4, 8$, $q = 1024$, $K = 512$, $P_{FA} = 0.1$ and 0.01 . The important observations are as follows:

- An improvement factor of 4 to 13 is possible at $P_{FA} = 0.1$ while 4 to 16 is possible for $P_{FA} = 0.01$ in the SNR range of $-40dB$ to $+10dB$.
- A comparison with the Fig 4.12 for fixed threshold acquisition performance clearly shows better results are possible using the adaptive thresholding technique.

Fig 4.15 The improvement factor for variance of acquisition time is plotted in Fig 4.15 for $q = 1024$, $K = 512$, $M = 4$, $P_{FA} = 0.1$ and 0.01 . An improvement factor of 5 to 15 is possible, while similar curves for fixed threshold method in Fig 4.13 have shown an improvement of 4 to 11 times.

4.5 Acquisition time performance in Nakagami- m fading environment Adaptive threshold method

Fig 4.16 and Fig 4.17 The improvement factors for the mean and variance of the acquisition time when the received signal is severely faded is shown in Fig 4.16 and Fig 4.17 respectively for varying degree of severity. For fading more severe ($m < 1$) than Rayleigh ($m = 1$) an improvement factor of 3 to 6 times in mean acquisition time and 5 to 6 times in variance has been obtained. For Rayleigh fading case ($m = 1$) the two improvement factors are slightly higher. In general, as the fading severity is reduced the improvement curves shift upwards i.e., higher improvement is possible as the signal becomes more and more unfaded.

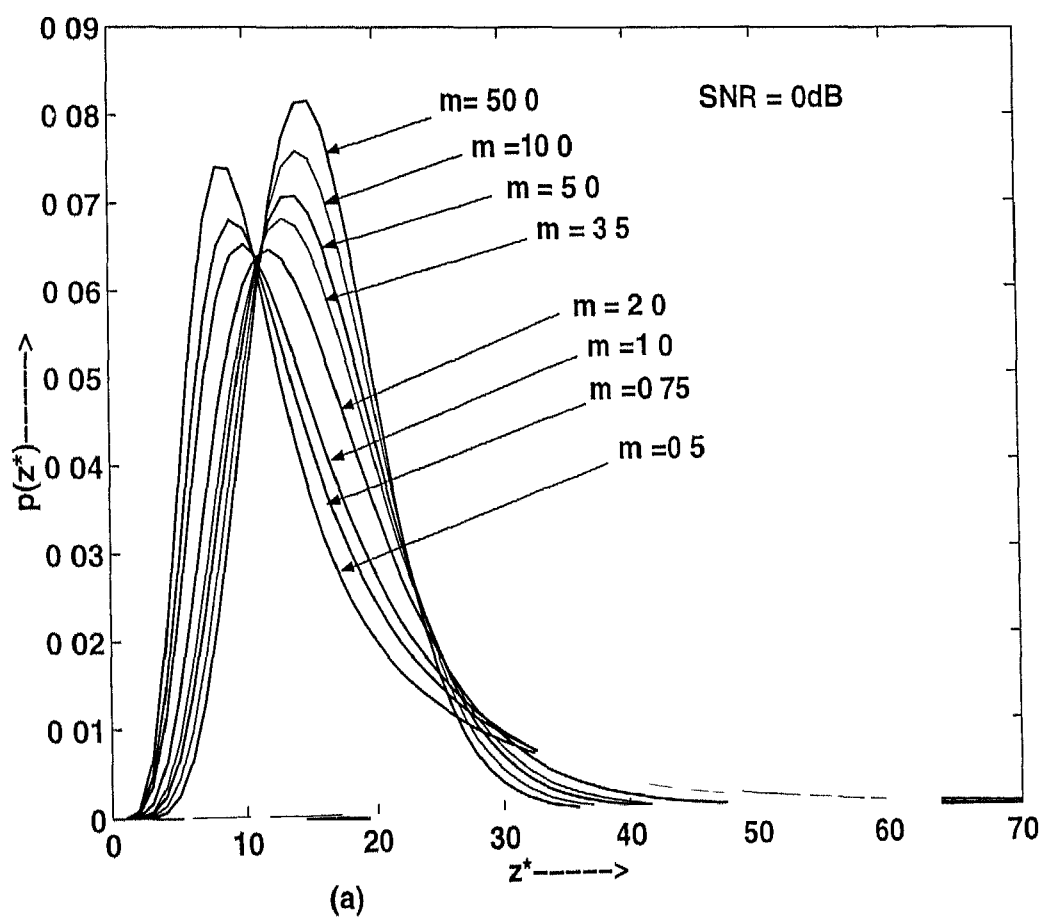
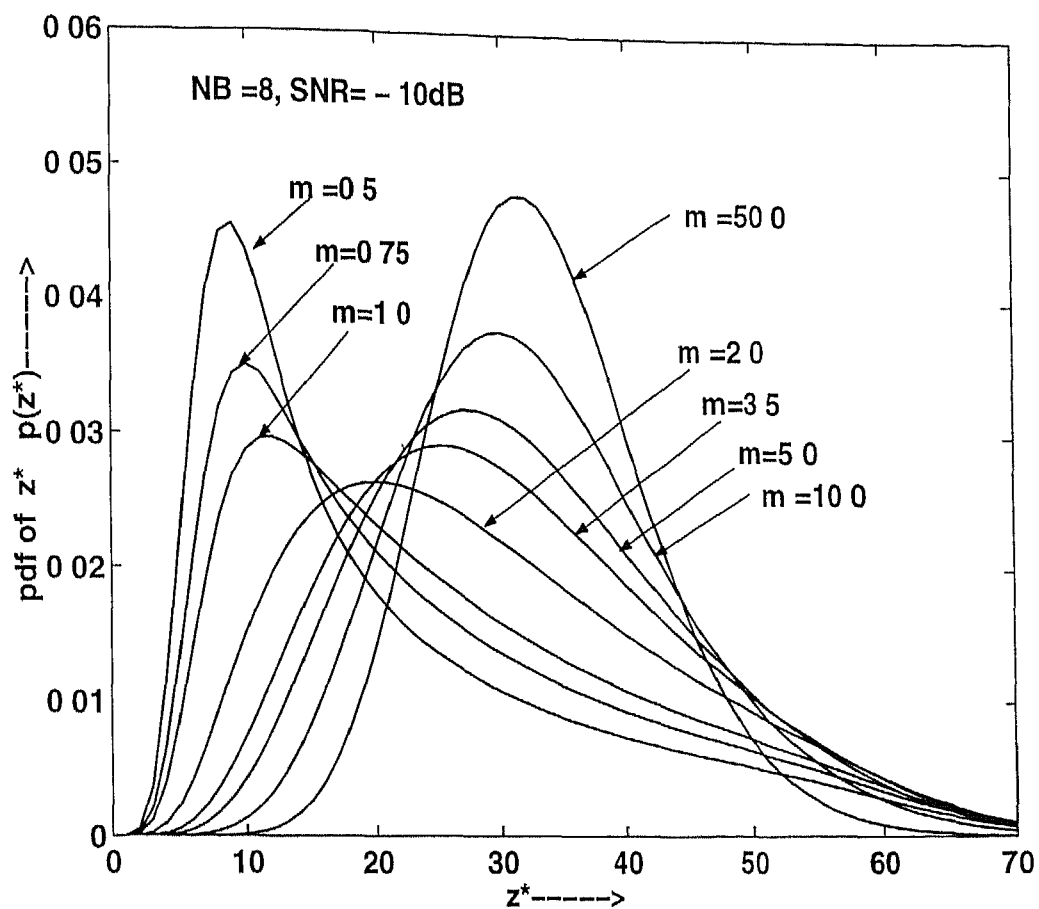


Figure 4.10 pdf of decision variable Z^* for Nakagami m faded received signal

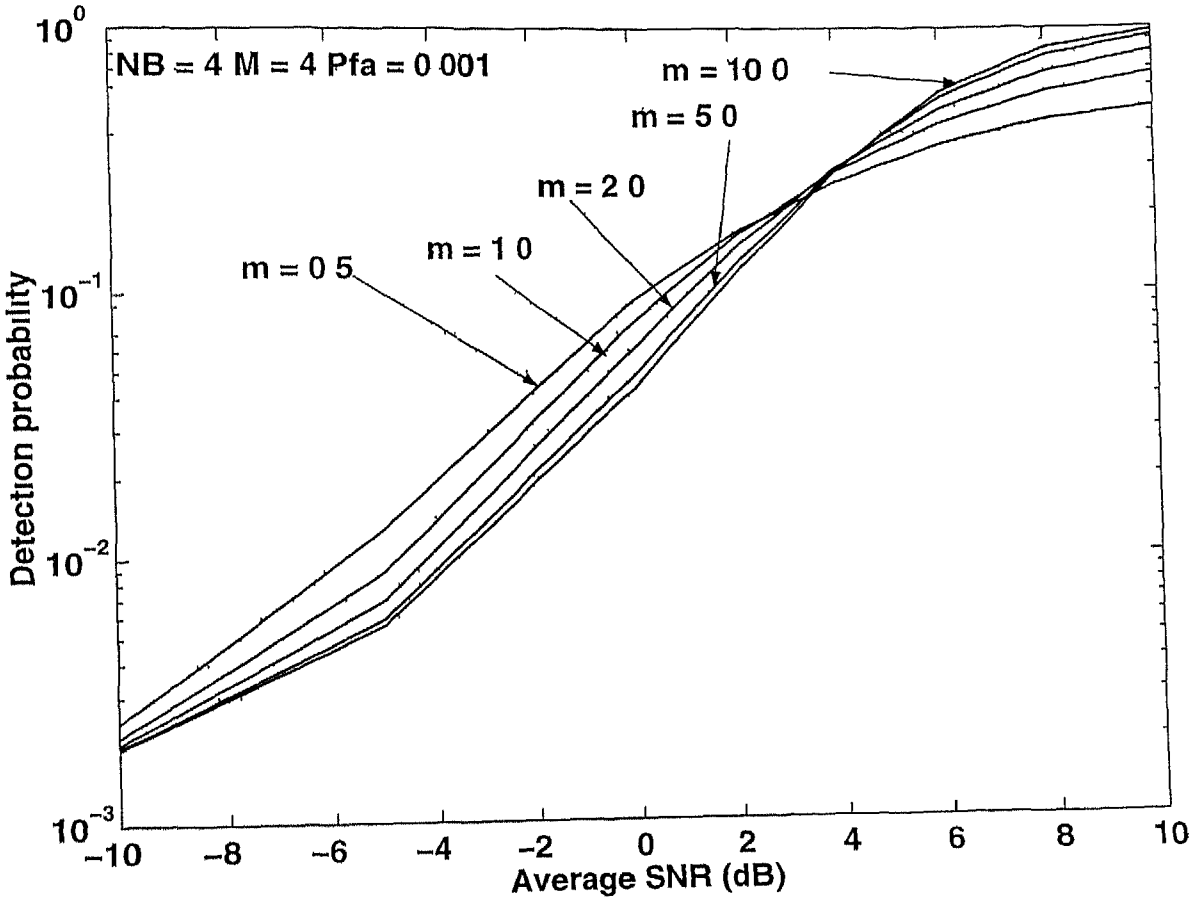


Figure 4.11 Detection probability vs SNR for Nakagami m faded received signal

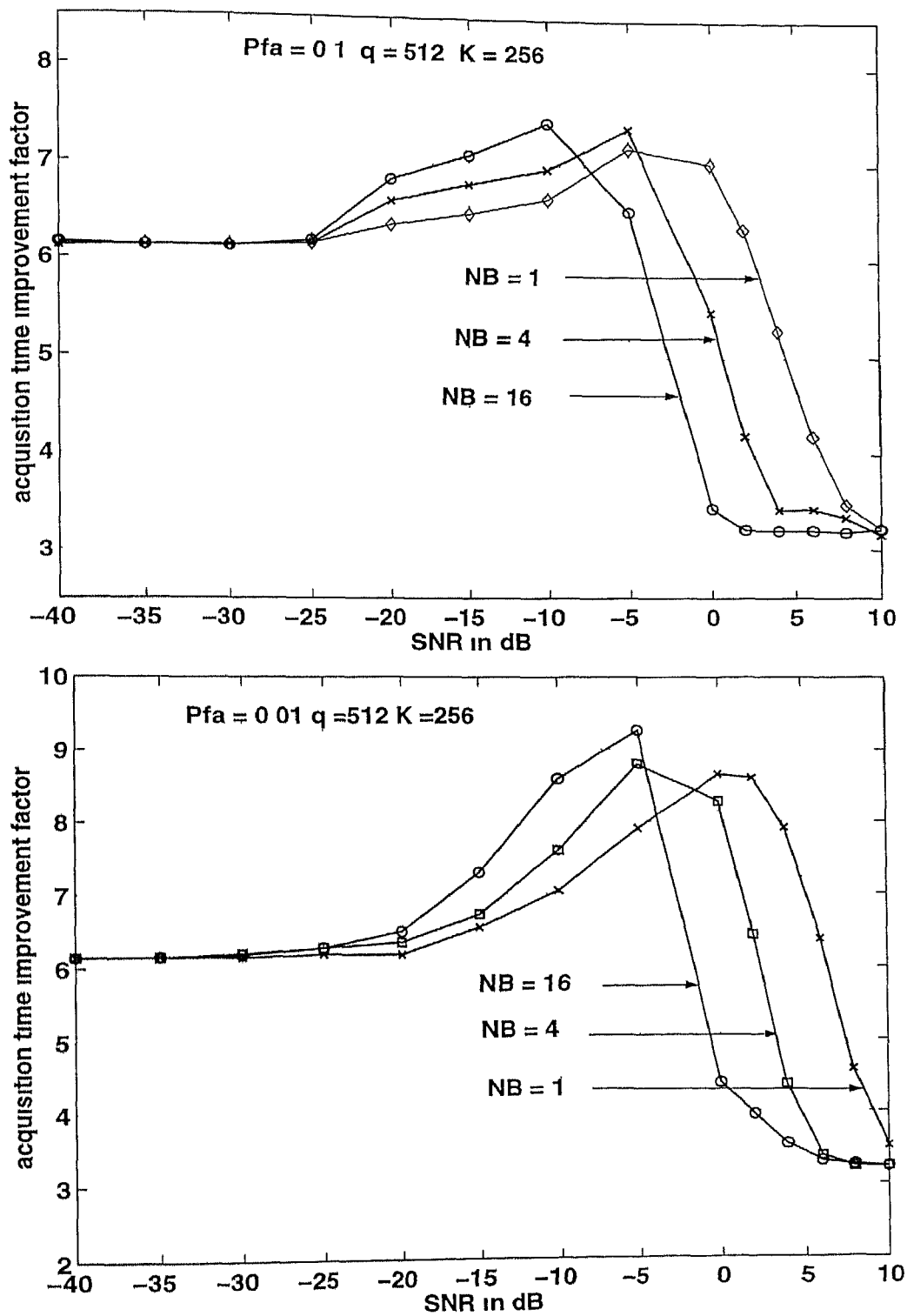


Figure 4.12 Improvement in mean acquisition time Fixed threshold method

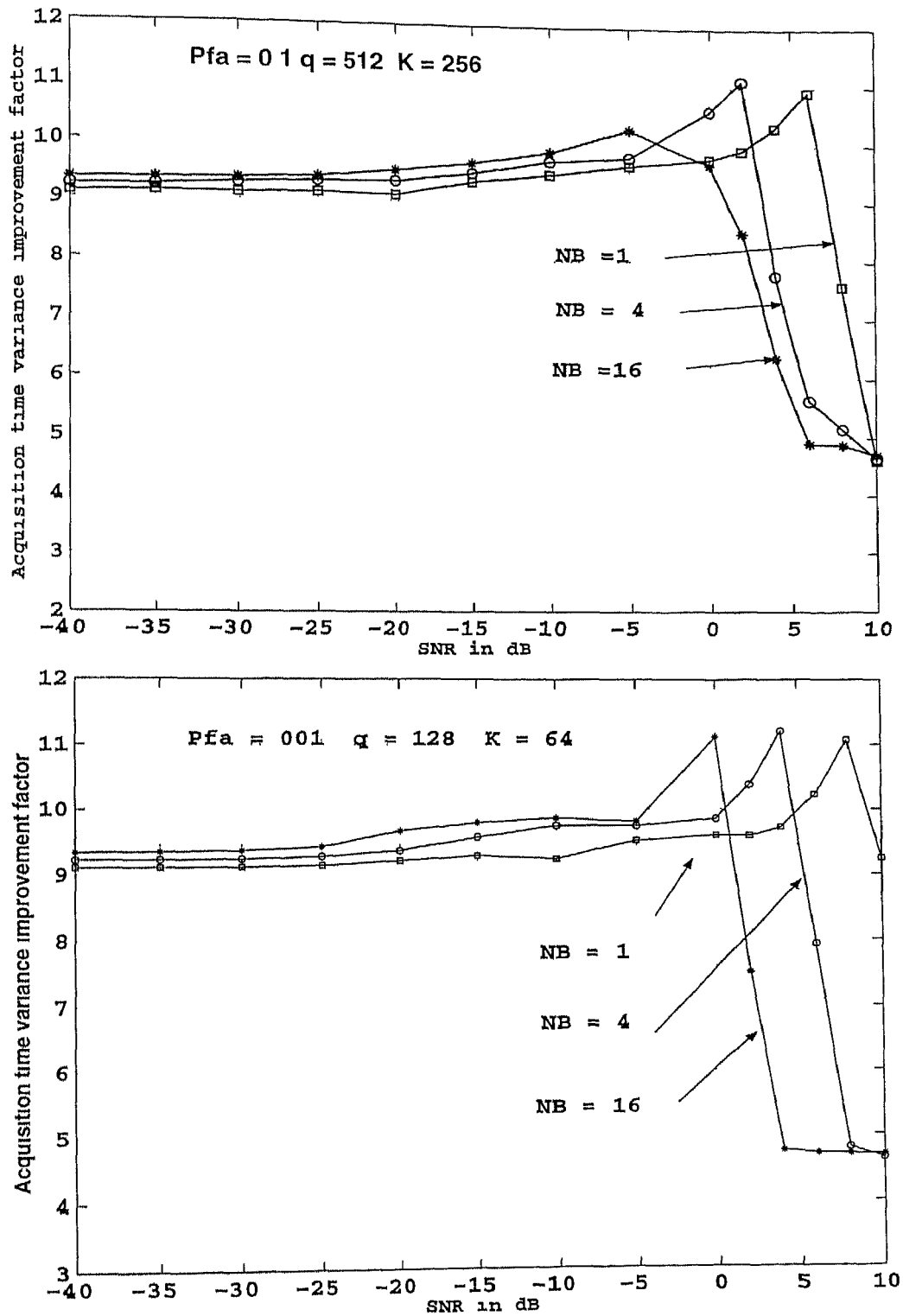


Figure 4.13 Improvement in variance of acquisition time Fixed threshold method

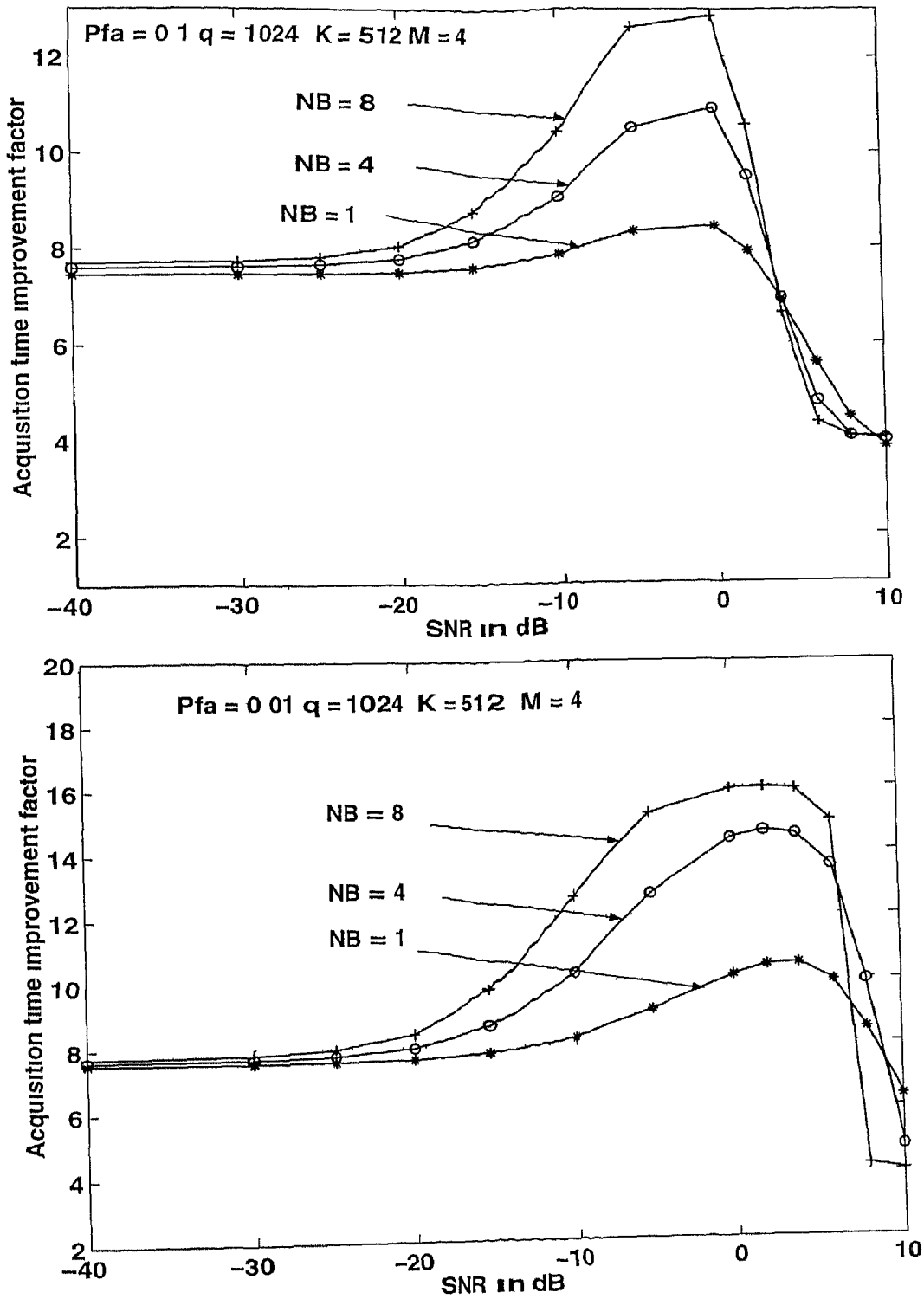


Figure 4.14 Improvement in mean acquisition time Adaptive threshold method

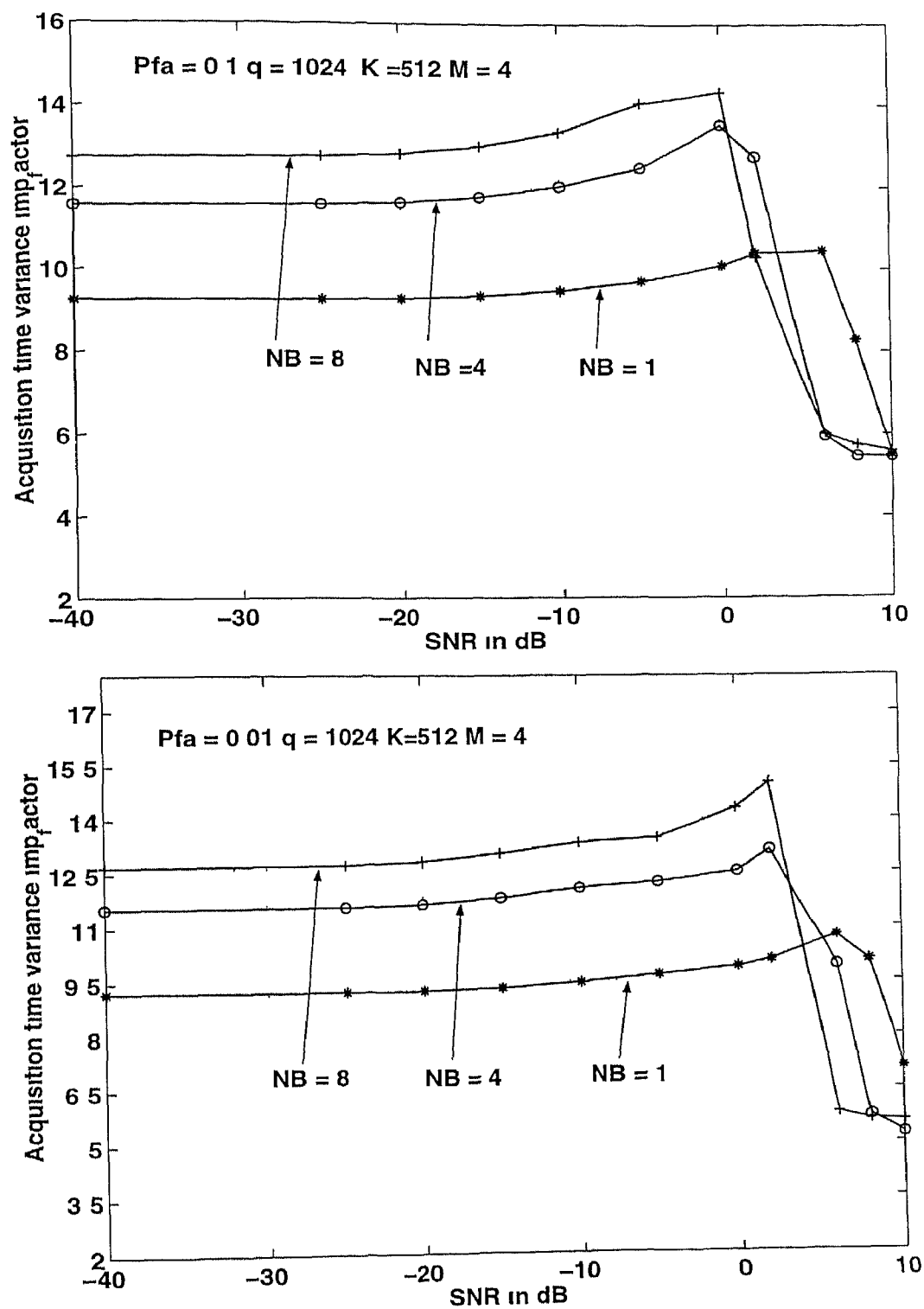


Figure 4.15 Improvement in variance of acquisition time Adaptive Thresh old method

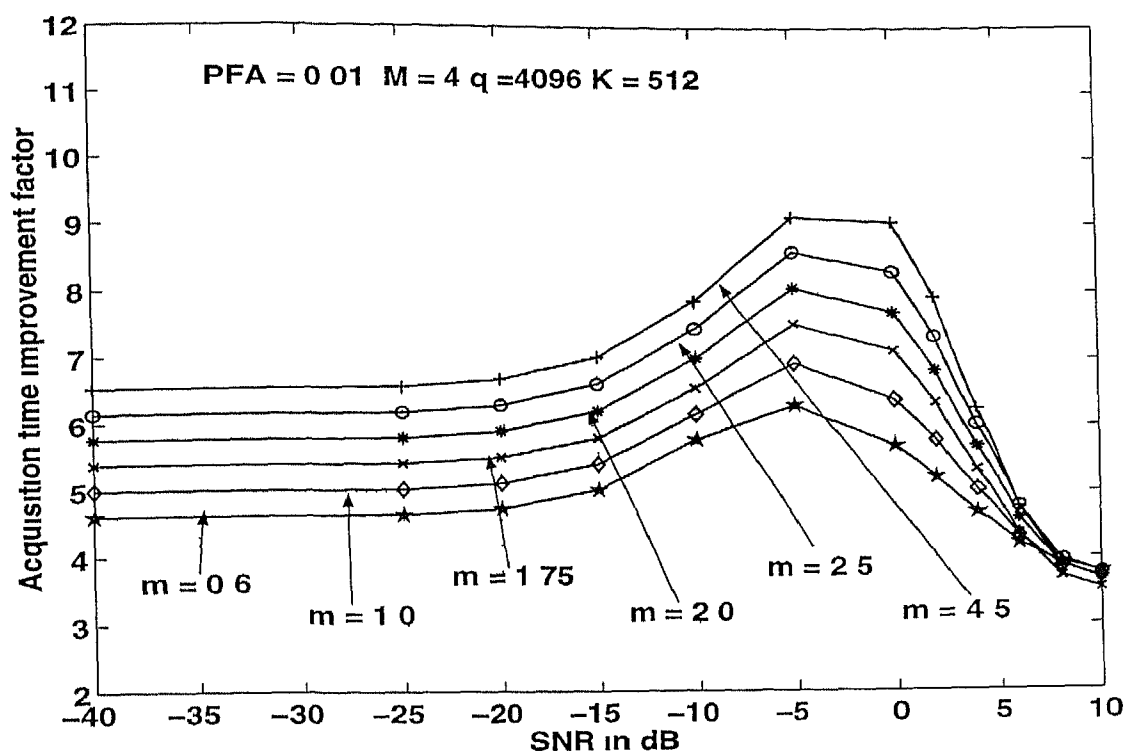


Figure 4.16 Improvement in Mean of the acquisition time Nakagami-m faded received signal using adaptive threshold method

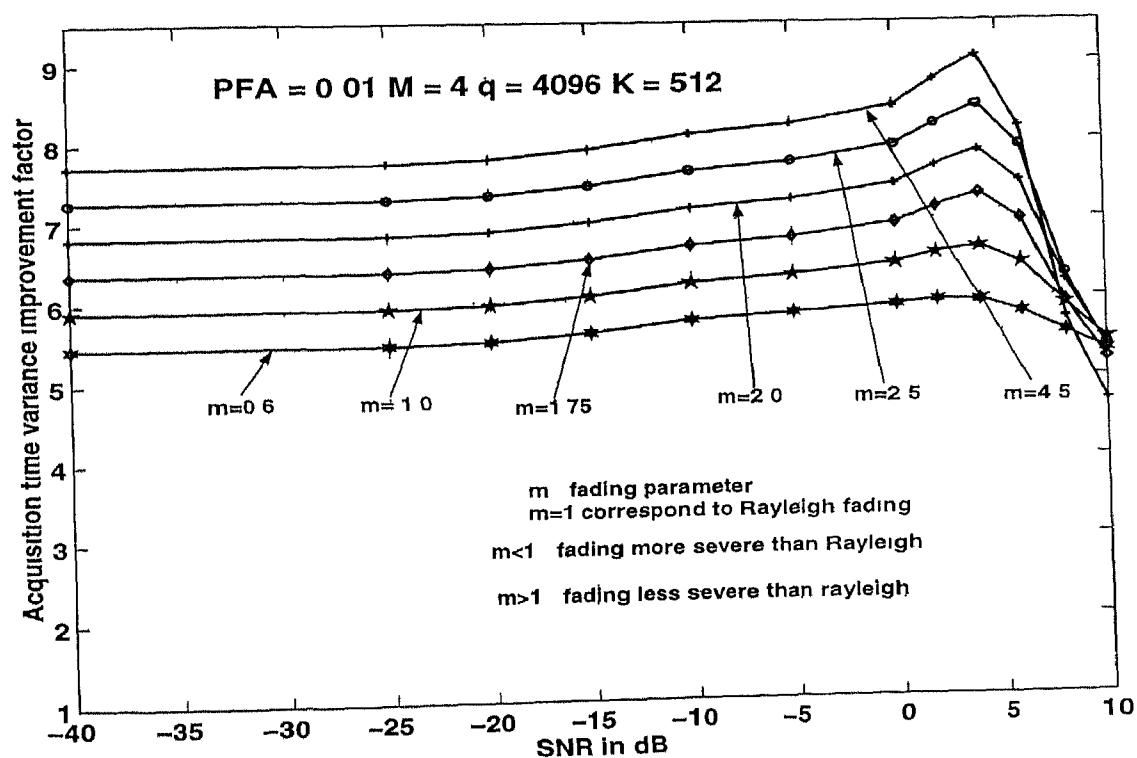


Figure 4.17 Improvement in variance of the acquisition time Nakagami-m faded received signal using adaptive threshold method

Chapter 5

Conclusions and Suggestions for Further Work

In this work a recently proposed [15] approach for PN code acquisition based on the recirculation loop principle has been modified and analyzed in terms of code acquisition parameters using fixed and adaptive threshold detection methods

Performance analysis of these algorithms have shown that for very low SNR range ($-40dB$ to $0dB$) considerably high improvement is possible over the existing serial search techniques. For moderate SNR range ($0dB$ to $10dB$) the improvement is still significant. In particular, the average acquisition time and its variance can be reduced up to *5 times* at $SNR = -15dB$. The overhead involved is not very significant as additional component e.g. post detection integration block (PDI) and adaptive decision processor can be easily incorporated in the integrated circuits. The former range of SNR is of interest during the period of initial synchronization.

5.1 Scope for further work

Some of the unresolved issues are

- What should be the filter bandwidth (B) ? The answer depends upon the allocated width of frequency band of operation and partially lies in the hands of frequency regulatory authorities and partially on the system variables such as the number of post detection integrations (N_B) employed. Since each test requires summation over N_B samples, the total search time will be proportional to N_BP , where P is the PN code period. This implies that N_B should be reduced

to decrease the search time. On the other hand, requirements of high detection probability and acceptable false alarm probability need N_B to be high. This fact was also observed in chapter 4 in the case of detection performance in Nakagami fading environment. Moreover, $N_B = B\tau_d$ and B is chosen such that $B = 1/T$ where T is sampling period, therefore, choosing faster sampling rate will increase B and hence N_B . Now the choice of integration dwell time (τ_d) dictates the optimization problem. Thus parameters B , N_B and τ_d need careful examination from optimization point of view so as to satisfy the constraint of reduced search time on one hand and acceptable detection performance on the other. For a given bandwidth B one possible approach as applicable to fixed threshold detection method could be as follows:

For a given false alarm probability P_{FA} solve for η . For a given detection probability P_{D_i} and SNR (γ_i) solve transcendently for N_B now using the relation $N_B = B\tau_d$ determine the τ_d . Finally using the τ_d , P_{FA} and P_{D_i} determine mean acquisition time and its variance.

Similar approach for adaptive detection method could also be devised keeping in view the fact that there is one more parameter M (number of reference cell in the adaptive decision processor) that needs to be optimized. Larger value of M will give better estimate of noise or interference. However, no procedure exists in the literature cited [18, 31] which gives optimum M for given P_{FA} and P_{D_i} .

- Another factor on which the acquisition time directly depends is false alarm penalty (K), i.e., number of integration needed to detect a false proposition. Though K should be chosen according to the criterion $K \ll q$, procedure for finding optimum K is far from being understood in contemporary literature.
- In the standard serial search technique a single code phase is examined at a time for possible synchronization. A natural extension of this technique will be to use two or more branches for simultaneous search of code phase uncertainty region. This approach, on one hand, will reflect in the increase of hardware complexity, which is quite affordable with present state of the art ASICs. On the other hand, by searching more than one code phase at a time it is expected that the acquisition time will decrease in direct relation to the number of parallel branches used. Specifically, devise a system where the entire q cell uncertainty region is subdivided into $N_p \geq 2$ equal components each containing $\frac{q}{N_p}$ cells. Each of N_p branches will be responsible for searching one component in parallel with remaining $(N_p - 1)$ branches. Furthermore, since the N_p searches progress

in parallel under a common control at any point along the way all N_p alignment examinations must be dismissed before search can proceed further

- When known code Doppler is present the acquisition time performance of system shown in fig 3.4 is affected in two ways. The first being relative shift between locally generated and received PN code phase to be time varying i.e. relative phase between the two codes is smeared during the dwell time of integrate and dump. The result is either an increase or decrease of detection probability depending upon whether code Doppler is causing relative code phase to increase or decrease. Thus the signal flow graph of fig 3.5 should be appropriately modified. The second and potentially more dominant effect is that code Doppler affects the average search rate (sweep rate), which in extreme cases can reduce it to zero thereby increasing the acquisition time to a very high value and hence needs critical examination. A brief description for the effect of code Doppler on the average search rate is provided in [2, 6]
- For unknown code Doppler, a code rate uncertainty region of the spreading code will be introduced which can also be partitioned into many discrete bands for either serial or parallel search. This search procedure will now be more complicated in the sense that it is two dimensional now one in code rate and another in time.
- The ideas of parallel search and recirculation loop can also be applied to the other forms of serial code search processes such as sequential detection etc.

References

- [1] A. J. Viterbi, *CDMA Principles of Spread Spectrum Communication* Reading MA Addison Wesley 1995
- [2] J. K. Holmes, *Coherent Spread Spectrum Systems* John Wiley Newyork 1982
- [3] J. S. Lee, J. L. Miller *CDMA System Engineering Handbook* Artech House, Boston 1998
- [4] R. L. Peterson, R. E. Ziemer D. E. Borth *Introduction to Spread Spectrum Communications* Pricntice Hall, Englewood Cliff New Jersey 1995
- [5] R. E. Ziemer, R. L. Peterson *Digital Communications and Spread Spectrum Systems*, Macmillan Publishing Company Newyork 1985
- [6] M. K. Simon *etal* , *Spread Spectrum Communications Handbook*, Vol III, Computer Science Press, Maryland, 1985
- [7] M. K. Simon *etal* , *Spread Spectrum Communications Handbool* Vol II Computer Science Press, Maryland, 1985
- [8] M. K. Simon *etal* , *Spread Spectrum Communications Handbook*, Vol I, Computer Science Press, Maryland, 1985
- [9] D. I. Tominelli, *Principles Of Secure Communication Systems*, Artech House Norwood, MA 1985
- [10] A. Polydoros and S. Ghisic, *Code Synchronization A Review of Principles and Techniques*, Reading MA Kluwer academic 1995
- [11] M. Schwartz, W. R. Bennet, S. Stein, "Communication Systems and Techniques" McGraw Hill, 1966
- [12] A. Papoulis "Probability, Random Variables, and Stochastic Processes" 3rd ed McGraw Hill International, Singapore 1991

- [13] H L Vantrees, *Detection Estimation and Linear Modulation Theory* Part I John Wiley Newyork 1968
- [14] M Abramowitz and I A Stegun *Handbook of Mathematical Function with Formulas Graph and Mathematical Tables* 9th ed Newyork Dover 1970
- [15] S Glisic *etal* 'New PN code acquisition scheme for CDMA network with low SNR', *IEEE Trans on commun* vol 47 pp 300 309 Feb 1999
- [16] M Katz and S Glisic "Modeling of code acquisition process in CDMA network Quasi synchronous systems" *IEEE Trans on commun* vol 46 pp 1564 1568 no 12 Dec 1998
- [17] S G Glisic, "Automatic decision threshold level control in direct sequence spread spectrum systems," *IEEE Trans Commun* , vol 39, No 2 pp 187 192 Feb 1991
- [18] C J Kim H J Lee, H S Lee "Adaptive Acquisition of PN sequences for DS SS communications" *IEEE Trans on commun* vol 46, No 8 pp 993 996 August 1998
- [19] A Polydoros, M K Simon, "Generalized serial search code acquisition The equivalent circular state diagram approach," *IEEE Trans on commun* COM 32 pp 1260 1268, Dec 1984
- [20] A Polydoros, C Weber, "A unified approach to serial search spread spectrum code acquisition Part I, General Theory,' *IEEE Trans on commun* , COM 32 pp 542 549, May 1984
- [21] A Polydoros, C Weber, "A unified approach to serial search spread spectrum code acquisition Part II, A Matched Filter Receiver,' *IEEE Trans on commun* COM 32, pp 550 560, May 1984
- [22] D M D'Amico, C L Weber, "Multiple dwell serial search Performance and application to direct sequence code acquisition ," *IEEE Trans on commun* , COM 31 No 5 pp 650 659, May 1983
- [23] D M D'Amico, C L Weber, " Statistical performance of single dwell serial synchronization systems," *IEEE Trans on commun* COM 28 No 8 pp 1382 1388 August 1980
- [24] G F Sage, " serial synchronization of pseudonoise systems,' *IEEE Trans on commun* , COM 12, pp 123 127, Dec 1964

- [25] R B Wuid Acquisition of pseudonoise signals by sequential estimation *IEEE Trans on commun* COM 13 pp 475 483 Dec 1965
- [26] R B Wuid, K P Yiu, 'Acquisition of pseudonoise signals by recursion aided sequential estimation,' *IEEE Trans on commun* COM 25 pp 784 794 Aug 1977
- [27] Y H Lee S Tuntari 'Acquisition of PN sequences for DS/SS system Design and performance,' *IEEE Journal in selected area of commun* vol SAC 10 pp 750 759, May 1992
- [28] J J Stiffel, 'Rapid Acquisition sequences,' *IEEE Trans on Inf theory* vol IT 14 No 2 pp 221 225 Mar 1968
- [29] D V Sarwate, M B Pursley, 'Cross correlation properties of pseudorandom and related sequences" *proc IEEE* vol 68 pp 593 619 Mar 1980
- [30] M K Simon, 'Non coherent pseudonoise code tracking performance of spread spectrum receivers," *IEEE trans on commun* , vol COM 25, No 3 pp 327 345 Mar 1977
- [31] X Y Hou, N Morinaga T Namekawa, "Direct evaluation of radar detection probabilities," *IEEE trans Aerosp Electron Syst* , vol AES 23, pp 418 424 July 1987
- [32] H Suzuki, "A statistical model for urban multipath propagation" *IEEE Trans Commun* , vol COM 25, pp 673 680, July 1977
- [33] M Nakagami, "The m distribution A general formula of intensity distribution for rapid fading," *in statistical methods in Radio wave propagation* New York Pergamon, 1960, pp 3 36
- [34] J K Holmes and C C Chen, "Acquisition time performance of PN Spread Spectrum system", *IEEE Trans on commun* , Vol com 25 pp 778 783 Aug 1977
- [35] [http //www qualcom com](http://www.qualcom.com)

Appendix A

Derivation of Acquisition Time Parameters

A 1 Mean acquisition time for serial search

Taking natural logarithm of (3.49) we get

$$\ln U(z) = -\ln q + \ln \sum_{l=0}^{q-1} H^l(z) + \ln \left[\frac{\beta_j z}{1 - (1 - \beta_j) z H^{q-1}(z)} \right] \quad (A.1)$$

differentiation of (A.1) with respect to z will give

$$\begin{aligned} \frac{d}{dz} \ln U(z) &= \frac{\sum_{l=0}^{q-1} \{l H^{l-1}(z) [\alpha(K+1)z^K + (1-\alpha)]\}}{\sum_{l=0}^{q-1} H^l(z)} \\ &+ \frac{1}{\sum_{j=1}^N \frac{\beta_j}{1 - (1-\beta_j)z H^{q-1}(z)}} \sum_{j=1}^N \frac{\{1 - (1-\beta_j)z H^{q-1}(z)\} \beta_j + z \beta_j (1-\beta_j) \frac{d[z H^{q-1}(z)]}{dz}}{[1 - (1-\beta_j)z H^{q-1}(z)]^2} \quad (A.2) \end{aligned}$$

$$d1 = \frac{d[z H^{q-1}(z)]}{dz} = H^{q-2}(z) [(q-1)\{\alpha(K+1)z^{K+1} + (1-\alpha)z\} + H(z)] \quad (A.3)$$

Since $H(z) = \alpha z^{K+1} + (1-\alpha)z$, therefore, $[H(z)]_{z=1} = 1$ so that

$$[d1]_{z=1} = \left[\frac{d[z H^{q-1}(z)]}{dz} \right]_{z=1} = (q-1)(1 + \alpha K) + 1 \quad (A.4)$$

Substituting (A.3) in (A.2) and recognizing the fact that $\sum_{l=0}^{q-1} l = \frac{q(q-1)}{2}$ the result after much simplification can be written as

$$\left[\frac{d[\ln U(z)]}{dz} \right]_{z=1} = \frac{(q-1)(1 + K\alpha)}{2} + \frac{1}{N} \left[\sum_{j=1}^N \left(1 + \frac{(1-\beta_j)\{(q-1)(1 + K\alpha) + 1\}}{\beta_j} \right) \right] \quad (A.5)$$

Since $(q-1)(1+K\alpha) \gg 1$, therefore after some cumbersome manipulation the desired expression for mean acquisition time is found out to be

$$\frac{\overline{T}_{acq}}{\tau_d} = \left[\frac{d[\ln U(z)]}{dz} \right]_{z=1} = (q-1)(1+K\alpha) \left[\left(\frac{1}{N} \sum_{j=1}^N \frac{1}{\beta_j} \right) - 0.5 \right] + 1 \quad (A 6)$$

A 2 Variance of acquisition time for serial search

Starting with the double differentiation of (A 1), we have

$$\begin{aligned} \frac{d^2}{dz^2} \ln U(z) &= \underbrace{\frac{d^2}{dz^2} \ln z}_{D_1} + \underbrace{\frac{d^2}{dz^2} \ln \left[\sum_{l=0}^{q-1} H^l(z) \right]}_{D_2} \\ &+ \underbrace{\frac{d^2}{dz^2} \ln \left[\sum_{j=1}^N \frac{\beta_j}{1 - (1 - \beta_j)z^{q-1}} \right]}_{D_3} \end{aligned} \quad (A 7)$$

$$[D_1]_{z=1} = -1 \quad (A 8)$$

$$[D_2]_{z=1} = \frac{(q-1)}{2} \left[\frac{(q-5)}{6} (1+K\alpha)^2 + K\alpha(K+1) \right] \quad (A 9)$$

$$\begin{aligned} [D_3]_{z=1} &= \frac{2(q-1)^2(1+K\alpha)^2}{N} \sum_{j=1}^N \left[\frac{1-\beta_j}{\beta_j} \right]^2 \\ &+ \left(\sum_{j=1}^N \frac{1-\beta_j}{\beta_j} \right) \left[\frac{(q-1)\{(q-2)(1+K\alpha)^2 + 2(1+K\alpha) + 1\} \alpha(K+1)}{N} \right. \\ &\quad \left. - \frac{(q-1)^2(1+K\alpha)^2}{N^2} \sum_{j=1}^N \frac{1-\beta_j}{\beta_j} \right] \end{aligned} \quad (A 10)$$

Therefore, variance of acquisition time can be written as

$$\begin{aligned} \frac{\sigma_{acq}^2}{\tau_d^2} &= [D_1]_{z=1} + [D_2]_{z=1} + [D_3]_{z=1} \\ &= \frac{(q-1)(1+K\alpha)}{2} + 1 + (q-1)(1+K\alpha) \frac{1}{N} \left(\sum_{j=1}^N \frac{1-\beta_j}{\beta_j} \right) \end{aligned} \quad (A 11)$$

Substituting (A 8), (A 9) and (A 10) in (A 11) and using the fact $(q-1)(1+K\alpha) \gg 1$ the result can be expressed as

$$\begin{aligned} \frac{\sigma_{acq}^2}{\tau_d^2} &= \left[\frac{(q-1)(1+K\alpha)}{N} \sum_{j=1}^N \frac{1-\beta_j}{\beta_j} \right] \left[3 + (q-2)(1+K\alpha) + \frac{K\alpha(K+1)}{(q-1)(1+K\alpha)} \right] \\ &+ \left[\frac{\{2(q-1)(1+K\alpha)\}^2}{N} \sum_{j=1}^N \left(\frac{1-\beta_j}{\beta_j} \right)^2 - \left(\frac{(q-1)(1+K\alpha)}{N} \sum_{j=1}^N \frac{1-\beta_j}{\beta_j} \right)^2 \right] \\ &+ \frac{(q-1)}{2} \left[(1+K\alpha) + (1+K\alpha)^2 \left(\frac{q-5}{6} \right) + \frac{K\alpha(K+1)}{2} \right] \end{aligned} \quad (A 12)$$

Appendix B

Probability Density Function of Decision Variable

B 1 Pdf of decision variable for no post detection integration case Unfaded signal in AWGN

Transforming (3.9) to the polar coordinates i.e., $w(t) = R(t)\cos\theta$ and $v(t) = R(t)\sin\theta$. To find the distribution of R and θ we simply transform (w,v) to (R,θ) in two dimensions as there is one to one correspondence

$$\begin{aligned}(w, v) &\longrightarrow (R, \theta) \\ p(w, v)dw dv &= p(R, \theta)dR d\theta \\ dw dv &= R dR d\theta \\ p(R, \theta) &= \frac{1}{2\pi\sigma^2} \exp\left(-\frac{(w-A)^2 + v^2}{2\sigma^2}\right) dw dv \\ &= \frac{R}{2\pi\sigma^2} \exp\left(-\frac{R^2 + A^2 - 2AR\cos\theta}{2\sigma^2}\right) dR d\theta\end{aligned}\tag{B 1}$$

The random variable θ is assumed to be uniformly distributed in the interval $[0, 2\pi]$ therefore distribution of R can be found out by integrating the (B 1) with respect to θ in the above interval i.e.,

$$\begin{aligned}p(R) &= \int_0^{2\pi} p(R, \theta) d\theta \\ &= \int_0^{2\pi} \frac{R}{2\pi\sigma^2} \exp\left(-\frac{R^2 + A^2}{2\sigma^2}\right) \exp\left(\frac{AR\cos\theta}{\sigma^2}\right) d\theta \\ &= \frac{R}{\sigma^2} \exp\left(-\frac{R^2 + A^2}{2\sigma^2}\right) I_0\left(\frac{AR}{\sigma^2}\right)\end{aligned}\tag{B 2}$$

Where $I_0(\cdot)$ is the modified Bessel function of first kind and zeroth order and is defined as [11] $I_0(\cdot) = \frac{1}{\pi} \int_0^{2\pi} \exp(\gamma \cos \theta) d\theta$

Since $y(t) = h(t)$ therefore applying the fundamental theorem of probability [12] on (B 2) we obtain the distribution of $y(t)$ **under signal present condition**, (Hypothesis H_1) as

$$p_1(y) = \begin{cases} \frac{1}{\sigma^2} \exp\left(-\frac{y}{2\sigma^2} + \gamma_i\right) I_0\left(\sqrt{\frac{2y}{\sigma^2}} \gamma_i\right) & \text{for } y \geq 0 \\ 0 & \text{otherwise} \end{cases} \quad (\text{B } 3)$$

and the pdf of $y(t)$ when the signal is absent, (Hypothesis H_0) can be obtained by substituting $\gamma_i = 0$ in (B 3) and recognizing the fact that $I_0(0) = 1$

$$p_0(y) = \begin{cases} \frac{1}{2\sigma^2} \exp\left(-\frac{y}{2\sigma^2}\right) & \text{for } y \geq 0 \\ 0 & \text{otherwise} \end{cases} \quad (\text{B } 4)$$

B 2 Pdf of decision variable for post detection integration case Unfaded signal in AWGN

Letting $\gamma_i = \frac{y_i}{N_B}$ The pdf of γ_i under hypothesis H_0 can be written from (B 4) as

$$p_0(\gamma_i) = \frac{N_B}{2\sigma^2} \exp\left(-\frac{\gamma_i N_B}{2\sigma^2}\right) d\gamma_i \quad (\text{B } 5)$$

To find out the pdf of decision variable Z , characteristic function (CF) approach [12] will be followed i.e. take the Laplace transform of $p_0(\gamma_i)$ take its N_B^{th} power and invert the transform to obtain the pdf of Z under both the hypotheses

Therefore under the hypothesis H_0 , the CF denoted by $M_0(s)$ is given as

$$M_0(s) = \int_0^\infty \frac{N_B}{2\sigma^2} \exp\left(-\frac{\gamma_i N_B}{2\sigma^2}\right) \exp(-s\gamma_i) d\gamma_i \quad (\text{B } 6)$$

$$M_0(s) = \frac{N_B}{2\sigma^2} \left(\frac{1}{s + \frac{N_B}{2\sigma^2}} \right) \quad (\text{B } 7)$$

The equation (B 7) gives the CF of decision variable Z under the hypothesis H_0 for no post detection integration case. Therefore, the pdf of Z for post detection integration case can be expressed as

$$p_0(Z) = \frac{1}{2\pi i} \oint [M_0(s)]^{N_B} \exp(sZ) ds \quad (\text{B } 8)$$

$$= \frac{\left[\frac{N_B}{\sigma}\right]^{N_B}}{2\pi i} \oint_C \frac{e^s}{\left(s + \frac{N_B}{2\sigma}\right)^{N_B}} ds \quad (\text{B } 9)$$

Since there is a simple pole of N_B^{th} order at $s = -\frac{N_B}{2\sigma}$ and residue at this pole is found out to be

$$\lim_{s \rightarrow -\frac{N_B}{2\sigma}} \frac{1}{(N_B - 1)!} Z^{N_B-1} \exp(sZ) \\ \left(\frac{1}{(N_B - 1)!} Z^{N_B-1} \exp\left(-\frac{ZN_B}{2\sigma^2}\right) \right) \quad (\text{B } 10)$$

therefore making use of Cauchy's residue theorem [14] the likelihood pdf of decision variable Z under hypothesis H_0 is found out to be

$$p_0(z) = \begin{cases} \left(\frac{N_B}{2\sigma^2}\right)^{N_B-1} \frac{\left(\frac{N_B}{2\sigma}\right)}{(N_B-1)!} \exp\left(-\frac{zN_B}{2\sigma^2}\right) & \text{for } Z \geq 0 \\ 0 & \text{otherwise} \end{cases} \quad (\text{B } 11)$$

To find out the pdf of decision variable Z under the hypothesis H_1 we proceed as follows. Since $r = \frac{y_i}{N_B}$ therefore the pdf of r_i using (B 3) can be expressed as

$$p_1(r_i) = \frac{N_B}{2\sigma^2} \exp\left[-\frac{r_i N_B}{2\sigma^2} - \gamma_i\right] I_0\left(2\sqrt{\frac{z_i N_B \gamma_i}{2\sigma^2}}\right) \quad (\text{B } 12)$$

The CL under hypothesis H_1 denoted as $M_1(s)$ is then defined as

$$M_1(s) = \int_0^\infty p_1(r_i) \exp(-s r_i) dz_i \quad (\text{B } 13)$$

and expanding the modified Bessel function [14] $I_0(x) = \sum_{n=0}^\infty \frac{[x/2]^n}{(n!)^2}$ $M_1(s)$ can be expressed as

$$M_1(s) = \int_0^\infty \frac{N_B}{2\sigma^2} \exp\left[-\frac{N_B r_i}{2\sigma^2} - \gamma_i\right] \sum_{n=0}^\infty \frac{\left[\frac{r_i N_B \gamma_i}{2\sigma^2}\right]^n}{(n!)^2} dz_i \quad (\text{B } 14)$$

Rearranging the terms of r_i and interchanging the sign of integration and summation we have

$$= \frac{N_B}{2\sigma^2} \exp(-\gamma_i) \sum_{n=0}^\infty \frac{\left[\frac{N_B \gamma_i}{2\sigma^2}\right]^n}{(n!)^2} \underbrace{\int_0^\infty r_i^n \exp\left(-s r_i - \frac{N_B r_i}{2\sigma^2}\right) dz_i}_{I_1} \quad (\text{B } 15)$$

The integral I_1 can be evaluated by making a substitution $r_i \left(s + \frac{N_B}{2\sigma^2}\right) = \theta$ and then using the definition of Gamma function [14] i.e., $\Gamma(n+1) = n! \triangleq \int_0^\infty \theta^n \exp(-\theta) d\theta$

$$I_1 = \frac{n!}{\left(s + \frac{N_B}{2\sigma^2}\right)^{n+1}} \quad (\text{B } 16)$$

substituting the L_1 in (B 15) and performing some routine algebra the final result can be expressed as

$$M_1(s) = \frac{\left(\frac{N_B}{2\sigma}\right)}{\left(s + \frac{N_B}{2\sigma}\right)} \exp \left[-\frac{\gamma_i s}{s + \frac{N_B}{2\sigma}} \right] \quad (\text{B } 17)$$

Therefore pdf of decision variable Z under the hypothesis H_1 is given as

$$p_1(Z) = \frac{1}{2\pi i} \oint [M_1(s)]^{N_B} \exp(sZ) ds$$

$$p_1(Z) = \frac{\left[\frac{N_B}{2}\right]^{N_B}}{2\pi i} \oint \frac{1}{\left(s + \frac{N_B}{2\sigma}\right)^{N_B}} \exp \left[-\frac{\gamma_i s N_B}{s + \frac{N_B}{2\sigma}} + sZ \right] ds \quad (\text{B } 18)$$

multiplying in numerator and denominator of (B 18) by $\exp \left[N_B \left(\gamma_i + \frac{Z}{2\sigma} \right) \right]$ letting $s + \frac{N_B}{2\sigma} = u$ so that $ds = du$ the $p_1(Z)$ then becomes

$$= \left[\frac{N_B}{2\sigma^2} \right]^{N_B} \exp \left[-N_B \left(\gamma_i + \frac{Z}{2\sigma} \right) \right] \frac{1}{2\pi i} \oint \frac{1}{u^{N_B}} \exp \left[\frac{Zu + \frac{\gamma_i N_B}{2\sigma^2}}{u} \right] du \quad (\text{B } 19)$$

The modified Bessel function of n^{th} order can be expressed in transform domain [11] by

$$I_n(ab) = \left(\frac{b}{a} \right)^n \frac{1}{2\pi j} \oint \frac{1}{s^{n+1}} \exp \left(\frac{a^2 s}{2} + \frac{b^2}{2s} \right) ds \quad (\text{B } 20)$$

letting $a = \sqrt{2Z}$ and $b = \sqrt{\frac{2N_B \gamma_i}{2\sigma}}$, we can write

$$\frac{1}{2\pi j} \oint \frac{1}{u^{N_B}} \exp \left(Zu + \frac{\gamma_i N_B^2}{u 2\sigma^2} \right) du = \left(\sqrt{\frac{2\sigma^2 Z}{N_B^2 \gamma_i}} \right)^{N_B-1} I_{N_B-1} \left(2\sqrt{\frac{Z \gamma_i N_B^2}{2\sigma^2}} \right) \quad (\text{B } 21)$$

using (B 21) in (B 19) the likelihood pdf of $p_1(Z)$ can then be expressed as

$$p_1(Z) = \left(\frac{N_B}{2\sigma^2} \right)^{N_B} \exp \left[-N_B \left(\gamma_i + \frac{Z}{2\sigma} \right) \right] \left[\frac{2Z\sigma^2}{\gamma_i N_B^2} \right]^{\frac{N_B-1}{2}} I_{N_B-1} \left(2\sqrt{\frac{Z \gamma_i N_B^2}{2\sigma^2}} \right) \quad (\text{B } 22)$$

Finally after some routine algebra the result can be expressed in simpler form

$$p_1(Z) = \begin{cases} \left(\frac{N_B}{2\sigma^2} \right) \exp \left[-N_B \left(\gamma_i + \frac{Z}{2\sigma} \right) \right] \left[\frac{Z}{2\sigma^2 \gamma_i} \right]^{\frac{N_B-1}{2}} I_{N_B-1} \left(2\sqrt{\frac{Z \gamma_i N_B}{2\sigma}} \right) & \text{for } Z \geq 0 \\ 0 & \text{otherwise} \end{cases} \quad (\text{B } 23)$$

Normalizing Z by $2\sigma^2/N_B = N_0 \tau_d$ or, equivalently, letting $Z \triangleq \frac{ZN_B}{2\sigma^2}$ we can rewrite (B 11) and (B 23), respectively, in a simpler form

$$p(Z^*) = \begin{cases} \left(\frac{\gamma}{(N_B-1)\gamma}\right)^{N_B-1} \exp(-Z^*) & \text{for } Z^* \geq 0 \\ 0 & \text{otherwise} \end{cases} \quad (\text{B } 24)$$

and

$$p_1(Z^*) = \begin{cases} \left(\frac{\gamma}{N_B\gamma}\right)^{\frac{N_B-1}{2}} \exp(-Z^* - N_B\gamma_i) I_{N_B-1}(2\sqrt{N_B\gamma_i Z^*}) & \text{for } Z^* \geq 0 \\ 0 & \text{otherwise} \end{cases} \quad (\text{B } 25)$$

B 3 Pdf of decision variable for post detection integration case Nakagami-m faded signal in AWGN

Expressing the modified Bessel function of $(N_B - 1)^{\text{th}}$ order in series summation form as [14]

$$I_{N_B-1}(2\sqrt{N_B Z^* \gamma_i}) = \sum_{r=0}^{\infty} \frac{(N_B Z^* \gamma_i)^{\frac{N_B-1}{2} + r}}{r!(N_B + r - 1)!} \quad (\text{B } 26)$$

putting (B 26) in (B 25) the resulting function will be

$$p_1(Z^*) = \left(\frac{\gamma}{N_B\gamma_i}\right)^{\frac{N_B-1}{2}} \exp[-Z^* - \gamma_i N_B] \sum_{r=0}^{\infty} \frac{(N_B Z^* \gamma_i)^{\frac{N_B-1}{2} + r}}{r!(N_B + r - 1)!} \quad (\text{B } 27)$$

Substituting (3 19) and (B 27) in (3 20), the resulting function will be

$$p_1(\gamma^*) = \int_0^{\infty} \frac{1}{\Gamma(m)} \left(\frac{m}{\Omega}\right)^m \gamma_i^{m-1} \exp\left(\frac{-m\gamma_i}{\Omega}\right) \left[\frac{\gamma}{N_B\gamma_i}\right]^{\frac{N_B-1}{2}} \exp[-Z^* - \gamma_i N_B] \sum_{r=0}^{\infty} \frac{(N_B Z^* \gamma_i)^{\frac{N_B-1}{2} + r}}{r!(N_B + r - 1)!} d\gamma_i \quad (\text{B } 28)$$

$$p_1(\gamma^*) = \frac{\left(\frac{m}{\Omega}\right)^m}{\Gamma(m)} \left(\frac{\gamma^*}{N_B}\right)^{\frac{N_B-1}{2}} \exp(-Z^*) \sum_{r=0}^{\infty} \frac{(N_B Z^*)^{\frac{N_B-1}{2} + r}}{r!(N_B + r - 1)!} \underbrace{\int_0^{\infty} \gamma_i^{m-1+r} \exp\left[-\gamma_i \left(\frac{m}{\Omega} + N_B\right)\right] d\gamma_i}_{I_1} \quad (\text{B } 29)$$

letting $\gamma_i \left(\frac{m}{\Omega} + N_B\right) = \theta$ and using the definition of $\Gamma(\cdot)$ function [14] the integral I_1 reduces to

$$I_1 = \frac{1}{\left(\frac{m}{\Omega} + N_B\right)^{m+r}} \int_0^{\infty} \theta^{m+r-1} \exp(-\theta) d\theta = \frac{\Gamma(m+r)}{\left(\frac{m}{\Omega} + N_B\right)^{m+r}} \quad (\text{B } 30)$$

Substituting (B 30) in (B 29) the result will be

$$p_1(\mathcal{Z}^*) = \frac{(m/\Omega)^m}{1(m)} \left[\frac{\mathcal{Z}^*}{N_B} \right]^{N_B-1} e^{\mathcal{Z}^*} p(-\mathcal{Z}^*) \sum_{i=0}^{\infty} \frac{(N_B \mathcal{Z}^*)^{\frac{N_B+i}{2}-1} \Gamma(m+i)}{i! \Gamma(N_B+i) \left(\frac{1}{\Omega} + N_B \right)^{m+i}} \quad (\text{B 31})$$

$$p_1(Z) = \frac{(m/\Omega)^m}{1(m) \left(\frac{m}{\Omega} + N_B \right)^m} [\mathcal{Z}^*]^{N_B-1} e^{\mathcal{Z}^*} p(-\mathcal{Z}^*) \sum_{i=0}^{\infty} \frac{(N_B \mathcal{Z}^*)^{\frac{N_B+i}{2}-1} \Gamma(m+i)}{i! \Gamma(N_B+i) \left(\frac{m}{\Omega} + N_B \right)^i} \quad (\text{B 32})$$

Letting $u = \frac{N_B \Omega}{m}$ remembering $\Omega = E(\gamma_i)$ and rearranging the terms we get

$$= \frac{(\mathcal{Z}^*)^{N_B-1} e^{\mathcal{Z}^*} p(-\mathcal{Z}^*)}{1(m) (1+u)^m} \sum_{i=0}^{\infty} \frac{\Gamma(m+i)}{i! \Gamma(N_B+i)} \left(\frac{u \mathcal{Z}^*}{1+u} \right)^i \quad (\text{B 33})$$

Multiplying numerator and denominator by $\Gamma(N_B)$ the final result can be expressed as

$$p_1(\mathcal{Z}^*) = \frac{(\mathcal{Z}^*)^{N_B-1} e^{\mathcal{Z}^*} p(-\mathcal{Z}^*)}{(1+u)^m (N_B-1)!} {}_1I_1 \left(m, N_B, \frac{u \mathcal{Z}^*}{1+u} \right) \quad (\text{B 34})$$

Where ${}_1I_1(a, b, i)$ is **confluent Hypergeometric function** defined as [3 14]

$${}_1I_1(a, b, i) = \frac{1(b)}{\Gamma(a)} \sum_{i=0}^{\infty} \frac{i! \Gamma(i+a)}{i! \Gamma(i+b)} \quad (\text{B 35})$$

Appendix C

Evaluation of Detection Probabilities P_{FA} and P_D

C.1 Unladed signal in AWGN Fixed threshold case

C.1.1 Probability of false alarm for post detection case

The probability of false alarm $P_{f,1}$ for fixed signal in AWGN can be obtained by integrating the likelihood pdf $P_0(Z)$

$$P_{f,1} = \int_{\eta}^{\infty} p_0(Z^*) dZ$$

$$\int_{\eta}^{\infty} \frac{(Z^*)^{N_B-1} \exp(-Z^*)}{(N_B-1)!} dZ \quad (C.1)$$

Using the definition of incomplete gamma function i.e.,

$$\Gamma(n+1) = \int_0^{\infty} \theta^n \exp(-\theta) d\theta = (n-1)! \exp(-1) \sum_{p=0}^{n-1} \frac{1^p}{p!} \quad (C.2)$$

Using (C.2) in (C.1) the result can be expressed as

$$P_{f,1} = \exp(-\eta^*) \sum_{p=0}^{N_B-1} \frac{\eta^{*p}}{p!} \quad (C.3)$$

where η^* is normalized threshold and is defined as $\eta^* \triangleq \frac{\eta N_B}{2\sigma^2}$

C 1 2 Probability of false alarm for no post detection integration case

The probability of false alarm under no post detection integration case can be obtained by substituting $N_B = 1$ in equation (C 3) i.e.

$$P_{FA} = \exp(-\eta^*) \quad (\text{C 4})$$

C 1 3 Probability of detection for post detection integration case

The probability of detection P_{Di} for i^{th} receive cycle of accumulation loop can be obtained by

$$\begin{aligned} P_{Di} &= \int_{\eta}^{\infty} p_1(Z^*) dZ^* \\ P_{Di} &= \int_{\eta}^{\infty} \left(\frac{Z^*}{N_B \gamma_i} \right)^{N_B-1} \exp(-Z^* - \gamma_i N_B) I_{N_B-1}(2\sqrt{N_B \gamma_i Z^*}) dZ^* \\ &\quad \left(\frac{1}{N_B \gamma_i} \right)^{N_B-1} \exp(-\gamma_i N_B) \int_{\eta}^{\infty} (Z^*)^{\frac{N_B-1}{2}} I_{N_B-1}(2\sqrt{N_B \gamma_i Z^*}) dZ^* \end{aligned} \quad (\text{C 5})$$

The modified Bessel function $I_{N_B-1}(\cdot)$ can be expressed in series sum form i.e.

$$I_{N_B-1}(2\sqrt{N_B \gamma_i Z^*}) = \sum_{r=0}^{\infty} \frac{(N_B \gamma_i Z^*)^{\frac{N_B+r-1}{2}}}{r!(N_B+r-1)!} \quad (\text{C 6})$$

Substituting (C 6) in (C 5) and performing some routine algebra the result can be expressed as

$$P_{Di} = \exp(-\gamma_i N_B) \sum_{r=0}^{\infty} \frac{(N_B \gamma_i)^r}{r!(N_B+r-1)!} \underbrace{\int_{\eta}^{\infty} (Z^*)^{N_B+r-1} \exp(-Z^*) dZ^*}_{K_1} \quad (\text{C 7})$$

The integral K_1 can be evaluated using the definition of incomplete gamma function given in (C 2) i.e.

$$K_1 = (N_B+r-1)! \exp(-\eta^*) \sum_{p=0}^{N_B+r-1} \frac{(\eta^*)^p}{p!} \quad (\text{C 8})$$

Finally substituting (C 8) in (C 7) the detection probability expression can be expressed as

$$P_D = \exp(-\gamma N_B - \eta) \sum_{r=0}^{\infty} \frac{(N_B \eta)^r}{r!} \sum_{l=0}^{N_B \tau - 1} \frac{(\eta)^l}{l!} \quad (\text{C } 9)$$

C 1 4 Probability of detection for no post detection integration

The detection probability for no post detection integration case may be obtained by putting $N_B = 1$ in equation (C 9) i.e

$$P_{D_i} = \exp(-\gamma_i - \eta) \sum_{r=0}^{\infty} \frac{\gamma_i^r}{r!} \sum_{p=0}^{\infty} \frac{(\eta)^p}{p!} \quad (\text{C } 10)$$

Which if desired can be expressed in Marcum Q function form

C 2 Unfaded signal in AWGN Adaptive threshold case

C 2 1 Probability of false alarm for post detection integration case

The probability of false alarm for a given value of \mathbf{T} is obtained by integrating the detection probability conditioned on a threshold $\eta = T\lambda$ over $p(\lambda)$

$$P_{FA} = \int_0^{\infty} p(\lambda) \int_{T\lambda}^{\infty} p_0(Z^*) dZ d\lambda \quad (\text{C } 11)$$

Since λ is defined as

$$\lambda = \sum_{i=-M}^M Z_i \quad \text{for } i \neq 0 \quad (\text{C } 12)$$

where each of Z_i consists of N_B independent white Gaussian noise samples the pdf of λ therefore can be written as

$$p(\lambda) = \frac{\lambda^{L-1} \exp(-\lambda)}{(L-1)!} \quad \text{where } L = M N_B \quad (\text{C } 13)$$

Therefore substituting (C 13) in (C 11) we have

$$P_{FA} = \int_0^{\infty} \frac{\lambda^{L-1} \exp(-\lambda)}{(L-1)!} \int_{T\lambda}^{\infty} \underbrace{\frac{(Z)^{N_B-1} \exp(-Z)}{(N_B-1)!}}_{\substack{p(Z) \\ I_1}} dZ d\lambda \quad (\text{C } 14)$$

using the definition of incomplete gamma function given in [14] the inner integral I_1 can be evaluated i.e

$$I_1 = (N_B - 1)! \exp(-T\lambda) \sum_{l=0}^{N_B-1} \frac{(T\lambda)^l}{l!} \quad (\text{C 15})$$

substituting (C 15) in (C 14) and changing the order of summation and integration we get

$$= \sum_{p=0}^{N_B-1} \frac{T^p}{(L-1)!p!} \underbrace{\int_0^\infty \lambda^{L+p-1} \exp\{-(1+T)\lambda\} d\lambda}_I \quad (\text{C 16})$$

Now making use of definition of Gamma function [14] the integral I is found out to be $(L+p-1)!$. Substituting it in (C 16) and performing some minor algebra the final result can be written in simplified form i.e

$$P_{FA} = \frac{1}{(1+T)^{MN_B}} \sum_{p=0}^{N_B-1} \binom{MN_B + p - 1}{p} \frac{T^p}{(1+T)^p} \quad (\text{C 17})$$

where notation $\binom{a}{b}$ is used to denote $\frac{a!}{b!(a-b)!}$ when a and b are positive integer and also for representing $\frac{\Gamma(a+1)}{\Gamma(b+1)\Gamma(a-b+1)}$ when a and b are positive non integer

C 2 2 Probability of false alarm for no post detection integration case

the probability of false alarm for no post detection integration case may be obtained by substituting $N_B = 1$ in (C 17) i.e

$$P_{FA} = \frac{1}{(1+T)^M} \quad (\text{C 18})$$

C 2 3 Probability of detection for post detection integration case

The detection probability for a given value of \mathbf{T} is obtained by averaging the detection probability over the pdf $p(\lambda)$ i.e ,

$$P_{Di} = \int_0^\infty \frac{\lambda^{L-1} \exp(-\lambda)}{(L-1)!} \underbrace{\int_{T\lambda}^\infty \left(\frac{Z^*}{N_B \gamma_i} \right)^{\frac{N_B-1}{2}} \exp(-Z^* - \gamma_i N_B) I_{N_B-1}(2\sqrt{N_B Z^* \gamma_i}) dZ^*}_{p_1(Z^*)} d\lambda \quad (\text{C 19})$$

Expanding the modified Bessel function $I_{N_B-1}(\cdot)$ into series summation form i.e

$$I_{N_B-1}(2\sqrt{N_B Z \gamma}) = \sum_{r=0}^{\infty} \frac{(N_B Z \gamma)^{\frac{N_B+r-1}{2}}}{r!(N_B+r-1)!} \quad (\text{C } 20)$$

Substituting (C 20) into (C 19) and interchanging the sign of summation and integration we have

$$\sum_{r=0}^{\infty} \frac{(N_B)^r \gamma}{r!(N_B+r-1)!} \exp(-\gamma N_B) \underbrace{\int_{T\lambda}^{\infty} (Z)^{N_B+r-1} \exp(-Z) dZ}_I \quad (\text{C } 21)$$

The integral I_3 can easily be evaluated using the definition of incomplete gamma function [14] i.e

$$I_3 = \Gamma(N_B+r, T\lambda) = (N_B+r-1)! \exp(-T\lambda) \sum_{p=0}^{N_B+r-1} \frac{(T\lambda)^p}{p!} \quad (\text{C } 22)$$

putting (C 22) into (C 21) and after some simplification the result can be written as

$$P_{D_i} = \sum_{r=0}^{\infty} \frac{(N_B \gamma_i)^r}{r!(L-1)!} \exp(-\gamma_i N_B) \sum_{p=0}^{N_B+r-1} \frac{T^p}{p!} \underbrace{\int_0^{\infty} \lambda^{L+p-1} \exp\{-(1+T)\lambda\} d\lambda}_{I_1} \quad (\text{C } 23)$$

The integral I_1 can be evaluated using the definition of gamma function i.e $I_1 = (L+p-1)!$ upon substitution in (C 23). Finally after some cumbersome manipulation the result can be expressed as

$$P_{D_i} = \frac{\exp(-\gamma_i N_B)}{(1+T)^{MN_B}} \sum_{r=0}^{\infty} \frac{(N_B \gamma_i)^r}{r!} \sum_{p=0}^{N_B+r-1} \binom{MN_B+p-1}{p} \left(\frac{T}{1+T}\right)^p \quad (\text{C } 24)$$

C 2 4 Probability of detection for no post detection integration case

The detection probability for no post detection integration case may be obtained by simply putting $N_B = 1$ in equation (C 24) i.e

$$P_{D_i} = \frac{\exp(-\gamma_i)}{(1+T)^M} \sum_{r=0}^{\infty} \frac{\gamma_i^r}{r!} \sum_{p=0}^r \binom{M+p-1}{p} \left(\frac{T}{1+T}\right)^p \quad (\text{C } 25)$$

C 3 Nakagami-m faded signal in AWGN Adaptive threshold case

$$P_{D_i} = \int_0^{\infty} \int_{T\lambda}^{\infty} p(\lambda) p_1(Z) dZ d\lambda \quad (\text{C } 26)$$

$$= \int_0^\infty p(\lambda) \left[\int_{T\lambda}^\infty \frac{Z^{(N_B-1)} \exp(-Z)}{(1+u)^m (N_B-1)!} {}_1F_1 \left(m, N_B, \frac{uZ}{1+u} \right) dZ \right] d\lambda \quad (C 27)$$

$$= \int_0^\infty p(\lambda) \underbrace{\left[\int_{T\lambda}^\infty \frac{Z^{(N_B-1)} e^{-Z}}{(1+u)^m (N_B-1)!} \sum_{r=0}^\infty \binom{m+r-1}{r} \left(\frac{uZ}{1+u} \right)^r dZ \right]}_{I_1} d\lambda \quad (C 28)$$

$$I_1 = \frac{1}{(1+u)^m} \sum_{r=0}^\infty \binom{m+r-1}{r} \frac{\left(\frac{u}{1+u} \right)^r}{(N_B+r-1)!} \underbrace{\int_{T\lambda}^\infty (Z)^{N_B+r-1} e^{-Z} p(-Z) dZ}_I \quad (C 29)$$

The integral I_2 is incomplete gamma function and is defined as

$$\Gamma(n, \theta) = \int_\theta^\infty e^{-t} t^{n-1} dt = (n-1)! e^{-\theta} \sum_{l=0}^{n-1} \frac{\theta^l}{l!} \quad (C 30)$$

Substituting C 30 in C 29 we get

$$I_1 = \frac{e^{-T\lambda}}{(1+u)^m} \sum_{r=0}^\infty \binom{m+r-1}{r} \left(\frac{u}{1+u} \right)^r \sum_{l=0}^{N_B+r-1} \frac{(T\lambda)^l}{l!} \quad (C 31)$$

Now $p(\lambda)$ is given by

$$p(\lambda) = \frac{\lambda^{L-1} \exp(-\lambda)}{(L-1)!} \quad (C 32)$$

substituting (C 31) and (C 32) in (C 29) we get

$$P_{D_i} = \int_0^\infty \frac{\lambda^{L-1} e^{-\lambda} p(-\lambda)}{(L-1)!} \frac{e^{-T\lambda}}{(1+u)^m} \sum_{r=0}^\infty \binom{m+r-1}{r} \left(\frac{u}{1+u} \right)^r \sum_{l=0}^{N_B+r-1} \frac{(T\lambda)^l}{l!} d\lambda \quad (C 33)$$

$$= \frac{1}{(1+u)^m (L-1)!} \sum_{r=0}^\infty \binom{m+r-1}{r} \left(\frac{u}{1+u} \right)^r \sum_{l=0}^{N_B+r-1} \frac{T^l}{l!} \underbrace{\int_0^\infty \lambda^{L+p-1} \exp(-(1+T)\lambda) d\lambda}_{I_3} \quad (C 34)$$

substituting $(1+T)\lambda = \theta$ the integral I_3 reduces to gamma function defined as $\Gamma(n) = \int_0^\infty \theta^{n-1} e^{-\theta} d\theta$. Hence integral I_3 reduces to

$$I_3 = \frac{\Gamma(L+p)}{(1+T)^{L+p}} \quad (C 35)$$

Therefore P_{D_i} could be written as

$$P_{D_i} = \frac{1}{(1+u)^m} \sum_{r=0}^\infty \binom{m+r-1}{r} \left(\frac{u}{1+u} \right)^r \sum_{p=0}^{N_B+r-1} \frac{T^p (L+p-1)!}{p! (L-1)! (1+T)^{L+p}} \quad (C 36)$$

Finally rearranging the like power terms we get the desired expression for detection probability i.e

$$P_{D_1} = \frac{1}{(1+u)^n(1+T)^L} \sum_{r=0}^{\infty} \binom{m+r-1}{r} \left(\frac{u}{1+u}\right)^r \sum_{p=0}^{N_B+r-1} \binom{L+p-1}{p} \left(\frac{T}{1+T}\right)^p \quad (C.57)$$

C.4 Rayleigh faded signal in AWGN Adaptive threshold case

The probability of detection for Rayleigh Faded signal in AWGN can be found out in a manner similar to Nakagami-m faded case. Since Rayleigh fading is the special case of Nakagami m fading, therefore direct substitution of $m = 1$ will yield the detection probability expression i.e

$$P_D = \frac{1}{((1+u)(1+T))^L} \sum_{r=0}^{\infty} \left(\frac{u}{1+u}\right)^r \sum_{p=0}^{N_B+r-1} \binom{L+p-1}{p} \left(\frac{T}{1+T}\right)^p \quad (C.58)$$

A130930

A130930

Date Slip

This book is to be returned on the
date last stamped

--



A130930